

Evaluation of a novel Dual Resin Substrate Feed- Product Removal (SFPR) strategy applied to an oxidative bioconversion

A thesis submitted to University College London for the degree of
Doctor of Philosophy

by

Naqash Yasin Raja

The Advanced Centre for Biochemical Engineering
Department of Biochemical Engineering
University College London
Torrington Place
London
WC1E 7JE
UK

Declaration

I, Naqash Raja, confirm that the work presented in this thesis is my own. Where information has been derived from other sources, I confirm that this has been indicated in the thesis.

Abstract

A novel dual resin based, substrate feed and product removal (SFPR) strategy has been investigated to overcome the substrate and product inhibition in an industrially important Baeyer-Villiger monooxygenase catalysed bioconversion in order to enhance the productivity of the bioconversion process. The bioconversion of the ketone substrate, bicyclo[3.2.0]hept-2-en-6-one, to the lactone products, (1R,5S)-3-oxabicyclo[3.3.0]oct-6-en-2-one and (1S,5R)-2-oxabicyclo[3.3.0]oct-6-en-3-one, catalysed by a recombinant whole cell biocatalyst, *Escherichia coli* TOP10 [pQR239], expressing cyclohexanone monooxygenase from *Acinetobacter calcoaceticus*, was used as the model reaction to prove the feasibility of the novel dual resin SFPR concept.

Before the application of the dual resin SFPR strategy to the Baeyer-Villiger bioconversion, adsorption of the ketone and lactone onto non-specific resins was investigated. Several resins were initially characterised at the bench scale by determining adsorption isotherms for the ketone and lactone compounds. Thereafter adsorption isotherms were generated via a high throughput resin screening (HTRS) method using both 96 wells and 24 wells microplate platforms.

Comparison of the adsorption isotherm data between the bench scale and the two HTRS platforms, together with results of resin mixing in wells of the 96 wells and 24 wells microplate platforms, as investigated by high speed imaging experiments, shows that the 24 well microplate platform was the most suitable to investigate adsorption kinetics of the ketone and lactone on the resins.

Based on the adsorption studies, resins Dowex[®] Optipore L493 and Amberlite[®] XAD7 were chosen to be separately used for substrate feeding in the dual resin SFPR strategy. Dowex[®] Optipore L493 was chosen for its high capacity of 0.21 g/g_{adsorbent} for ketone, whereas Amberlite[®] XAD7 was chosen for its high selectivity of ketone over lactone compared to any other resin. Amberlite[®] IRC50 was chosen for lactone removal in the

dual resin SFPR strategy because of its high selectivity of lactone over ketone than any other resin.

To demonstrate the feasibility of the dual resin SFPR strategy, the Baeyer-Villiger bioconversion was performed in shake flasks and compared to bioconversions without the use of resins and with the use of a single resin based SFPR strategy. At an initial ketone concentration of 3g/l, both resin based strategies performed significantly better than the bioconversion performed without resins. The dual resin SFPR strategy, carried out with both types of resins free in suspension without spatial separation, also showed improvement compared to results obtained with the single resin SFPR strategy. The dual resin SFPR strategy was also performed with the spatial separation of the two resins by housing one of the resins in a porous bag. This allowed observation of the majority of lactone product adsorbed onto the Amberlite[®] IRC50 resin as expected based on adsorption studies.

Carrying out the Baeyer-Villiger bioconversion with the implementation of the dual resin SFPR strategy in shake flasks saw an increase of productivity compared to the Baeyer-Villiger bioconversions carried out without resins by as much as 132% and in comparison with the single resin SFPR strategy by as much 10%, thus demonstrating a ‘proof of concept’ of the novel dual resin SFPR bioconversion strategy.

After demonstrating a ‘proof of concept’ for the dual resin SFPR strategy, its application in a miniature stirred tank bioreactor was investigated to open the way for scale up studies. Two configurations were investigated, namely the conventional reactor system where both resins were added directly into the bioreactor, and the recycle reactor system where a column housed one of the two types of resins. Using resins with low adsorption capacities and the need of an extra resin type in a dual resin SFPR strategy, makes the recycle reactor configuration a more attractive system, however it was the conventional reactor configuration that performed better than the recycle reactor system.

The L493-IRC50 combination in the conventional reactor configuration achieves a 21% greater productivity than in the recycle reactor. The dual resin SFPR strategy using the

L493-IRC50 combination performed better than any other resin based SFPR strategy when carried out with both resins in the reactor. It reached a productivity of 0.85g/l/h after 2.5 hours of reaction, 5% higher than the productivity achieved with the single resin strategy in the conventional reactor configuration.

The novel dual resin based SFPR strategy and the HTRS method developed in this work has the potential to be applied in any bioconversion that needs to overcome substrate and product inhibition.

Acknowledgments

I praise All Mighty Allah for giving me the ability, knowledge, strength and patience to perform and complete this work. All that is good is from Him and any shortcomings are of my own. I pray to Him that the research presented here brings further progress to its field and beyond.

I would like to show my utmost respect and gratitude for my Supervisor Dr Frank Baganz for trusting me with this project and giving me support and guidance throughout the programme. I would also like to thank Professor Gary Lye, who acted as the project Advisor, the research and non-research staff in the Department of Biochemical Engineering, UCL, for the help they provided, and the Biotechnology and Biological Sciences Research Council (BBSRC) for funding this project. I am also grateful to this project for enhancing my skills as a researcher.

A special mention to Dr Shaukat Ali who provided company on those late work days, Miguel Angel Perez-Pardo for caring for my project like it was his own and Omar Al-Ramadhani for the many important advice that has helped me in my life.

I must express my love for my family who have shown tremendous patience during my PhD research. I would like to thank my older sisters Samara and Furrah (Bobby), my little brother Bilal and my brother-in-law Usman for taking care of many things in my life so that I can focus on my research. Thank you to my nieces, princess Rumaysa and princess Umaymah, whose innocence got rid of all my worries. And I express love and gratitude for my wife Tabassum, who entered my life to give me the motivation to overcome the last hurdle on the way to achieving this success.

Finally, words cannot express how much I am thankful to the two most important people in my life, my parents Muhammad Yasin and Ishrat. They have afforded me material and emotional support but have asked nothing in return except success and happiness for their children. I dedicate this PhD to them.

Table of Contents

Declaration.....	2
Abstract.....	3
Acknowledgments.....	6
Table of Contents	7
List of Figures	13
List of Tables	20
Chapter 1. Introduction	22
1.1 Prospect of biocatalysis.....	22
1.2 The Baeyer-Villiger oxidation.....	25
1.2.1 Reaction and mechanism	25
1.2.2 Chemical methods	26
1.2.3 Biological methods.....	27
1.3 Baeyer-Villiger oxidation using Cyclohexanone Monooxygenase	29
1.3.1 Cyclohexanone Monooxygenase from <i>Acinetobacter calcoaceticus</i> (NCIMB 9871).....	29
1.3.2 Overexpression of Cyclohexanone Monooxygenase in <i>E. coli</i> TOP10 [pQR239].....	32
1.3.3 BVMO as the model bioconversion system.....	34
1.4 <i>in situ</i> Substrate Feeding and Product Removal (SFPR)	34

1.4.1	General.....	34
1.4.2	Resin based SFPR.....	35
1.4.3	High throughput resin screening (HTRS).....	36
1.4.4	Choice of reactor for resin based systems.....	37
1.5	Thesis Aims.....	39
Chapter 2. Materials and Methods.....		41
2.1	Materials.....	41
2.1.1	Chemicals.....	41
2.1.1.1	Preparation of ketone and lactone solutions in buffer.....	41
2.1.1.2	Fermentation media composition.....	41
2.1.2	Resins.....	41
2.1.2.1	Resin water content.....	42
2.1.3	Microorganism.....	42
2.1.3.1	<i>E. coli</i> TOP10 [pQR239] seed stock preparation.....	42
2.2	Analytical methods.....	43
2.2.1	Ketone and lactone quantification by gas chromatography (GC).....	43
2.2.1.1	Sample preparation.....	43
2.2.1.2	Gas Chromatography Operation and Quantification.....	43
2.2.2	Dry cell weight (DCW) measurement.....	44
2.2.3	Analysis of ketone and lactone load on resin.....	44
2.2.4	Measurement of glycerol concentration in bioconversion medium.....	44
2.3	Resin Screening.....	45
2.3.1	Millilitre scale adsorption isotherms.....	45
2.3.2	High throughput resin screening (HTRS).....	46
2.3.2.1	Adsorption isotherms.....	46
2.3.2.2	Dual compound adsorption kinetics.....	47

2.3.3	Investigation of resin suspension behaviour in 96 and 24 wells microplate formats using high speed imaging	47
2.3.3.1	High speed camera equipment.....	47
2.3.3.2	Investigation of resin suspension behaviour in mimics of 96 and 24well microplate	47
2.4	<i>E. coli</i> TOP10 [pQR239] fermentation.....	48
2.4.1	Preparation of inoculum.....	48
2.4.2	Shake flask fermentation and CHMO induction	48
2.4.3	Cell harvest and storage	48
2.5	Shake flask bioconversions	49
2.5.1	Bioconversions without the implementation of a SFPR strategy.....	49
2.5.2	Bioconversion with the implementation of the single resin SFPR strategy	49
2.5.3	Bioconversions with the implementation of the dual resin SFPR strategy	50
2.5.3.1	Dual resin SFPR bioconversion without separation of the two types of resins	50
2.5.3.2	Dual resin SFPR bioconversion with separation of the two types of resins	50
2.6	Miniature stirred tank reactor (STR) bioconversions	52
2.6.1	Operation of miniature STR system	52
2.6.2	Bioconversions without the implementation of a SFPR strategy.....	52
2.6.3	Bioconversion with the implementation of the single resin SFPR strategy	53
2.6.4	Bioconversions with the implementation of the dual resin SFPR strategy	53
2.7	Resin based SFPR bioconversions performed in the recycle reactor configuration.....	54
2.7.1	Specifications of column.....	54
2.7.2	Preparation of column for use in bioconversion	54

2.7.3	Set up and operation of the miniature STR in the recycle reactor configuration.....	55
2.7.4	Bioconversion with the implementation of the single resin SFPR strategy	55
2.7.5	Bioconversion with the implementation of the dual resin SFPR strategy .	56
Chapter 3. Resin screening		57
3.1	Aims.....	57
3.2	Introduction	57
3.3	Theory.....	58
3.3.1	Adsorption capacity	58
3.3.2	Adsorption isotherm models	58
3.3.3	Determining selectivity based on initial rate of adsorption	59
3.4	Results.....	60
3.4.1	Bench scale resin screening	60
3.4.2	High-throughput resin screening (HTRS).....	67
3.4.2.1	Charaterisation of resin suspension behaviour analysis using high-speed image analysis.....	67
3.4.3	Determination of adsorption isotherms from microwell experiments	72
3.5	Adsorption kinetics studies	82
3.6	HTRS efficiency.....	86
3.7	Conclusions	87
Chapter 4. Demonstrating a ‘proof of concept’ of the novel dual resin SFPR strategy in shake flasks		89
4.1	Aims.....	89
4.2	Introduction	89

4.3	Results.....	90
4.3.1	Demonstration of substrate inhibition in the BV bioconversion.....	90
4.3.2	Single resin SFPR strategy.....	92
4.3.3	Dual resin SFPR strategy	94
4.3.3.1	Dual resin SFPR using two resins free in suspension.....	95
4.3.3.2	Dual resin SFPR with the substrate feeding resin in filter bag.....	97
4.3.4	Comparison of single resin and dual resin SFPR	100
4.4	Conclusions	104
Chapter 5. Miniature stirred tank reactor evaluation of SFPR strategy		105
5.1	Aims.....	105
5.2	Introduction	105
5.3	Results.....	106
5.3.1	Baeyer-Villiger bioconversion	106
5.3.2	Single SFPR strategy	107
5.3.3	Dual SFPR strategy	109
5.3.4	Recycle STR SFPR strategy.....	111
5.3.5	Comparison of single and dual SFPR strategies	114
5.4	Conclusions	116
Chapter 6. Overall Conclusions.....		117
Chapter 7. Future Work.....		121
7.1	Automated HTRS and design of experiments (DoE)	121
7.2	Scale up of the dual resin SFPR bioconversion strategy	122
Chapter 8. References		124

List of Abbreviations and Symbols.....	132
Appendix.....	135

List of Figures

Figure 1.1 Mechanism of the Baeyer-Villiger reaction (from Kamerbeek <i>et al.</i> , 2003).	26
Figure 1.2 Mechanism of CHMO-mediated oxidation (from Kamerbeek <i>et al.</i> , 2003).	30
Figure 1.3 CHMO-mediate bioconversion of bicyclo[3.2.0]hept-2-ene-6-one to its corresponding regioisomeric lactones, (-)-(1 <i>S</i> ,5 <i>R</i>)-2-oxabicyclo[3.3.0]oct-6-en-3-one and (-)-(1 <i>R</i> ,5 <i>S</i>)-3-oxabicyclo[3.3.0]oct-6-en-3-one.	31
Figure 1.4 Plasmid constructs that have led to the construction of pQR2349 (from Doig <i>et al.</i> , 2001).	32
Figure 1.5 Schematic showing internal and external modes of SFPR with direct and indirect cell contact (from Woodley <i>et al.</i> , 2008).	38
Figure 1.6 Schematic of dual resin SFPR concept	40
Figure 2.1 A schematic of the method of employing a filter bag for the separation of two types of resins used in the dual resin SFPR strategy	51
Figure 2.2 Recycle reactor with fixed bed of resins in an external loop.	55
Figure 3.1 Adsorption isotherms generated using resins (A) XAD7 and (B) IRC50 for the adsorption of (●) ketone and (○) lactone in experiments described in section 2.3.1.	61
Figure 3.2 Adsorption isotherms generated using resins (A) L493 and (B) XAD4 for the adsorption of (●) ketone and (○) lactone in experiments described in section 2.3.1	62

Figure 3.3 Adsorption isotherms generated using resins (A) XAD16 and (B) XAD1180 for the adsorption of (●) ketone and (○) lactone in experiments described in section 2.3.1 63

Figure 3.4 High speed camera images of (A) XAD7 (B) IRC50 (C) L493 (D) XAD4 (E) XAD16 (F) XAD1180 resins obtained under the following conditions: 800rpm, 3mm throw, 0.01g resin, 1ml volume..... 68

Figure 3.5 Suspension percentages of resins (●) XAD7 (○) IRC50 (▼) L493 (Δ) XAD4 (■) XAD16 and (□) XAD1180 in a well mimic from the 24 well microplate performed as described in section 2.3.3..... 70

Figure 3.6 High speed camera images of (A) XAD7 (B) IRC50 (C) L493 (D) XAD4 (E) XAD16 (F) XAD1180 resins obtained in a well mimic from a 24 wells microplate platform under the following conditions: 800rpm, 3mm throw, 0.15g resin, 1.5ml volume..... 71

Figure 3.7 Adsorption isotherms generated using XAD7 for the adsorption of (A) ketone (B) lactone in the (●) 96 wells and (○) 24 wells microplate platforms in experiments described in section 2.3.2.1 73

Figure 3.8 Adsorption isotherms generated using IRC50 for the adsorption of (A) ketone (B) lactone in the (●) 96 wells and (○) 24 wells microplate platforms in experiments described in section 2.3.2.1 74

Figure 3.9 Adsorption isotherms generated using L493 for the adsorption of (A) ketone (B) lactone in the (●) 96 wells and (○) 24 wells microplate platforms in experiments described in section 2.3.2.1 75

Figure 3.10 Adsorption isotherms generated using XAD4 for the adsorption of (A) ketone (B) lactone in the (●) 96 wells and (○) 24 wells microplate platforms in experiments described in section 2.3.2.1 76

Figure 3.11 Adsorption isotherms generated using XAD16 for the adsorption of (A) ketone (B) lactone in the (●) 96 wells and (○) 24 wells microplate platforms in experiments described in section 2.3.2.1	77
Figure 3.12 Adsorption isotherms generated using XAD1180 for the adsorption of (A) ketone (B) lactone in the (●) 96 wells and (○) 24 wells microplate platforms in experiments described in section 2.3.2.1	78
Figure 3.13 Time course of the dual compound adsorption of (●) ketone and (○) lactone on (A) XAD7 and (B) IRC50 in experiments described in section 2.3.2.2	83
Figure 3.14 Time course of the dual compound adsorption of (●) ketone and (○) lactone on (A) L493 and (B) XAD4 in experiments described in section 2.3.2.2	84
Figure 3.15 Time course of the dual compound adsorption of (●) ketone and (○) lactone on (A) XAD16 and (B) XAD1180 in experiments described in section 2.3.2.2.....	85
Figure 4.1 Production of lactone by <i>E. coli</i> TOP10 [pQR239] biocatalyst (8g _{DCW} /l) using initial ketone concentrations of (●) 0.4g/l and (○) 3g/l, without the use of a resin SFPR strategy as described in section 2.5.1.....	91
Figure 4.2 Single resin SFPR strategy, with use of L493 (8g/l) resin, for the production of lactone by <i>E. coli</i> TOP10 [pQR239] biocatalyst (8g _{DCW} /l) using an initial ketone concentration of 3g/l on the resin as described in section 2.5.2.....	93
Figure 4.3 Dual resin SFPR, with use of L493 (8g/l) and IRC50 (300g/l) as substrate and product reservoirs respectively, for the production of lactone by <i>E. coli</i> TOP10 [pQR239] biocatalyst (8g _{DCW} /l) using an initial ketone concentration of 3g/l, as described in section 2.5.3.1.....	95
Figure 4.4 Dual resin SFPR, with use of XAD7 (60g/l) and IRC50 (300g/l) as substrate and product reservoirs respectively, for the production of lactone by <i>E. coli</i> TOP10	

[pQR239] biocatalyst (8g _{DCW} /l) using an initial ketone concentration of 3g/l, as described in section 2.5.3.1	96
Figure 4.5 Dual resin SFPR, with use of L493 (8g/l) and IRC50 (300g/l) as substrate and product reservoirs respectively, for the production of lactone by <i>E. coli</i> TOP10 [pQR239] biocatalyst (8g _{DCW} /l) using an initial ketone concentration of 3g/l, as described in section 2.5.3.2.....	98
Figure 4.6 Dual resin SFPR, with use of XAD7 (60g/l) and IRC50 (300g/l) as substrate and product reservoirs respectively, for the production of lactone by <i>E. coli</i> TOP10 [pQR239] biocatalyst (8g _{DCW} /l) using an initial ketone concentration of 3g/l, as described in section 2.5.3.2.....	99
Figure 4.7 Calculated mass balances from all bioconversions performed without resins ('0.4g/l' and '3g/l'), with the single resin SFPR strategy ('L493 single SFPR') and with the dual resin SFPR strategy where both types of resins are free in suspension ('L493-IRC50 (free)' and 'XAD7-IRC50 (free)') and where they have been physically separated ('L493-IRC50 (filter bag)' and 'XAD7-IRC50 (filter bag)').....	103
Figure 5.1 Production of lactone by <i>E. coli</i> TOP10 [pQR239] biocatalyst (8g _{DCW} /l) using initial ketone concentrations of (●) 0.4g/l and (○) 3g/l, without the use of a resin SFPR strategy in a miniature STR as described in section 2.6.2	107
Figure 5.2 Single resin SFPR strategy, with use of L493 (8g/l) resin contained in a miniature STR, for the production of lactone by <i>E. coli</i> TOP10 [pQR239] biocatalyst (8g _{DCW} /l) using an initial ketone concentration of 3g/l on the resin. (●) ketone in aqueous phase, (○) lactone in aqueous phase, (■) ketone on L493 and (■) lactone on L493. Experiment performed as described in section 2.6.2	108
Figure 5.3 Dual resin SFPR, with use of L493 (8g/l) and IRC50 (300g/l) as substrate and product reservoirs respectively contained in a miniature STR, for the production of lactone by <i>E. coli</i> TOP10 [pQR239] biocatalyst (8g _{DCW} /l) using an initial ketone	

concentration of 3g/l. (●) ketone in aqueous phase, (○) lactone in aqueous phase, (■) ketone on resins and (■) lactone on resins. Experiment performed as described in section 2.6.3 109

Figure 5.4 Dual resin SFPR, with use of XAD7 (60g/l) and IRC50 (300g/l) as substrate and product reservoirs respectively contained in a miniature STR, for the production of lactone by *E. coli* TOP10 [pQR239] biocatalyst (8g_{DCW}/l) using an initial ketone concentration of 3g/l. (●) ketone in aqueous phase, (○) lactone in aqueous phase, (■) ketone on resins and (■) lactone on resins. Experiment performed as described in section 2.6.3 110

Figure 5.5 Single resin SFPR strategy, using a combination of a miniature STR and miniature column containing L493 (8g/l), for the production of lactone by *E. coli* TOP10 [pQR239] biocatalyst (8g_{DCW}/l) using an initial ketone concentration of 3g/l on the resin. (●) ketone in aqueous phase, (○) lactone in aqueous phase, (■) ketone on L493 and (■) lactone on L493. Experiment performed as described in section 2.7.4 112

Figure 5.6 Dual resin SFPR, with use of L493 (8g/l) (housed in a miniature column) and IRC50 (300g/l) (free in suspension inside a miniature STR) as substrate and product reservoirs respectively, for the production of lactone by *E. coli* TOP10 [pQR239] biocatalyst (8g_{DCW}/l) using an initial ketone concentration of 3g/l. (●) ketone in aqueous phase, (○) lactone in aqueous phase, (■) ketone on L493, (■) lactone on L493, (■) ketone on IRC50 and (■) lactone on IRC50. Experiment performed as described in section 2.7.5..... 113

Figure 7.1 Mass of resin Amberlite IRC50 dispensed by a wide bore tip as slurry from a 10g/l resin suspension mixed by a 3 blade marine impeller at 350rpm..... 122

Figure A.1 Calibration curves for ketone (●) and lactone (○) in ethyl acetate. Samples were prepared as described in section 2.2.1.1 and analysed as described in section 2.2.1.2..... 135

Figure A.2 Calibration of OD _{600nm} measurements from an <i>E. coli</i> TOP10 [pQR239] fermentation with DCW measurements determined as described in section 2.2.2	136
Figure A.3 Adsorption isotherms generated using XAD7 for the adsorption of (A) ketone (B) lactone in the 96 wells and 24 wells microplate platforms in experiments described in section 2.3.2.1	137
Figure A.4 Adsorption isotherms generated using IRC50 for the adsorption of (A) ketone (B) lactone in the 96 wells and 24 wells microplate platforms in experiments described in section 2.3.2.1	138
Figure A.5 Adsorption isotherms generated using L493 for the adsorption of (A) ketone (B) lactone in the 96 wells and 24 wells microplate platforms in experiments described in section 2.3.2.1	139
Figure A.6 Adsorption isotherms generated using XAD4 for the adsorption of (A) ketone (B) lactone in the 96 wells and 24 wells microplate platforms in experiments described in section 2.3.2.1	140
Figure A.7 Adsorption isotherms generated using XAD16 for the adsorption of (A) ketone (B) lactone in the 96 wells and 24 wells microplate platforms in experiments described in section 2.3.2.1	141
Figure A.8 Adsorption isotherms generated using XAD1180 for the adsorption of (A) ketone (B) lactone in the 96 wells and 24 wells microplate platforms in experiments described in section 2.3.2.1	142
Figure A.9 Production of lactone by <i>E. coli</i> TOP10 [pQR239] biocatalyst (8g _{DCW} /l) using initial ketone concentration of 0.4g/l in (●) 50mM phosphate buffer (working volume 10%) and (○) fermentation media (working volume 20%), without the use of a resin SFPR strategy as described in section 2.5.1	143

Figure A.10 Characterisation of the peristaltic Pump P-1 (Pharmacia Biotech, Sweden) by passing 50mM phosphate buffer through the Tricorn 5/50 column (GE Healthcare, Buckinghamshire, UK) packed with 1.2g of resin Optipore L493.....	144
Figure A.11 Flow rate of 8g _{DCW} /l of cells resuspended in 50mM phosphate buffer passed through the Tricorn 5/50 column (GE Healthcare, Buckinghamshire, UK) packed with 1.2g of resin Optipore L493 using the the peristaltic Pump P-1 (Pharmacia Biotech, Sweden) at a flow rate of 6.4ml/min.....	145
FigureA.12 Mechanical drawing of a cross section of the miniature stirred tank reactor (taken from Gill <i>et al</i> 2008).....	146
Figure A.13 Calculated mass balances from all bioconversions performed in the miniature STR without resins ('0.4g/l' and '3g/l'), with the single resin SFPR strategy in the conventional reactor ('L493 (conventional reactor)') and recycle reactor ('L493 (recycle reactor)') configurations and with the dual resin SFPR strategy in the conventional reactor ('L493-IRC50 (conventional reactor)' and 'XAD7-IRC50 (conventional reactor)') and recycle reactor ('L493-IRC50 (recycle reactor)') configurations.....	147

List of Tables

Table 1.1 Different technological approaches and measures used by fine chemical, pharmaceutical and other related industries towards sustainability (Watson, 2012)	23
Table 1.2 Examples of recently developed industrial applications of biocatalysis (Bornscheuer <i>et al.</i> , 2012; Aldridge, 2013).....	24
Table 1.3 Selected BVMOs and their characteristics (Willems, 1997; Kamerbeek <i>et al.</i> , 2003).....	28
Table 1.4 Common <i>in situ</i> substrate supply and product removal techniques (Schmid <i>et al.</i> , 2001).	35
Table 2.1 Water content in six resins screened	42
Table 2.2 Dimensions of 96 wells and 24 wells microplate	46
Table 3.1 Resin properties and derived parameters of Langmuir and Freundlich adsorption models. All resin particles range from 1-2mm in diameter and are polyaromatics except for XAD7 which is an acrylic ester.....	65
Table 3.2 Adsorption capacity of six resins at a ketone equilibrium concentration of 0.5g/l.	67
Table 3.3 Comparison of Langmuir parameters for adsorption on ketone and lactone at the three different scales	80
Table 3.4 Comparison of adsorption capacities of six resins at three different scales, at a ketone equilibrium concentration of 0.5g/l.....	81

Table 3.5 Selectivity for ketone and lactone, as determined by equation 4, for each of the six resins	86
Table 4.1 Comparison of performance of three different strategies to undertake Baeyer Villiger bioconversion. Results based on data after 2.5 hours of bioconversion.	102
Table 5.1 Comparison of performance of three different strategies to undertake Baeyer Villiger bioconversion using two different reactor configurations- recycle reactor and conventional STR.	115

Chapter 1. Introduction

1.1 Prospect of biocatalysis

A need for more sustainable technologies in the chemical industry has brought biocatalysts in the spot-light for application in ‘green chemistry’ (Fahrenkamp-Uppenbrink, 2002). This is demonstrated by an increasing trend for use of enzymatic based bioconversions for the production of fine and bulk chemicals (Straathof *et al.*, 2002). Particularly, more sustainable methods are actively sought for drug synthesis. Initiatives such as the CHEM21 project (<http://www.imi.europa.eu/content/chem21>) has so far received a total of €26.4 million at the half stage of the 2 year project (start date 01/10/2012), to look into using more common metals instead of rarer and expensive precious metals, enzymes, methods to use less solvents and synthetic biology to make the drug development process more environmentally friendly. The importance of this area is demonstrated by the European participants of the CHEM21 which include multinational corporations (e.g. GSK Research and Development Ltd, Sanofi Chimie and Pfizer Ltd) from the European Federation of Pharmaceutical Industries and Associations (EFPIA), Universities (e.g. University of Manchester, Technische Universität Graz and Universität Stuttgart) and also SMEs.

Table 1.1 Different technological approaches and measures used by fine chemical, pharmaceutical and other related industries towards sustainability (Watson, 2012)

Solvents	Using water and ionic liquids as alternative solvents to more toxic and harsh DCM, chloroform and dipolar aprotic solvents
Microwave heating	Traditionally adopted in medicinal chemistry, microwave heating is making its way into process research and development as a result of scale-up investigations
Flow chemistry	Generally used by non-pharma industry because of operation at larger scales and established procedures for handling hazardous reagents
Avoiding certain reagents/reactions	Companies have started to avoid using certain toxic reagents and reactions for safety reasons when there is a suitable alternative. Examples include HCN, LiAlH ₄ and nitrations and Wittig reactions

There is also a demand for effective medicines, i.e. those with few or no side effects and high specificity, which means that there will be a need to produce more structurally complex molecules (Lye and Woodley, 1999), which can also be fulfilled by biocatalysis. Around 200 processes alone are already implemented in the pharmaceutical industry (Woodley *et al.*, 2013), with 45% of big pharmaceutical companies having dedicated biotransformations group (Watson, 2011). Despite the challenges (see Table 1.1 above), such a vast application of biocatalysts in the pharmaceutical industry (see Table 1.2 below) is seen as a result of the latest wave of technological research and innovations, with the pioneering research in molecular biology in the late 1990s being the catalyst (Bornscheuer *et al.*, 2012).

Table 1.2 Examples of recently developed industrial applications of biocatalysis (Bornscheuer *et al.*, 2012; Aldridge, 2013).

Product (Trade name)	Company
Atorvastatin (Lipitor)	Pfizer
Sitagliptin (Januvia)	Merck
Reboxetine (Edronax)	Pfizer
Simvastatin	Codexis

The use of biocatalytic processes as an alternative or as a supplementary tool to conventional chemical methods, not only in the sectors mentioned above but also in the agrochemicals and food industries, is getting greater attention as the discovery, characterisation and application potentials of a range of enzymes expand (Rich *et al.*, 2002).

Bioconversions can be performed using either whole-cell or isolated enzymes, application of which will be limited by commercial availability, cost (including of the process), stability and requirements of reaction, for example the need for regeneration of cofactors (Wohlgemuth, 2007).

The attractiveness of enzymatically driven chemical processes as opposed to conventional chemistry include their ability of high stereo-, regio-, chemo- and enantio-selectivity, to avoid the use of harsh/toxic solvents and the potential of producing complex, optically pure molecules in fewer steps as protection and deprotection steps are avoided (Bull *et al.*, 1999; Lye *et al.*, 2003; Pollard and Woodley, 2007). As a result, the use of biocatalysts for industrial scale asymmetric synthesis, rather than racemic resolutions, is becoming more common (Lye and Woodley, 1999; Blaser and Schmidt, 2004).

In spite of the potential and attractiveness of enzyme mediated processes, their widespread industrial application remains elusive (Straathof *et al.*, 2002). Several reasons can account for this, for example, (1) biocatalytic processes are hindered by operation at high substrate and/or product concentrations, (2) biocatalyst longevity, i.e. activity of the biocatalyst decreases over time and (3) reaction requirements e.g. cofactors.

1.2 The Baeyer-Villiger oxidation

1.2.1 Reaction and mechanism

The chemical conversion of ketones into esters or cyclic ketones into lactones, otherwise known as the Baeyer-Villiger (BV) reaction, named after its discoverers, has been known for more than a century (Baeyer and Villiger, 1899).

The mechanism is accepted as being a two-step oxidation with the formation of an unstable 'Criegee intermediate' after the nucleophilic attack on the ketone by a peracid (Figure 1.1) (Criegee, 1948).

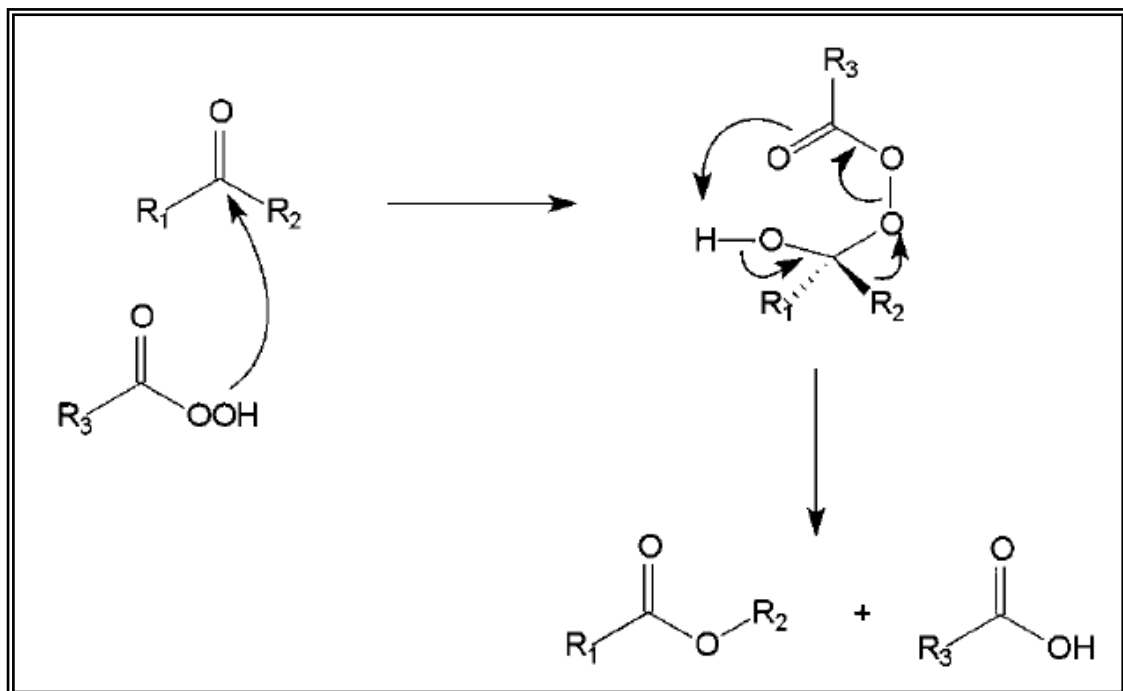


Figure 1.1 Mechanism of the Baeyer-Villiger reaction (from Kamerbeek *et al.*, 2003).

1.2.2 Chemical methods

The BV oxidation is commonly achieved by use of peracid reagents, such as hydrogen peroxide (H_2O_2), *m*-chloroperbenzoic acid (*m*-CPBA), peroxybenzoic acid and trifluoroperacetic acid ($\text{CF}_3\text{CO}_3\text{H}$) (Renz and Meunier, 1999; ten Brink *et al.*, 2004), in stoichiometric quantities (Baldwin *et al.*, 2008) which become very hazardous and often unstable at industrial level. Another disadvantage of chemical syntheses is that they proceed with poor enantioselectivities and enantiomeric excesses (ee) (Baldwin and Woodley, 2006).

Limited success has been achieved by use of metal-based catalysts (Strukul, 1998; Watanabe *et al.*, 2002; ten Brink *et al.*, 2004) and metal-free, biomimetic compounds (Murahashi *et al.*, 2002) to carry out asymmetric BV reactions. Therefore, for application of BV oxidation at industrial scale, oxygen should become the first choice of oxidant instead of unstable, toxic and unsustainable peracids mentioned above.

1.2.3 Biological methods

Many researchers (including Mihovilovic, 2006; ten Brink *et al.*, 2004; Kamerbeek *et al.*, 2003) have recognised enzyme-based, asymmetric BV oxidation as a valuable and efficient method, compared to conventional chemical syntheses, to acquire enantiopure products (e.g. optically active lactones have been efficiently transformed from racemic or prochiral ketones), thus justifying the importance of BV biooxidations in synthetic chemistry.

The most common class of enzyme known to catalyse the BV biooxidation are BV monooxygenase (BVMO) and over twenty BVMOs have been identified (Willems, 1997). Characterised BVMOs thus far are co-factor dependent flavoproteins and incorporate an atom of molecular oxygen into the substrate (Kamerbeek *et al.*, 2003), reaction of which proceeds similarly to that of conventional BV oxidation using peracids.

BVMOs can be categorised into two types: Type I are NADPH- and FAD-dependent and Type II enzymes are NADH- and FMN-dependent (Willems, 1997). They have been discovered in several organisms, both bacteria and fungi (Table 1.3), catalysing the nucleophilic and electrophilic oxygenation of a range of substrates.

Table 1.3 Selected BVMOs and their characteristics (Willems, 1997; Kamerbeek *et al.*, 2003).

Enzyme <i>Microorganism</i>	Molecular mass (kDa)	Cofactor	Coenzyme
Cyclohexanone monooxygenase <i>Acinetobacter calcoaceticus</i> (NCIMB 9871)	59	NADPH	FAD
Cyclohexanone monooxygenase <i>Nocardia globerula</i> CL1	53	NADPH	FAD
Cyclopentanone monooxygenase <i>Comamonas</i> sp. NCIMB 9872	200	NADPH	FAD
Cyclododecanone monooxygenase <i>Rhodococcus ruber</i>	67.5	NADPH	FAD
Tridecan-2-one monooxygenase <i>Pseudomonas cepacia</i>	123	NADPH	FAD
Oxocineole monooxygenase <i>Pseudomonas flava</i> UQM 1742	70	NADH	FMN
Diketocamphane monooxygenase <i>Pseudomonas putida</i> NCIMB 10007	78	NADH	FMN

1.3 Baeyer-Villiger oxidation using Cyclohexanone Monooxygenase

1.3.1 Cyclohexanone Monooxygenase from *Acinetobacter calcoaceticus* (NCIMB 9871)

Cyclohexanone monooxygenase (CHMO – EC 1.14.13.22) from *Acinetobacter calcoaceticus* (NCIMB 9871) is one of the best characterised BVMOs. It is an FAD-/NADPH-dependent monomeric protein with a molecular mass of 59kDa and was first purified from *Acinetobacter* and *Nocardia* species (Donoghue *et al.*, 1976).

In its wild-type host *Acinetobacter*, CHMO catalyses the oxidation of cyclohexanone to ϵ -caprolactone via the BV mechanism, one of a sequence of catabolic steps of cyclohexanol to produce diacid precursors of acetyl-CoA (Secundo *et al.*, 2005). As well as ketones and aldehydes, this enzyme is also capable of selective heteroatom electrophilic oxygenation, including that of sulphur, phosphorous, selenium and nitrogen (Willets *et al.*, 1997; Zambianchi *et al.*, 2002; ten Brink *et al.*, 2004).

The catalytic mechanism of CHMO has been studied by Ryerson *et al.* (1982) and Sheng *et al.* (2001) and proceeds as follows (Kamerbeek *et al.*, 2003) (figure 1.2):

- A reduced enzyme-NADP⁺ complex is formed from the reduction of the protein-bound FAD by NADPH.
- This complex goes on to form a flavin-peroxide as a result of the reaction between the enzyme-NADP⁺ complex and oxygen.
- This initiates the nucleophilic attack by the flavin-peroxide species on the carbonyl group of a ketone substrate.
- Formation of a flavin-hydroxide occurs whilst the Criegee intermediate rearranges to the corresponding product.
- The catalytic cycle is completed with the elimination of water from flavin-hydroxide, regenerating oxidised FAD and releasing NADP⁺.

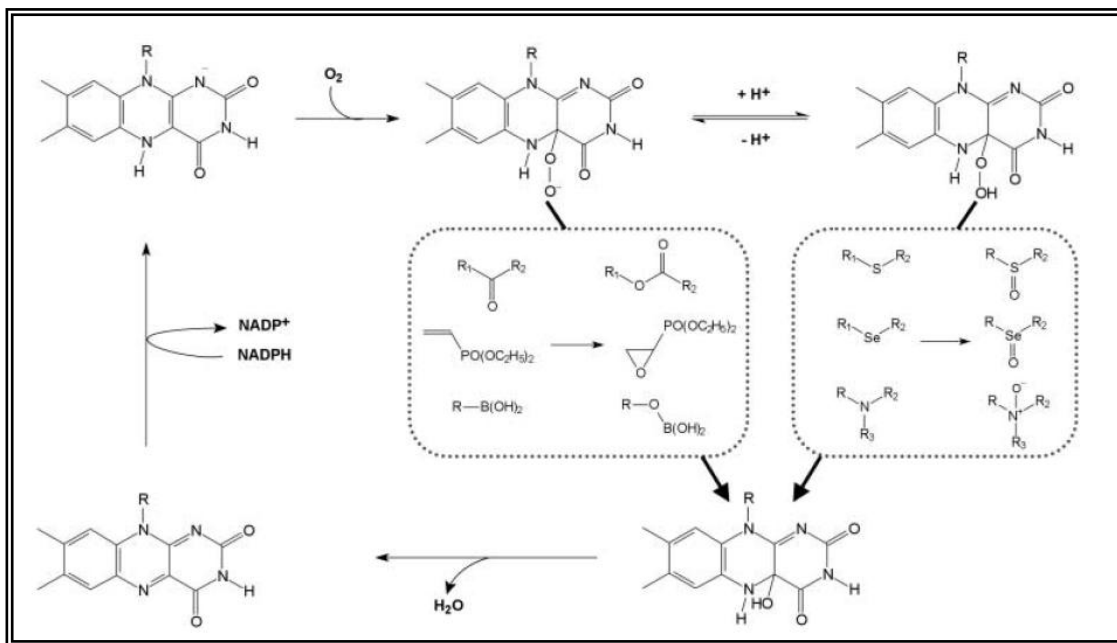


Figure 1.2 Mechanism of CHMO-mediated oxidation (from Kamerbeek *et al.*, 2003).

High regio- and enantio-selectivity has been exhibited by CHMO in a natural variant of *Acinetobacter*, TD63 (Alphand *et al.*, 1989). The ketone, bicyclo[3.2.0]hept-2-ene-6-one was oxidised, producing two region-isomeric lactones: (-)-(1*S*,5*R*)-2-oxabicyclo[3.3.0]oct-6-en-3-one and (-)-(1*R*,5*S*)-3-oxabicyclo[3.3.0]oct-6-en-3-one (an unexpected formation and unattainable using conventional chemical methods (Strukul, 1998)) in a 1:1 ratio and enantiomerically pure (figure 1.3). This work opened the door to research of similar substrates which increased the potential of synthetic applications.

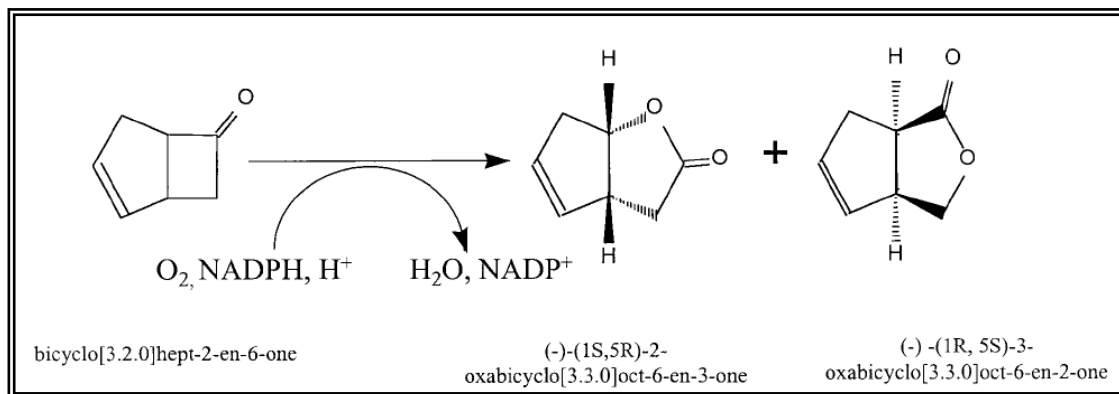


Figure 1.3 CHMO-mediate bioconversion of bicyclo[3.2.0]hept-2-ene-6-one to its corresponding regioisomeric lactones, (-)-(1*S*,5*R*)-2-oxabicyclo[3.3.0]oct-6-en-3-one and (-)-(1*R*,5*S*)-3-oxabicyclo[3.3.0]oct-6-en-3-one.

However, use of CHMO at industrial scale in its wild-type form is restricted due to (1) *Acinetobacter*'s pathogenic classification (class 2); (2) the existence of a lactone hydrolase (which means an occurrence of undesired side reactions); (3) low enzyme productivity, and (4) the need for stoichiometric quantities of cofactor NADPH, which makes the use of isolated CHMO undesirable as it necessitates an additional cofactor recycling system (Willems, 1997; Doig *et al.*, 2001; Zambianchi *et al.*, 2002).

Preference is for use of recombinant whole-cell biocatalysts expressing (and overexpressing) CHMO as they won't exhibit any unwanted enzyme activity and effectively regenerate and supply cofactors for conversions. As a result, CHMO has been cloned and overexpressed into yeast (Stewart *et al.*, 1996; Stewart *et al.*, 1998) and *E. coli* (Chen *et al.*, 1999; Mihovilovic *et al.*, 2001) and have shown to be resourceful, performing effective Baeyer-Villiger biooxidations on a range of substrates.

1.3.2 Overexpression of Cyclohexanone Monooxygenase in *E. coli* TOP10 [pQR239]

CHMO has been overexpressed in the *E. coli* strain TOP10 [pQR239], which requires the cheap L-arabinose as an inducer, to increase enzyme yield by a factor of 25 (Doig *et al.*, 2001). To construct the pQR239 strain, the *CHMO* gene was cloned from *A. calcoaceticus* (NCIMB 9871) into a pBAD vector and expression put under the control of the *araBAD* promoter (figure 1.4).

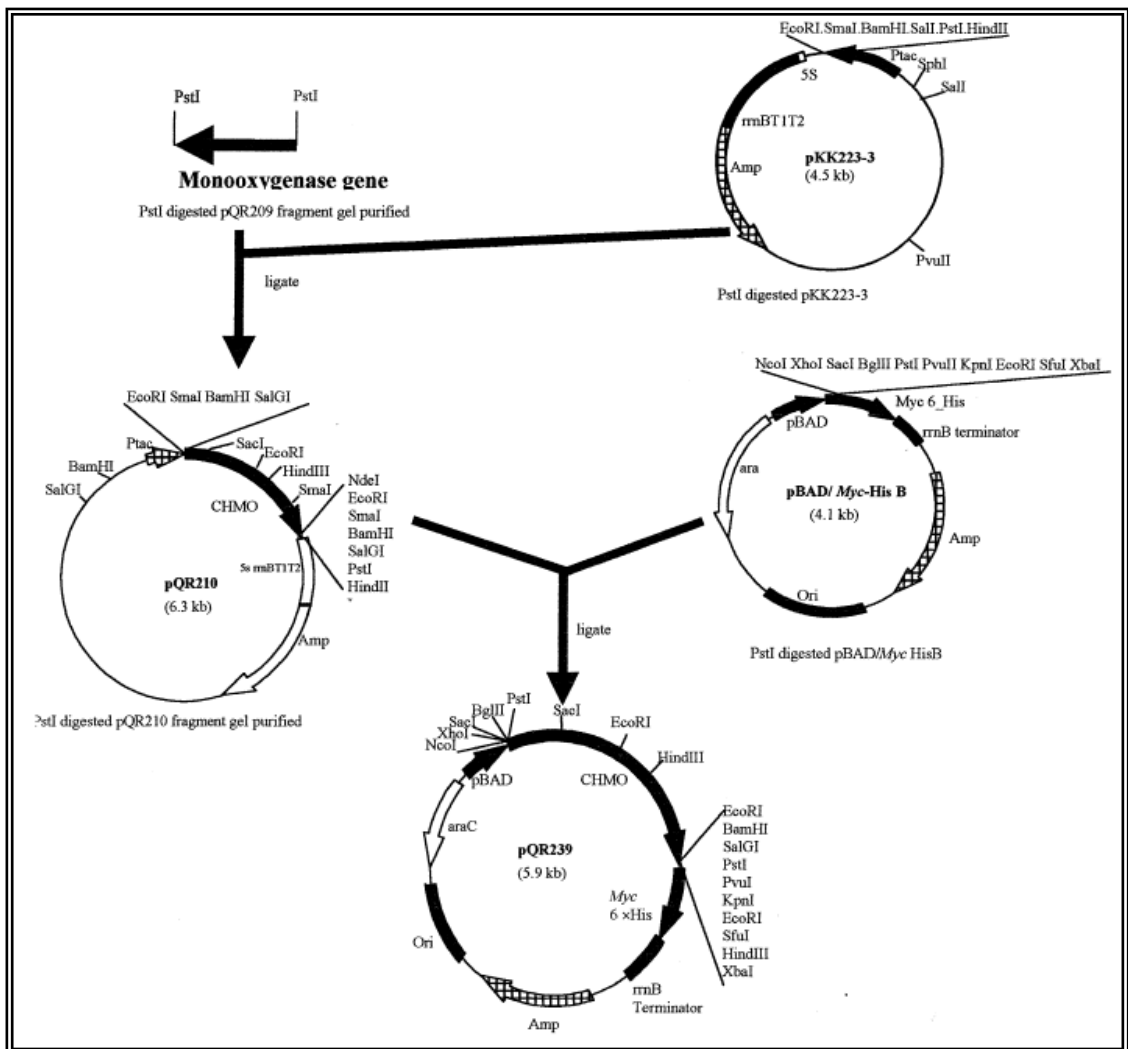


Figure 1.4 Plasmid constructs that have led to the construction of pQR2349 (from Doig *et al.*, 2001).

Expression of heterologous CHMO of 500-600 U/g_{dcw} on cyclohexanone had been observed in batch fermentations, with fast growth of *E. coli* TOP10 [pQR239] to 10 g_{DCW}l⁻¹ (Doig *et al.*, 2001). Further advantages of this expression system for large scale BV reactions are the *in vivo* cofactor recycling system and no unwanted enzyme activity. Also, comparative studies by Secundo *et al.* (2005) showed the recombinant and wild-type CHMOs to be practically identical, for example, in molecular mass and K_m values, except in their pH- and thermo-stability, which was attributed to protease contamination.

Very little in the way of preparative scale biocatalyst BV oxidation can be found. Doig *et al.* (2002) performed a fed-batch, 55 l scale, fermentation process using the aforementioned recombinant *E. coli*, but with increasing product concentration in the broth, productivity decreased as a result of an effect of product inhibition on biocatalytic activity.

Further work by the same group (Doig *et al.*, 2003) discovered limitations in rates of mass transfer of substrate (bicyclo[3.2.0]hept-2-ene-6-one) across the cell barrier and substrate and product inhibition. The optimum substrate concentration was found to be between 0.2-0.4 g l⁻¹ and of the corresponding products, specific activity of the whole cells dropped to zero at lactone concentrations above 4.5-5 g l⁻¹. This study (Doig *et al.*, 2003) produced the combined regioisomeric lactones at a level of 3.5 g l⁻¹, in a 45:55 ratio ((-)-(1*S*,5*R*)-2-oxabicyclo[3.3.0]oct-6-en-3-one to (-)-(1*R*,5*S*)-3-oxabicyclo[3.3.0]oct-6-en-3-one). Additionally, they exhibited optical purity of 94% and 99% ee, respectively.

Recently, Baldwin *et al.* (2008) achieved a 4.5 g l⁻¹ production of the aforementioned lactones at a 200 l scale by controlling the substrate concentration in solution. This whole-cell BV oxidation is the first at this scale without the use of an auxiliary phase.

As a result of limited large scale examples, it is important that an efficient and applicable preparative scale process needs to be developed to overcome the limitations and access the vast number of optically pure compounds produced from bioconversions (Alphand *et al.*, 2003).

1.3.3 BVMO as the model bioconversion system

The BVMO class of enzymes has got industrial applications in areas such as antibiotic synthesis and demonstrated high regio- and enantio-selectivity but their great potential still has to be unlocked. The challenges of inhibition, cell toxicity and substrate solubility seen with BVMO bioconversions are factors that make it ideal to be used as the model system to evaluate a new dual resin substrate feeding and product removal strategy.

1.4 *in situ* Substrate Feeding and Product Removal (SFPR)

1.4.1 General

As seen with whole cell CHMO-mediated BV oxidation (section 1.3.2), biocatalytic processes can be hindered by operation at high substrate and/or product concentrations. This can be due to their inhibitory effect on the enzyme, toxicity effect on the whole cell or low substrate solubility or a combination of these factors. Poor water-solubility of substrate and product can also result in low activity. Therefore, it has become clear that for an effective downstream operation and overall process economics there will be a need for a strategy that maintains the substrate and product at sub-inhibitory levels (Chen *et al.*, 2002).

A variety of *in situ* substrate supply and product removal approaches to solve this problem has been proposed (Table 1.4). The main objectives for employing such techniques are to (1) increase product concentration for easier downstream processing; (2) increase yield on biocatalyst, hence reducing biocatalyst cost; (3) increase yield on substrate, hence reducing substrate costs; and (4) increase volumetric productivity, which reduces reactor volume and processing time (Lye and Woodley, 1999).

Table 1.4 Common *in situ* substrate supply and product removal techniques (Schmid *et al.*, 2001).

Strategy	Description
Conservative liquid feed	Substrate fed into the reactor at limiting rates to prevent accumulation.
Liquid-liquid phase	An apolar solvent acts as a substrate reservoir and product sink, whilst the cells remain in the aqueous phase.
Gas-liquid phase	Substrate is fed in the gaseous phase and absorbed into the aqueous phase where the biocatalyst remains.
Solid-liquid phase	Works by a similar technique to the liquid-liquid phase.

1.4.2 Resin based SFPR

The use of macroporous resins for *in situ* product removal (ISPR) as to resolve the problem of product toxicity/inhibition has been applied in bioprocessing (Lye and Woodley, 1999; Stark and von Stockar, 2003) and works by extraction of product into the solid phase.

A solid-liquid phase strategy based on the use of an adsorbent polymeric resin has also been employed for concomitant substrate supply and product removal. The principle method is that the resin adsorbs the substrate before its introduction into the reaction mixture. Then mass transfer of the substrate from the resin to the reaction mixture occurs according to the adsorption/desorption equilibrium. Enzymatic conversion will yield the product which is adsorbed onto the resin, preventing its accumulation around the biocatalyst.

This strategy of *in situ* substrate feed product removal (SFPR) has been effectively applied to ketone reduction (Vicenzi *et al.*, 1997; D'Arrigo *et al.*, 1998; Conceicao *et al.*,

2003), sulfoxidation (Zambianchi *et al.*, 2004) and BV oxidation (Hilker *et al.*, 2004a; Rudroff *et al.*, 2006).

Whereas preparative scale BV biooxidation by conservative substrate feeding is a rarity (section 1.3.2) and only confined to the analytical scale, kilogram scale bioconversions of bicyclo[3.2.0]hept-2-ene-6-one to its corresponding regioisomeric lactones, by the recombinant *E. coli* TOP10 [pQR239] strain, have been demonstrated using the resin-based SFPR strategy (Hilker *et al.*, 2004a; Hilker *et al.*, 2004b; Rudroff *et al.*, 2006; Simpson *et al.*, 2001; Hilker *et al.*, 2005).

The induction of the resin allowed substrate concentrations of up to 20 g^l⁻¹ to be used while maintaining substrate and product concentrations in the reaction mixture at subinhibitory levels (Simpson *et al.*, 2001).

1.4.3 High throughput resin screening (HTRS)

The simpler and conservative route of feeding the substrate in concentrated form is more attractive for rapid scale up than use of a resin to supply the reactant because of the need to screen and select the appropriate resin and evaluate its recycle (Baldwin *et al.*, 2008). Therefore an efficient high throughput resin screening (HTRS) methodology needs to be designed and implemented in SFPR experiments.

High throughput processing in the initial phase of development of a biocatalytic process allows use of small quantities of biocatalysts, substrates, products, resins and other raw materials and enables data to be collected from several, rapid experiments in parallel.

Key data that a complete HTRS should be able to derive are reaction yield, biocatalyst activity and ee, all of which should be a function of substrate/resin ratio. Also, physical properties of the resin should be obtained, calculation of maximum substrate loading per unit of resin and substrate/product solubility in aqueous reaction bulk at various resin concentrations (Kim *et al.*, 2007).

High through experimentation has benefited greatly by microwell plate technology which has established itself as an analytical tool mainly in enzyme and gene assay screenings (Persidis, 1998). However, great strides have been made to apply the microwell plate technology to upstream processing as well as other downstream processing operations such as in areas of cell culture, microbial (Duetz *et al* 2000) and mammalian (Girard *et al* 2001), biotransformation studies (Stahl *et al* 2000) and filtration (Jackson *et al* 2006).

1.4.4 Choice of reactor for resin based systems

The choice and configuration of the bioreactor is important for the success of a resin based SFPR bioconversion. Also investigations have to be carried out determine whether there should be direct or indirect contact between the resins and cell broth (figure 1.5).

Hilker *et al* (2004a) tested a “two-in-one” SFPR system in a stirred tank reactor (STR), using direct, internal or external modes, and also in a bubble column, with direct and internal mode. Bioconversion of bicyclo[3.2.0]hept-2-ene-6-one, by the recombinant *E. coli* TOP10 [pQR239] strain, was carried out at the 1L scale. The bubble column configuration gave the best results which suggested that good aeration was one of the key factors.

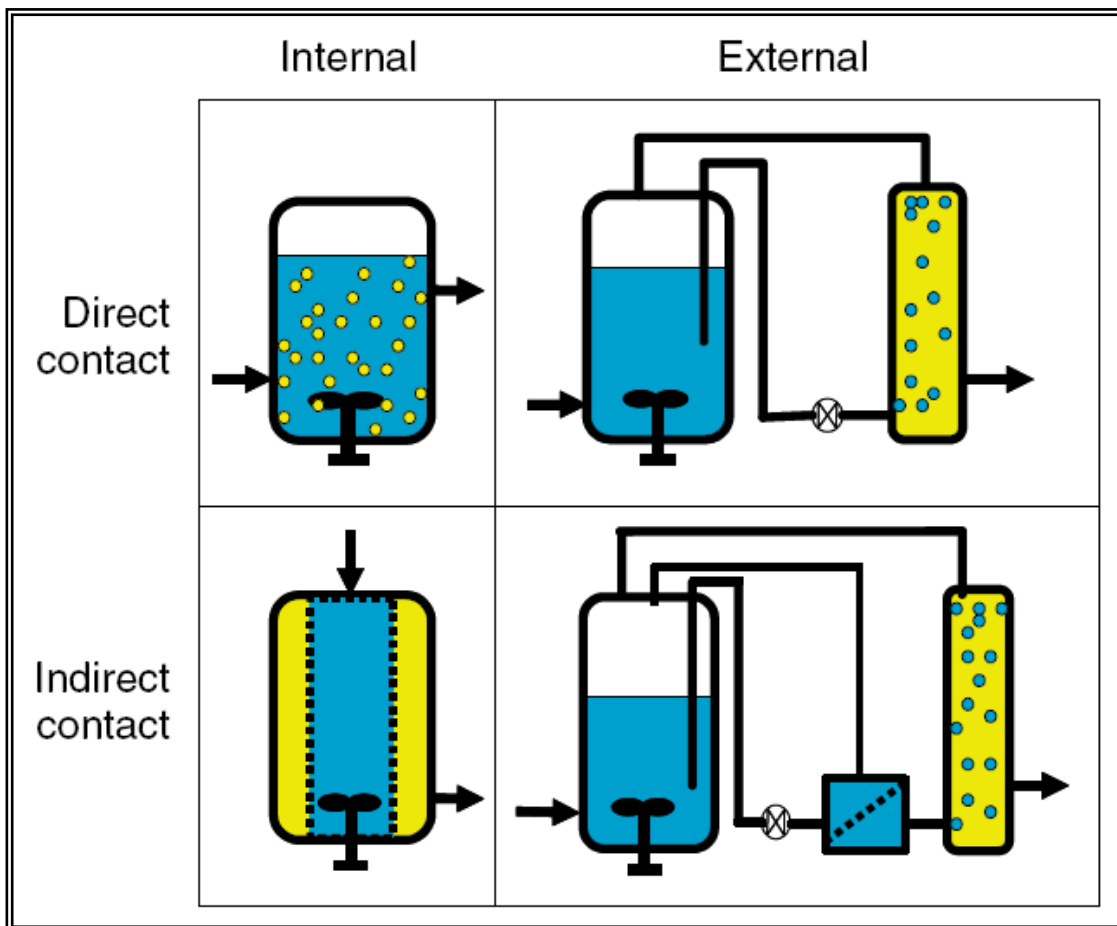


Figure 1.5 Schematic showing internal and external modes of SFPR with direct and indirect cell contact (from Woodley *et al.*, 2008).

1.5 Thesis Aims

This project aims to address the limitations of biocatalytic processes, specifically the inability of efficient operation at high substrate and product concentrations and strategies available to overcome this problem.

The examples of resin-based substrate supply and product removal mentioned in section 1.4.2 are all “two-in-one” resin-based methodologies, i.e. a single type of resin acts as the substrate reservoir and product sink. The work presented in this thesis proposes a new concept that uses a “dual resin” strategy. The principle method of deliverance of substrate to and removal of product from the broth is identical to that in “two-in-one” resin-based strategies, except that two different types of resins are used.

One type of resin is preloaded with the substrate and then added to the reaction system together with a second type of resin. This second type of resin does not have the substrate or another compound adsorbed, it acts as the sink for the product of the bioconversion (figure 1.6). The aim behind employing two resins instead of one is to exploit the differences in capacity, affinity and general compatibility of resins to different compounds.

The work presented in this thesis aims to demonstrate this novel dual resin based substrate feed- product removal (SFPR) concept to overcome both substrate and product inhibition that is exhibited in the oxidative Baeyer-Villiger bioconversion, using the recombinant whole cell biocatalyst *Escherichia coli* TOP10 [pQR239] expressing cyclohexanone monooxygenase.

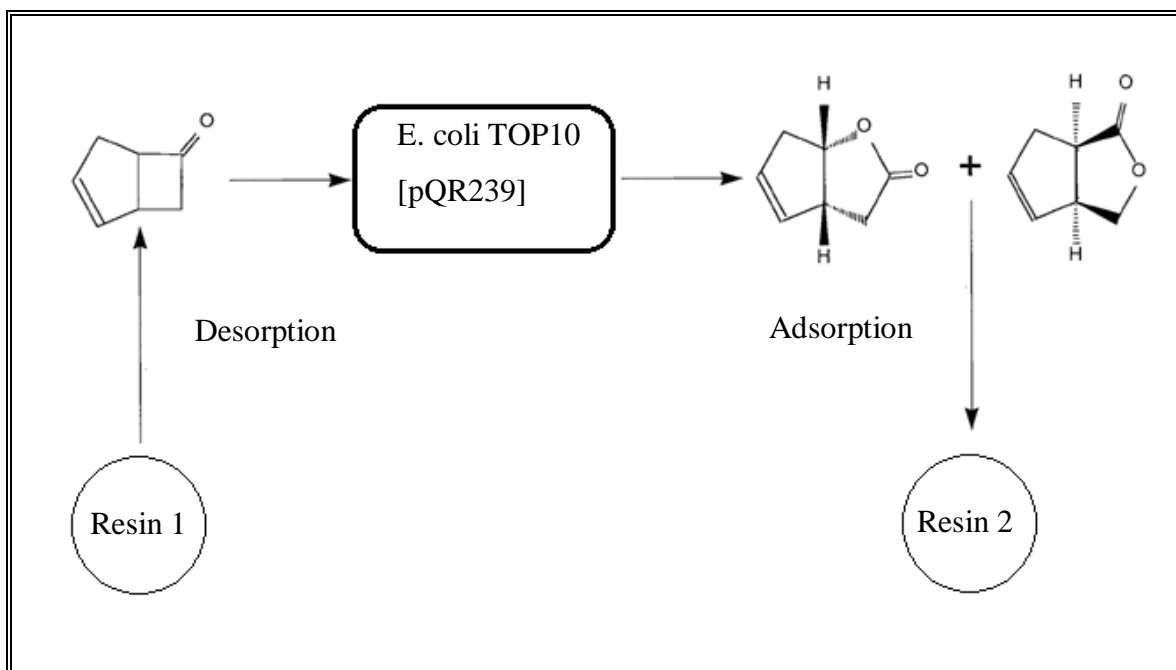


Figure 1.6 Schematic of dual resin SFPR concept

Chapter 3 aims to identify the best combination of resins to be used in the dual resin SFPR strategy by systematically evaluating different resin combinations to generate adsorption isotherms for substrate and product. This chapter further aims to develop a high throughput resin screening method that will assist in rapid determination of adsorption kinetics.

Chapter 4 aims to demonstrate a ‘proof of concept’ of the novel dual resin SFPR strategy by implementing the strategy at the bench scale in shake flasks by using data from the previous chapter that determined the best combination of resin to be employed in this strategy.

Chapter 5 aims demonstrate a ‘proof of concept’ of the novel dual resin SFPR strategy by implementing the strategy in a miniature stirred tank bioreactor. This investigation will be performed using two reactor configurations and will highlight limitations for further development, optimisation and scale up studies.

Chapter 2. Materials and Methods

2.1 Materials

2.1.1 Chemicals

Yeast extract, sodium chloride, ampicillin sodium salt, peptone, L(+)-arabinose, monosodium phosphate (monohydrate), disodium phosphate (heptahydrate), (±)-cis-bicyclo[3.2.0]hept-2-en-6-one and (1R,5S)-3-oxabicyclo[3.3.0]oct-6-en-2-one were all obtained from Sigma-Aldrich, Agar Technical (Agar No. 3) was obtained from Oxoid and Glycerol and Ethyl acetate were obtained from Alfa Aesar.

2.1.1.1 Preparation of ketone and lactone solutions in buffer

Bicyclo[3.2.0]hept-2-en-6-one and (1R,5S)-2-oxabicyclo[3.3.0]oct-6-en-3-one solutions were prepared by dissolving them at the required concentration in 50mM phosphate (monobasic, dibasic sodium phosphate) buffer at pH 7 (solubility: ketone 15.5g/l ±2.7%; lactone 54.1g/l ±0.9%) to be used for resin screening and bioconversions.

2.1.1.2 Fermentation media composition

Fermentation media for the growth of *E. coli* TOP10 [pQR239] composed of 10g/l of yeast extract, sodium chloride, peptone and glycerol (sterilised by autoclaving at a temperature of 121°C for 20 minutes) and 50mg/l ampicillin sodium salt (added after sterilisation through a 0.2µm Minisart[®], non-pyrogenic, sterile, single use filter unit).

2.1.2 Resins

Dowex[®] Optipore L493, Amberlite[®] XAD7, Amberlite[®] IRC50 (Sigma-Aldrich), Amberlite[®] XAD4, Amberlite[®] XAD1180, Amberlite[®] XAD16 (Alfa Aesar) were all ready to use from packaging, without any pre-treatment required.

2.1.2.1 Resin water content

Each resin was analysed for its water content by placing resins in a 100°C oven and left to dry overnight and/or until they achieved a constant weight. They were then weighed and their water content was calculated (table 2.1).

Table 2.1 Water content in six resins screened

Resin	XAD7	IRC50	L493	XAD4	XAD16	XAD1180
Water content (%)	67.6	51.4	62.7	56.5	67.9	69.2

2.1.3 Microorganism

Escherichia coli TOP10 [pQR239] was used throughout. This strain was constructed according to Doig et al (2001) as described in section 1.3.2 in Chapter 1 and stock culture were readily available in-house.

2.1.3.1 *E. coli* TOP10 [pQR239] seed stock preparation

Stock culture of the microorganism was prepared from an individual colony grown overnight at 37 °C on an agar plate containing growth medium (composed of 10g/l of yeast extract, sodium chloride, peptone and glycerol and 50mg/l ampicillin sodium salt). This was inoculated into a sterile 1 l shake flask containing 100 ml of the growth medium and grown overnight at 37°C and 200rpm. The culture was then added to 30 % v/v of sterile glycerol solution (final 15 % v/v of glycerol), mixed in aseptically and 1 ml aliquots were stored at -80°C.

2.2 Analytical methods

2.2.1 Ketone and lactone quantification by gas chromatography (GC)

2.2.1.1 Sample preparation

Samples were prepared by adding equal volume of ethyl acetate to the aqueous sample. The mixture was then vortex mixed for 30 seconds (determined to be sufficient) in a 1.5 ml Eppendorf tube, thereafter centrifuged at 13000 rpm for 2 minutes (Biofuge 13, Heraeus Sepatech, UK) The top solvent layer was transferred into a glass GC vial, diluted appropriately with ethyl acetate, which included 1g/l naphthalene as an internal standard, and analysed by GC.

2.2.1.2 Gas Chromatography Operation and Quantification

A Perkin-Elmer autosystem XL-2 gas chromatograph (Perkin-Elmer, Connecticut, USA), fitted with an AT-1701 column (reverse phase silica, 30 m x 0.54 mm) (Alltech, Carnforth, UK), was used for the analysis of ketone and lactone. 1 μ l samples were injected onto the column at 200 °C using the integrated autosampler and compounds exiting the column were detected by a flame ionisation detector (FID). The oven temperature programme included an initial holding step at 100 °C for 5 minutes and then the temperature was ramped at 10°C per minute until it reached 250 °C. Data capture and analysis was achieved using Perkin-Elmer Nelson Turbochrom™ software.

The FID response to a particular solute concentration in a sample was measured as an integrated peak area on a GC chromatogram. Calibration curves (Figure A1) were used to quantify these responses for the ketone and lactone compounds. Bicyclo[3.2.0]hept-2-en-6-one was used for the ketone standard and (1R,5S)-2-oxabicyclo[3.3.0]oct-6-en-3-one was used for the lactone standard. For each type of sample the coefficient of variance for a single peak area measurement was determined from triplicate measurements of ten ketone solutions (concentration range 0.1-1.8g/l) and six lactone solutions (concentration range 0.1-1.0g/l), and were found to be no more than ± 2 %.

2.2.2 Dry cell weight (DCW) measurement

Samples were taken from the fermentation of *E. coli* TOP10 [pQR239] at different stages of its growth. OD measurements were taken of the samples at 600nm (OD_{600nm}) using an Ultraspec 1110 Pro UV/Visible spectrophotometer (Amersham Biosciences, Buckinghamshire, UK). Samples were filtered on pre-weighed grade GF/F glass microfiber filter discs, pore size 0.7µm, using a Millipore[®] vacuum pump. The filters, retaining wet cell paste, were placed and left to dry in a 100°C oven overnight and/or until they achieved a constant weight. They were then weighed and the DCW calculated to produce a calibration curve (figure A2). The coefficient of variance for triplicate OD_{600nm} measurements were no more than ±0.5% and for triplicate DCW measurements coefficient of variance were no more than ±0.06%.

2.2.3 Analysis of ketone and lactone load on resin

Resins recovered from resin based SFPR bioconversions were separated from the bioconversion medium by pumping it through a Buchner funnel. The recovered resins were weighed and fully immersed and mixed in ethyl acetate, which included 1g/l naphthalene as an internal standard, overnight at 200rpm and room temperature to strip the loaded ketone and/or lactone from the resin. Sample was taken and analysed as described in section 2.2.1.2.

Preliminary experiments where resins were loaded with known concentrations of ketone and lactone were analysed as above and the coefficient of variance for triplicate experiments using all six resins were determined to be no more than ±8.2%.

2.2.4 Measurement of glycerol concentration in bioconversion medium

A 2ml sample from the bioconversion medium was centrifuged at 13000rpm for 2 minutes (Biofuge 13, Heraeus Sepatech, Brentwood, UK). The cell pellet was discarded but the supernatant retained to be assayed using a glycerol enzymatic test kit

(Boehringer-Mannheim Roche/R-Biopharm GmbH, Germany) for the determination of glycerol concentration. In this assay NADH oxidation is stoichiometrically linked to the amount of glycerol present via three enzyme catalysed reactions. Firstly glycerokinase catalyses the phosphorylation of glycerol by adenosine-5'-triphosphate (ATP) to L-glycerol-3-phosphate. The adenosine-5'-diphosphate formed in this reaction is reconverted into ATP by phosphoenolpyruvate with the aid of pyruvate kinase, and pyruvate is formed. In the presence of the enzyme L-lactate dehydrogenase, pyruvate is reduced to L-lactate by NADH with the oxidation of NADH to NAD. NADH oxidation was followed spectrophotometrically by measuring the total difference in absorbance at 340nm on completion of the above reactions using an Ultraspec 1110 Pro UV/Visible spectrophotometer (Amersham Biosciences, Buckinghamshire, UK). The coefficient of variance for triplicate glycerol standards solutions of a concentration range 4 to 10g/l were no more than 1%.

2.3 Resin Screening

2.3.1 Millilitre scale adsorption isotherms

1% (w/v) of resin (section 2.1.2) was agitated with 10ml of either ketone or lactone, prepared as described in section 2.1.1.1, at 250rpm and 37°C in an orbital shaker (New Brunswick Scientific). Concentrations of ketone and lactone ranged from 0.1-5g/l in 50mM phosphate buffer (2.9g/l monosodium phosphate, 7.7g/l disodium phosphate). After equilibrium was reached samples were analysed as described in section 2.2.1, and adsorption parameters calculated. Adsorption isotherm models were generated within SigmaPlot[®] version 10 (Systat[®], Chicago, USA).

Preliminary experiments were performed to determine when equilibrium is reached by mixing 1% (w/v) of resins with 10ml of ketone or lactone of concentration 5g/l, at 250rpm and 37°C, and taking samples every 1.5 hours. Samples were analysed as described in section 2.2.1 to see when solute concentration in aqueous phase becomes constant.f

2.3.2 High throughput resin screening (HTRS)

High throughput resin screening (HTRS) was performed using 96 and 24 deep square well (DSW) polypropylene microplate platforms (see table 2.2).

Table 2.2 Dimensions of 96 wells and 24 wells microplate

Platform	Well Width	Well Height	Well Volume
96 wells (Becton Dickinson, NJ, USA)	8mm	40mm	2ml
24 wells (Ritter Medical, Germany)	16mm	40mm	10ml

2.3.2.1 Adsorption isotherms

1% (w/v) of resin (section 2.1.2) was agitated with either ketone or lactone, prepared as described in section 2.1.1.1, at 1000rpm and 37°C on an Eppendorf Thermomixer Comfort, which has an orbital shaking pattern and a throw of 3mm (Eppendorf AG, Hamburg, Germany). Concentrations of ketone and lactone ranged from 0.1-5g/l and volumes of each solution were 1ml in 96 wells microplate and 1.5ml in 24 wells microplate. After equilibrium was reached samples were analysed as described in section 2.2.1, and adsorption parameters calculated. Adsorption isotherm models were generated within SigmaPlot[®] version 10 (Systat[®], Chicago, USA).

Preliminary experiments were performed to determine when equilibrium is reached by mixing 1% (w/v) of resins with 1ml in a 96 wells microplate and 1.5ml in 24 wells microplate of ketone or lactone of concentration 5g/l, at 1000rpm and 37°C, and taking samples every hour. Samples were analysed as described in section 2.2.1 to see when solute concentration in aqueous phase becomes constant.

2.3.2.2 Dual compound adsorption kinetics

Dual compound adsorption kinetic studies were carried out to determine the selectivity of the resins to the ketone and lactone compounds. 1g/l of ketone and lactone were mixed together with 1% (w/v) of resin at 1000rpm and 37°C and samples taken at regular intervals between 30 seconds and five minutes were analysed as described in section 2.2.1.

2.3.3 Investigation of resin suspension behaviour in 96 and 24 wells microplate formats using high speed imaging

2.3.3.1 High speed camera equipment

The camera equipment was loaned from the Engineering Instrument Pool, which is managed by the Science and Technology Facilities Council (STFC) (Rutherford Appleton Laboratory, Didcot, UK) on behalf of the Engineering and Physical Sciences Research Council (EPSRC).

A Photron FASTCAM MC-1 high speed monochrome video system was used to record high speed videos of resin mixing in a mimic of a single well from 96 and 24 wells microplate. Images were recorded with a Nikon 24-85mm zoom lens attached to the camera and the following settings:

- Frame rate: 240 fps
- Resolution: 512 x 512

2.3.3.2 Investigation of resin suspension behaviour in mimics of 96 and 24well microplate

Clear acrylic Perspex was used to construct (in-house workshop) mimics of a single well from 96 and 24 wells microplates. The mimic well was mounted and secured, alongside the Photron FASTCAM MC-1 high speed monochrome video camera, onto a Kuhner ShakerX LS-X bench top shaker set-up with a throw of 3mm. 1% (w/v) of resin was

added to the mimic wells and mixed at agitation speeds ranging from 325 to 800 rpm. Frames were visually analysed to record the number of resins in suspension.

2.4 *E. coli* TOP10 [pQR239] fermentation

2.4.1 Preparation of inoculum

A 1 ml frozen stock aliquot, as described in section 2.1.3.1, was thawed and inoculated into a 500ml unbaffled shake flask containing 100ml of fermentation medium as described in section 2.1.1. The shake flask was then incubated overnight at 37 °C in an orbital shaker (New Brunswick Scientific, Edison, USA) at 200 rpm.

2.4.2 Shake flask fermentation and CHMO induction

5% (v/v) of the overnight culture was inoculated into a 1 l baffled shake flask with a 10% working volume of fermentation medium as described in section 2.1.1. The shake flask was then incubated at 37°C and 250 rpm in an orbital shaker (New Brunswick Scientific, Edison, USA). The progress of the fermentation was followed by taking OD_{600nm} measurements, as described in section 2.2.2. When growth of *E. coli* TOP10 [pQR239] reached middle of exponential growth concentrated L(+)-arabinose solution was added via a 0.2 µm filter to a final concentration of 0.1 % w/v, inducing the expression of CHMO by the recombinant *E.coli* TOP10 [pQR239] cells. Fermentation continued until stationary phase of growth was reached.

2.4.3 Cell harvest and storage

Cell culture from fermentation was harvested as 50ml aliquots and centrifuged for 20 minutes at 3000g and 4°C (Avanti J-E, Beckman Coulter). Supernatant was discarded and the wet cell paste was either resuspended in phosphate buffer to be used immediately for bioconversion or stored at -80°C.

2.5 Shake flask bioconversions

Shake flask bioconversions were performed in 500ml baffled shake flasks with a 10% working volume. *E. coli* TOP10 [pQR239] cells harvested from fermentation (section 2.4) were resuspended in 50mM phosphate buffer, concentrated glycerol added to a final concentration of 10g/l and bioconversion initiated by the addition of substrate. Bioconversions were performed at 37°C and 250 rpm in an orbital shaker (New Brunswick Scientific, Edison, USA). Samples were taken at regular intervals and analysed as described in section 2.2.

2.5.1 Bioconversions without the implementation of a SFPR strategy

Bioconversions performed without the implementation of a SFPR strategy were carried out by the addition of ketone, prepared as described in section 2.1.1.1. Bioconversions were carried out at initial ketone concentrations of 0.4g/l or 3.0g/l.

2.5.2 Bioconversion with the implementation of the single resin SFPR strategy

Based on investigations described in section 2.3, a resin was chosen to be used for the implementation of the single resin SFPR strategy in the shake flask bioconversion experiments. The required amount of resin was mixed in a solution of ketone overnight at 37°C and 250 rpm in an orbital shaker (New Brunswick Scientific, Edison, USA) for the adsorption ketone on resin.

Resin loaded with ketone was then added to the resuspended cells and 10g/l glycerol to initiate the bioconversion at an initial ketone concentration of 3.0g/l. Samples were taken at regular intervals and analysed as described in section 2.2.

Prior to running the resin based bioconversions, experiments were carried out to see if the resins have an adverse effect on the whole biocatalyst. This was done by mixing 20g of the resins chosen for use in the resin based bioconversion with 8g_{DCW}/l of whole cells

in 50mM phosphate buffer for 6 hours at 37°C and 250 rpm in an orbital shaker (New Brunswick Scientific, Edison, USA) without ketone or lactone. There was no decrease of OD and, after filtering off the resins, there was no adverse effect on the whole cell biocatalyst activity.

2.5.3 Bioconversions with the implementation of the dual resin SFPR strategy

Based on investigations described in section 2.3, resins were chosen to be used for the implementation of the dual resin SFPR strategy in the shake flask bioconversion experiments. The required amount of resin, to be utilised for substrate feeding, was mixed in a solution of ketone overnight at 37°C and 250 rpm in an orbital shaker (New Brunswick Scientific, Edison, USA) for the adsorption ketone on resin.

Controlled experiments performed prior to resin based SFPR bioconversions showed that adding as much as 20g of resins to an *E. coli* TOP10 [pQR239] did not have an effect on either the OD or the whole cell biocatalyst activity.

2.5.3.1 Dual resin SFPR bioconversion without separation of the two types of resins

Resin loaded with ketone was added to resuspended cells and 10g/l glycerol to initiate the bioconversion at an initial ketone concentration of 3.0g/l. Based on adsorption kinetic studies described in section 2.3.2.2 and reaction kinetics from experiments described in section 2.5., set amounts of the second type of resin (used as the product removal tool) was added to the reaction system at regular intervals. Samples were taken at regular intervals and analysed as described in section 2.2.

2.5.3.2 Dual resin SFPR bioconversion with separation of the two types of resins

Bioconversions were performed as described in section 2.5.3.1 but with separation of the two types of resins. A filter bag (Teekanne, Dusseldorf, Germany), made of cellulose tissue, was used to house the resin used as the substrate feeding tool while the second

type of resin was kept free in suspension in the bioconversion medium (figure 2.1). Samples were taken at regular intervals and analysed as described in section 2.2.

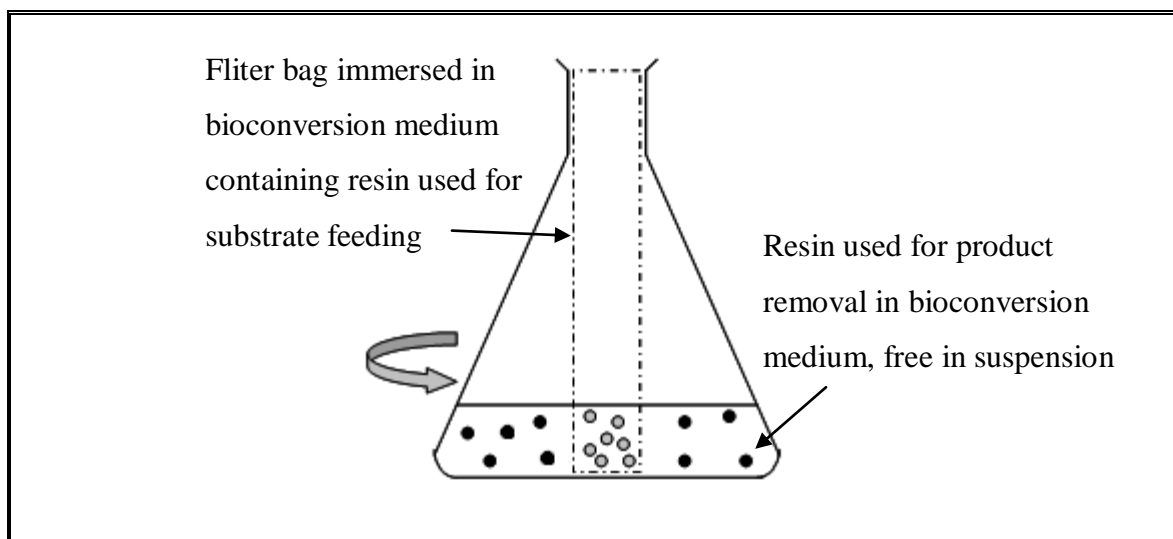


Figure 2.1 A schematic of the method of employing a filter bag for the separation of two types of resins used in the dual resin SFPR strategy

Controlled experiments performed prior to using the filter bag, to physically separate the two types of resins used in the dual resin SFPR bioconversions, showed that solute mass transfer from inside the filter bag to outside into phosphate buffer and *vice versa*, was not a limiting factor in the bioconversion. Also loss of ketone and lactone by adsorption onto the filter bag from the aqueous phase was only at 0.009g/l and 0.008g/l, respectively, from a starting solute concentration of 1g/l.

2.6 Miniature stirred tank reactor (STR) bioconversions

2.6.1 Operation of miniature STR system

The miniature STR system used has been designed and described by Gill *et al* (2008). Selected design and instrumentation features of the miniature STR are as follows:

- Borosilicate glass vessel (100ml maximum working volume), sealed with a stainless head plate
- Magnetically driven, six-blade miniature Rushton turbine impeller ($d_i = 20\text{mm}$, $d_i/d_T = 1/3$) with a stirring range of 100-2000rpm
- Four baffles of width 6mm
- A sparger fitted with a $15\mu\text{m}$ stainless steel sinter
- A standard laboratory rotameter in the range 0-200ml/min to regulated air flow rate
- Online monitoring of DOT and temperature by a polarographic oxygen electrode and a narrow K-type thermocouple, respectively

Agitation rate and air flow were manually regulated to keep DOT above 10% to ensure that bioconversions were not limited by oxygen mass transfer. Controlled experiments performed prior to the resin based SFPR bioconversions showed that the resins (amounts varying from 2 to 20g) did not have an effect on the DOT and did not interfere with the DOT probe at mixing rates between 800 to 2000rpm.

2.6.2 Bioconversions without the implementation of a SFPR strategy

Bioconversions performed without the implementation of a SFPR strategy were carried out by the addition of ketone, prepared as described in section 2.1.1.1, at the required concentration. Stirrer speed and air flow rate were maintained at 2000rpm and 1vvm, respectively. Samples were taken at regular intervals and analysed as described in sections 2.2.

2.6.3 Bioconversion with the implementation of the single resin SFPR strategy

Based on investigations described in section 2.3, a resin was chosen to be used for the implementation of the single resin SFPR strategy in the shake flask bioconversion experiments. The required amount of resin was mixed in a solution of ketone overnight at 37°C and 250 rpm in an orbital shaker (New Brunswick Scientific, Edison, USA) for the adsorption ketone on resin.

Resins loaded with ketone were then added to the resuspended cells and 10g/l glycerol to initiate the bioconversion at an initial ketone concentration of 3.0g/l. Stirrer speed and air flow rate were maintained at 2000rpm and 1vvm, respectively. Samples were taken at regular intervals and analysed as described in sections 2.2.

2.6.4 Bioconversions with the implementation of the dual resin SFPR strategy

Based on investigations described in section 2.3, resins were chosen to be used for the implementation of the dual resin SFPR strategy in the shake flask bioconversion experiments. The required amount of resin, to be utilised for substrate feeding, was mixed in a solution of ketone overnight at 37°C and 250 rpm in an orbital shaker (New Brunswick Scientific, Edison, USA) for the adsorption ketone on resin.

Resin loaded with ketone was added to resuspended cells and 10g/l glycerol to initiate the bioconversion at an initial ketone concentration of 3.0g/l. Based on adsorption kinetic studies described in section 2.3.2.2 and reaction kinetics from experiments described in section 2.5., set amounts of the second type of resin (used as the product removal tool) was added to the reaction system at regular intervals. Samples were taken at regular intervals and analysed as described in section 2.2.

2.7 Resin based SFPR bioconversions performed in the recycle reactor configuration

2.7.1 Specifications of column

The Tricorn 5/50 column (GE Healthcare, Buckinghamshire, UK) was used in the recycle reactor configuration to implement both single and dual resin SFPR strategies.

The specifications of the Tricorn 5/50 column are as follows:

- Inner diameter= 5mm
- Length= 50mm
- Operating pressure= 1450psi
- Operating temperature 4-40°C

The column was packed with the required amount of resin, assembled and connected to a peristaltic Pump P-1 (Pharmacia Biotech, Sweden) with PTFE tubing (Bohlender, Germany) with an internal diameter of 1mm.

2.7.2 Preparation of column for use in bioconversion

The required amount of resin for the resin based SFPR strategies was mixed in a solution of ketone overnight at 37°C and 250 rpm in an orbital shaker (New Brunswick Scientific, Edison, USA) for the adsorption ketone on resin. The resin was packed into the column by slowly pouring it into the column as slurry in the ketone solution. The column was assembled and ketone solution was drained, ready to be used for resin based SFPR bioconversions in the recycle reactor configuration.

2.7.3 Set up and operation of the miniature STR in the recycle reactor configuration

The column packed with loaded resin was connected to a peristaltic Pump P-1 (Pharmacia Biotech, Sweden) and the miniature STR, described in section 2.6.1, with PTFE tubing (Bohlender, Germany) with an internal diameter of 1mm. The tubing was inserted into the STR through openings, which were sealed by self-sealing septa, on a single multi-port on the headplate. This completed the full circuit of column, pump and STR (figure 2.2). The STR was operated as described in section 2.6.1 and the circulation of the bioconversion medium achieved at a flow rate of 6.4ml/min.

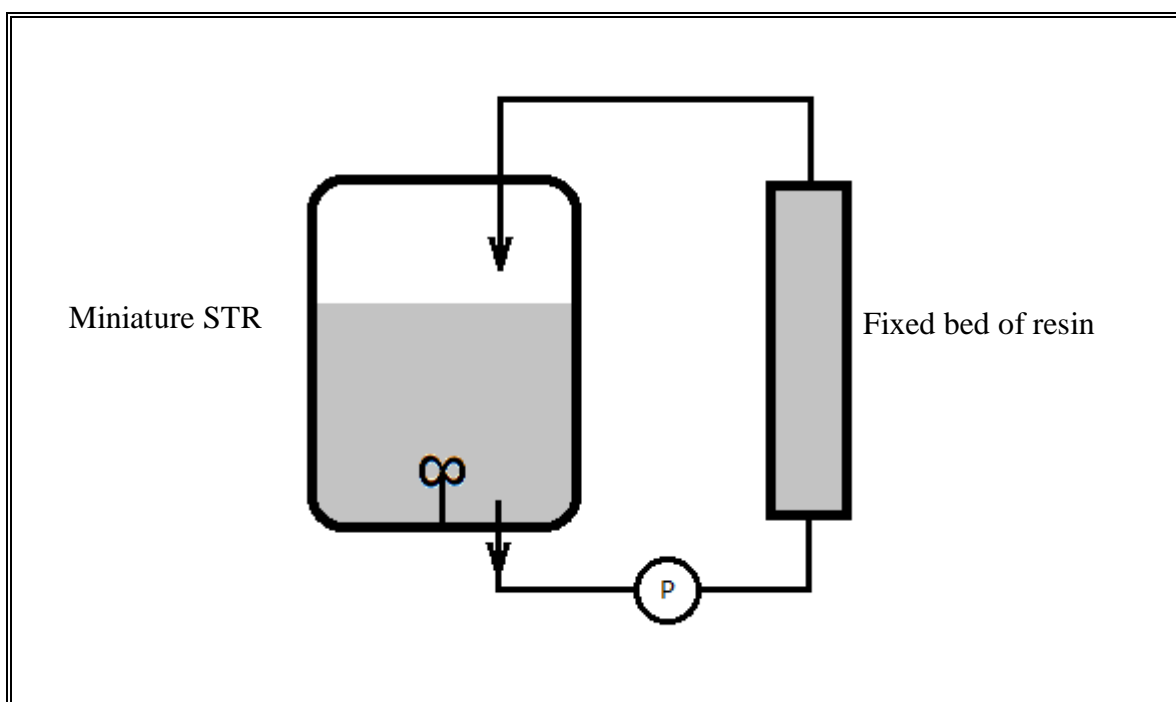


Figure 2.2 Recycle reactor with fixed bed of resins in an external loop.

2.7.4 Bioconversion with the implementation of the single resin SFPR strategy

The single resin SFPR strategy implemented in the recycle reactor configuration had the resin housed in the column outside the STR and no resins free in suspension inside the STR. The bioconversion was initiated by starting the pump (flow rate of 6.4ml/min) to

circulate the bioconversion medium with cells from the STR, through the packed column and back into the STR. Stirrer speed and air flow rate were maintained at 2000rpm and 1vvm, respectively. Samples were taken at regular intervals and analysed as described in sections 2.2. The amount of ketone and lactone loaded onto the resin inside the column at the end of bioconversion was analysed by dismantling the column and washing the resin out with ethyl acetate. Analysis was the performed as described in section 2.2.3.

2.7.5 Bioconversion with the implementation of the dual resin SFPR strategy

The dual resin SFPR strategy implemented in the recycle reactor configuration had the resin, which was chosen as the substrate feeding tool, housed in the column outside the STR. The second type of resin chosen as the product removal tool was added in set amounts at regular intervals into the STR free in suspension. The bioconversion was initiated by starting the pump (flow rate of 6.4ml/min) to circulate the bioconversion medium from the STR, through the packed column and back into the STR. Stirrer speed and air flow rate were manually regulated to ensure DOT was kept above 10%. Samples were taken at regular intervals and analysed as described in sections 2.2. The amount of ketone and lactone loaded onto the resin inside the column at the end of bioconversion was analysed by dismantling the column and washing the resin out with ethyl acetate. Analysis was the performed as described in section 2.2.3.

Chapter 3. Resin screening

3.1 Aims

The aim of this chapter is to characterise resins for selection as part of the dual resin SFPR strategy to be employed in the Baeyer-Villiger bioconversion, catalysed by CHMO expressed in *E. coli*. Additionally, high-throughput resin screening (HTRS) will also be developed to consider its potential for accelerating resin characterisation.

3.2 Introduction

Development of resin based SFPR systems requires an understanding of the interactions between the compounds in the biocatalytic reaction and the available resins that can be applied in such a system. One way is to generate adsorption isotherms which indicate the resin capacity, enable evaluation of performance and parameters to be improved, all of which are important in optimising the use of resins in biocatalytic processes.

However, examining the vast number of resins that have the potential of use in a resin based SFPR becomes a time and material consuming exercise, so a high throughput resin screening (HTRS) methodology which will pave the way for further development and optimisation of this system is needed.

3.3 Theory

3.3.1 Adsorption capacity

The adsorption capacity, Q_{ads} (g/g_{adsorbent}), was calculated using Equation 1:

$$Q_{ads} = \frac{V(C_i - C_{eq})}{M} \quad \text{Equation [1]}$$

Where C_i and C_{eq} are the initial concentration and concentration at equilibrium (g/l), respectively. V is the total volume of solution and M is the mass of resin (g).

3.3.2 Adsorption isotherm models

Langmuir isotherm:

The Langmuir model is the simplest model to describe monolayer adsorption and is widely used (Doran, 1995). It is shown in equation 2 where Q_{max} is the maximum loading of adsorbate corresponding to complete monolayer coverage of all available adsorption sites. At low adsorbate concentrations the Langmuir model approaches the linear model and at high concentrations adsorption approaches the monolayer capacity, Q_{max} . K_A is the equilibrium constant.

$$Q_{ads} = \frac{Q_{max}K_A C_{eq}}{1 + K_A C_{eq}} \quad \text{Equation [2]}$$

The assumptions of the Langmuir model are (i) that adsorbed molecules form no more than a monolayer on the surface, (ii) each site for adsorption is equivalent in terms of adsorption energy and (iii) there are no interactions between adjacent adsorbed molecules. In experimental systems one of these assumptions will often not be valid, largely because adsorbent surfaces are not homogeneous and adsorbate molecules may interact to form multi-layers of adsorption on the adsorbent particle.

Freundlich isotherm:

Another commonly used adsorption isotherm which attempts to incorporate surface heterogeneity is the Freundlich isotherm (Doran, 1995) which is described in equation 3. In this case n is a constant which represents the degree of surface heterogeneity and K_F is an equilibrium constant.

$$Q_{ads} = K_F C_{eq}^{1/n} \quad \text{Equation [3]}$$

Constant n can be taken as an indicator of the intensity of adsorption, so a value of $n > 1$ indicates a favourable adsorption, whereas a value of $n < 1$ indicates an unfavourable adsorption.

The isotherm parameters for Langmuir and Freundlich isotherms are determined from their linear forms. The regression coefficient (R^2) is used to determine the relationship between the experimental data and the isotherms.

3.3.3 Determining selectivity based on initial rate of adsorption

Selectivity, $S_{K,L}$, of resin for two different compounds is determined by equation 4, where K_K is the initial rate of adsorption of ketone and K_L is the initial rate of adsorption of lactone.

$$S_{K,L} = \frac{K_K}{K_L} \quad \text{Equation [4]}$$

3.4 Results

3.4.1 Bench scale resin screening

Results from the bench scale adsorption experiments are shown in figures 3.1 to 3.3. The most apparent trend of adsorption of ketone and lactone onto the six different resins (table 3.1) that can be taken from the graphs is that all six resins have a greater capacity for the adsorption of ketone than the lactone compound. This suggests that the less soluble ketone substrate exhibits a higher hydrophobic adsorption onto all resins compared to the lactone product.

The adsorption of both ketone and lactone on all six resins can be described by both Langmuir and Freundlich isotherm models, which can be visualised on each figure. The convex shape of all adsorption isotherms, figures 3.1 to 3.3, for both ketone and lactone compounds indicate favourable adsorption, with all isotherms reaching or moving towards saturation.

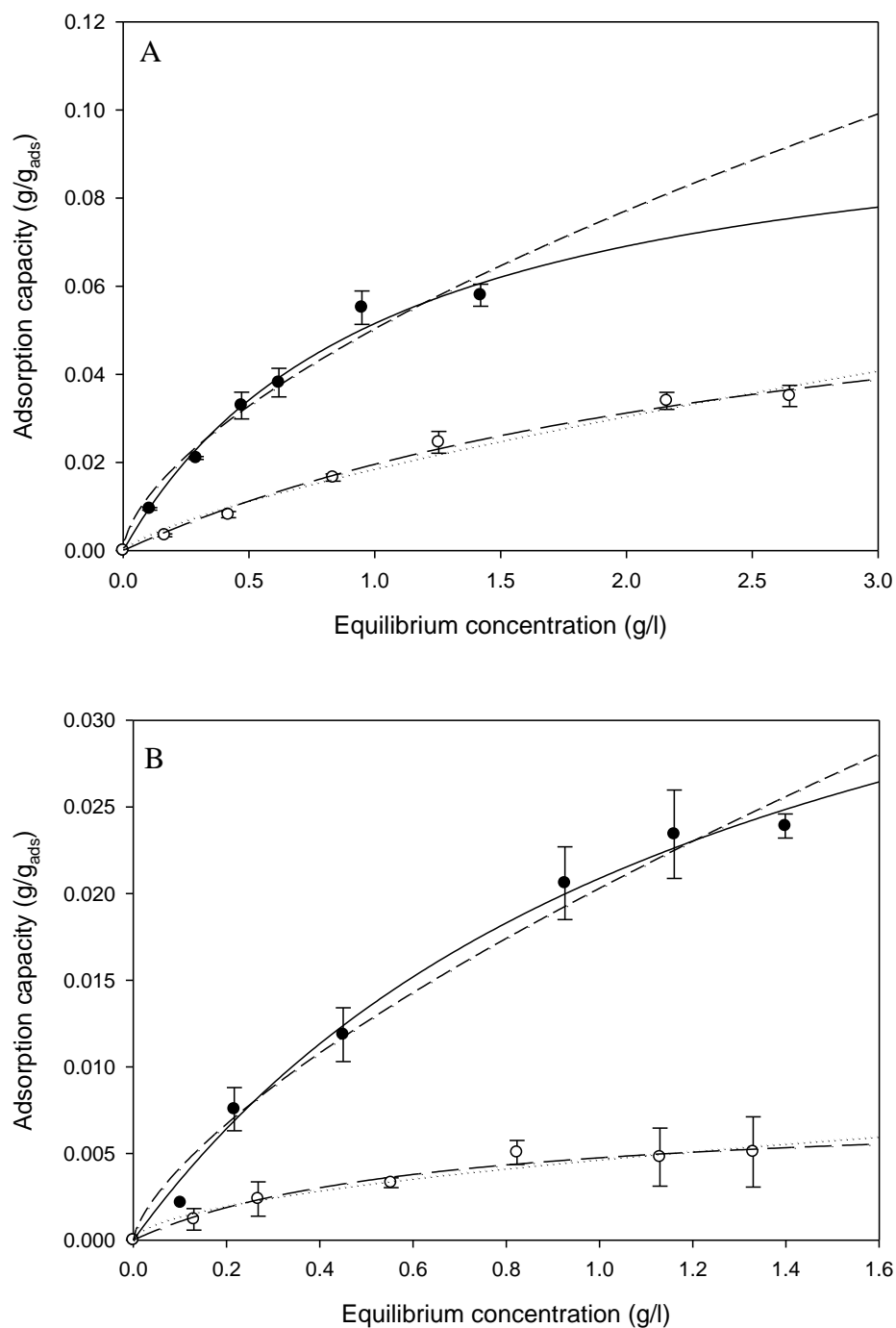


Figure 3.1 Adsorption isotherms generated using resins (A) XAD7 and (B) IRC50 for the adsorption of (●) ketone and (○) lactone in experiments described in section 2.3.1. Lines represent mathematical models fitted to the data as described in section 3.3.2 (Langmuir isotherm represented by solid and long dashed lines; Freundlich isotherm represented by medium dashed and dotted lines). Error bars represent one standard deviation based on triplicate experiments.

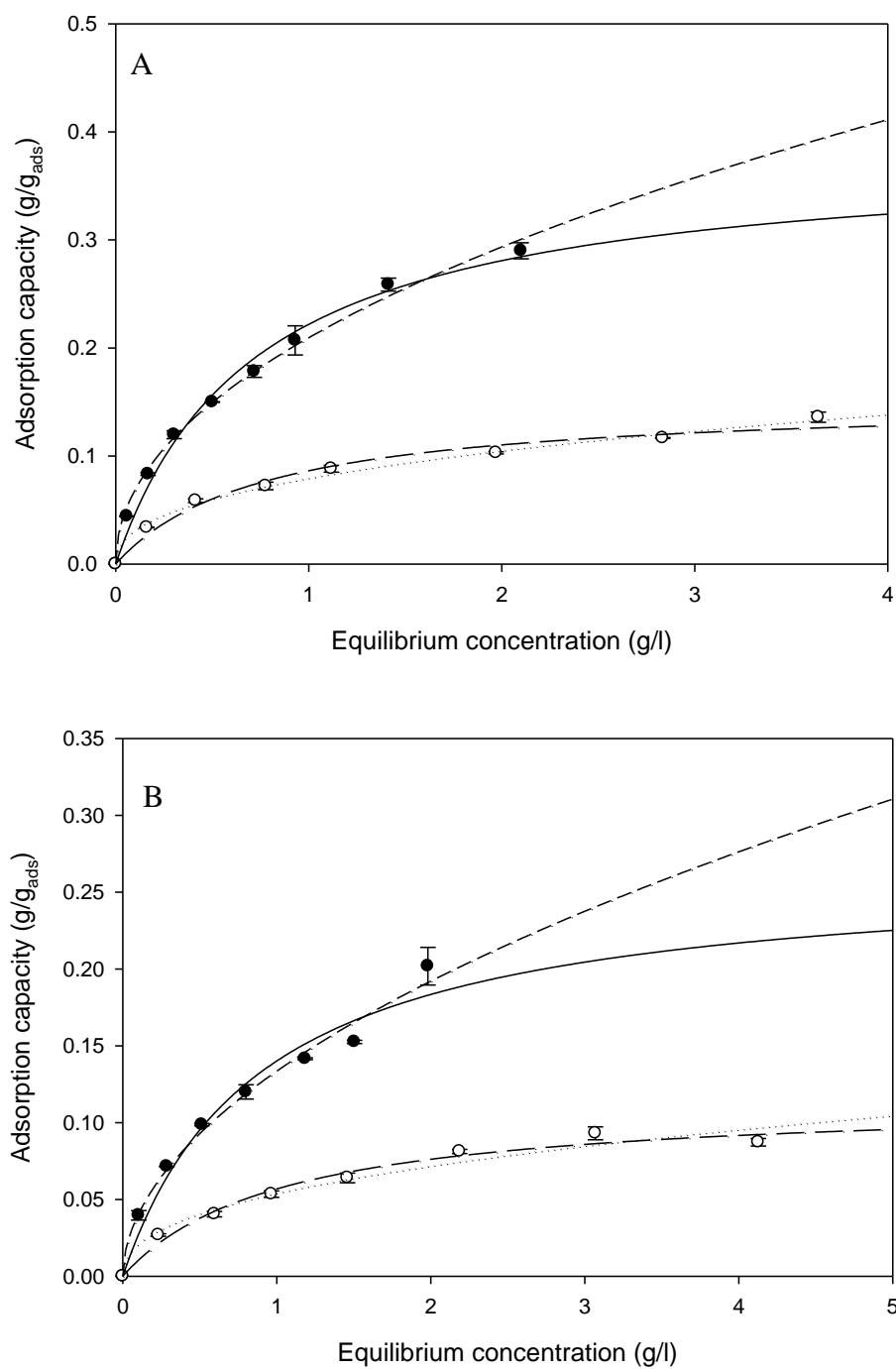


Figure 3.2 Adsorption isotherms generated using resins (A) L493 and (B) XAD4 for the adsorption of (●) ketone and (○) lactone in experiments described in section 2.3.1. Lines represent mathematical models fitted to the data as described in section 3.3.2 (Langmuir isotherm represented by solid and long dashed lines; Freundlich isotherm represented by medium dashed and dotted lines). Error bars represent one standard deviation based on triplicate experiments.

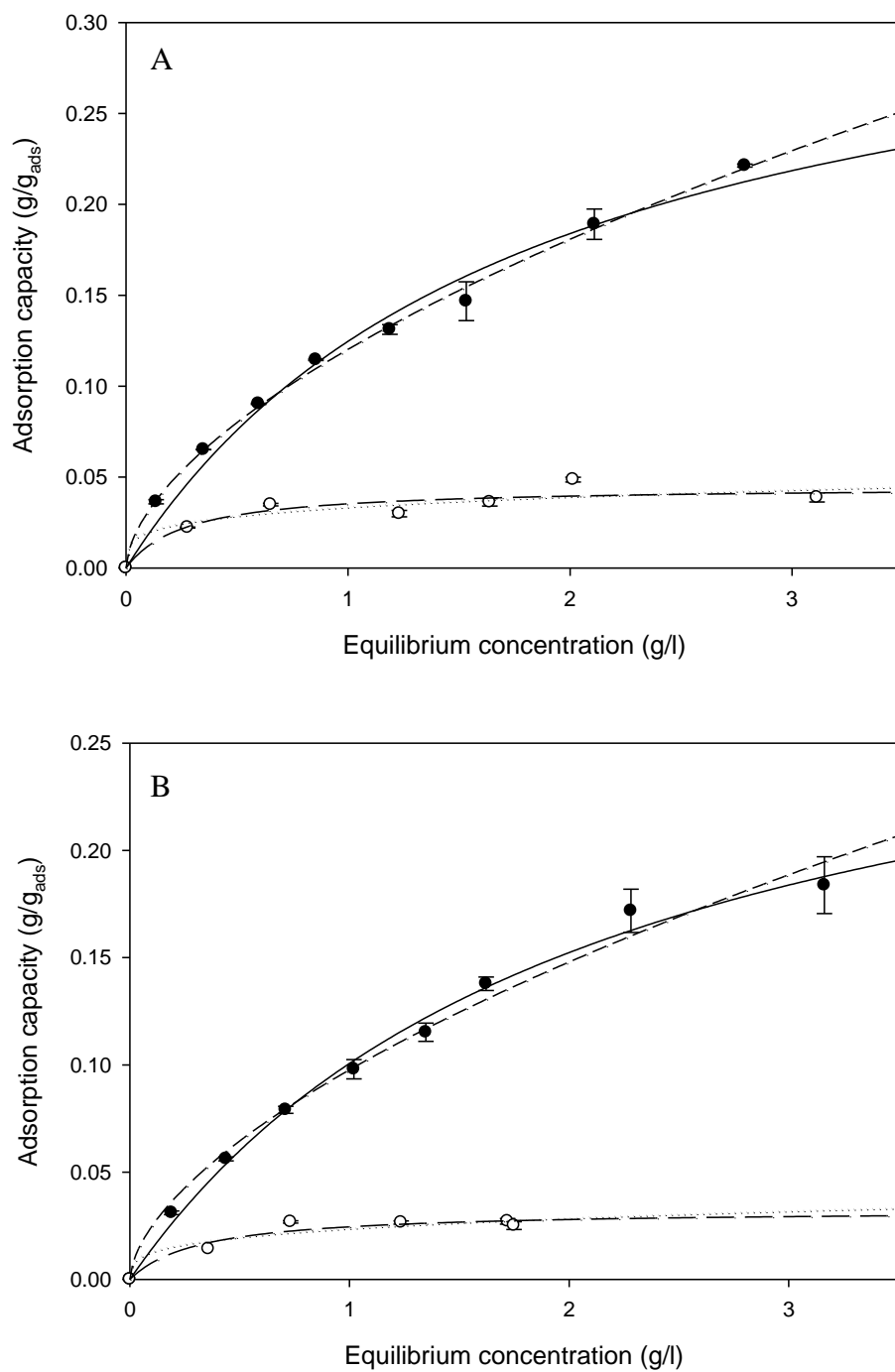


Figure 3.3 Adsorption isotherms generated using resins (A) XAD16 and (B) XAD1180 for the adsorption of (●) ketone and (○) lactone in experiments described in section 2.3.1. Lines represent mathematical models fitted to the data as described in section 3.3.2 (Langmuir isotherm represented by solid and long dashed lines; Freundlich isotherm represented by medium dashed and dotted lines). Error bars represent one standard deviation based on triplicate experiments.

Table 3.1 summarises the parameters calculated from both Langmuir and Freundlich adsorption isotherms shown in Figures 3.1 to 3.3 and compares the adsorption of ketone and lactone on all six resins.

The highest maximum adsorption capacity (Q_{\max}), as determined from the Langmuir adsorption isotherm, for the ketone compound was achieved using L493 at 0.383 g/g_{adsorbent}, and the lowest maximum adsorption capacity was seen using IRC50 at 0.048 g/g_{adsorbent}. Also a direct positive correlation can be seen between the maximum adsorption capacity of all six resins with their surface area, i.e. the larger the surface area the greater the adsorption capacity for ketone.

The same pattern is seen with adsorption of lactone with regards to the highest and lowest maximum adsorption capacity, i.e. L493 achieved the highest at 0.152 g/g_{adsorbent} and IRC50 the lowest at 0.008 g/g_{adsorbent}. However, unlike the trend seen with the adsorption of ketone, no positive relationship is seen between the adsorption of lactone and resin surface area. However, a negative correlation is observed between lactone adsorption and pore diameter, i.e. the smaller the pore diameter the greater the maximum adsorption capacity of resin for the lactone.

Observation of the equilibrium constants of both the Langmuir and Freundlich isotherms and constant n calculated from the Freundlich isotherm, shows no relationship between the intensity of adsorption with resin surface area and pore diameter, for both ketone and lactone compounds.

Table 3.1 Resin properties and derived parameters of Langmuir and Freundlich adsorption models. All resin particles range from 1-2mm in diameter and are polyaromatics except for XAD7 which is an acrylic ester.

Resin	Density (g/ml)	Surface area (m ² /g)	Pore diameter (Å)	Compound	Langmuir		Freundlich	
					Q _{max} (g/g _{adsorbent})	K _A	K _F	n
XAD7	1.24	450	90	Ketone	0.105	0.967	0.050	1.622
				Lactone	0.077	0.342	0.019	1.398
IRC50	0.66	-	300-3000	Ketone	0.048	0.781	0.020	1.452
				Lactone	0.008	1.621	0.005	1.893
L493	1.11	1100	46	Ketone	0.383	1.381	0.209	2.054
				Lactone	0.152	1.307	0.080	2.507

Table 3.1 continued

Resin	Density (g/ml)	Surface area (m ² /g)	Pore diameter (Å)	Compound	Langmuir		Freundlich	
					Q _{max} (g/g _{adsorbent})	K _A	K _F	n
XAD4	1.08	725	50	Ketone	0.265	1.118	0.134	1.906
				Lactone	0.115	0.975	0.054	2.444
XAD16	1.08	900	100	Ketone	0.351	0.552	0.120	1.699
				Lactone	0.045	3.677	0.034	4.399
XAD1180	1.04	600	300	Ketone	0.313	0.474	0.098	1.670
				Lactone	0.032	3.109	0.024	3.715

Another parameter that is important especially for designing a SFPR strategy for the Baeyer-Villiger bioconversion is the adsorption capacity of ketone on resin at an equilibrium concentration of 0.5g/l because it is above this concentration that biocatalysis is inhibited.

Table 3.2 presents the adsorption capacities for all six resins at an equilibrium concentration for ketone of 0.5g/l. It can be seen that resin L493 has the highest capacity at 0.21g/g_{adsorbent} and IRC50 the lowest at 0.012 g/g_{adsorbent} at the equilibrium concentration for ketone of 0.5g/l.

Table 3.2 Adsorption capacity of six resins at a ketone equilibrium concentration of 0.5g/l.

Resin	XAD7	IRC50	L493	XAD4	XAD16	XAD1180
Q _{ads} (g/g _{adsorbent})	0.035	0.012	0.21	0.11	0.082	0.059

3.4.2 High-throughput resin screening (HTRS)

3.4.2.1 Characterisation of resin suspension behaviour analysis using high-speed image analysis

Mixing of resins in both the 96 wells and 24 wells microplates were evaluated using a high speed camera. The experiment focused on the degree of suspension of the resins at different mixing speeds and was carried out as described in section 2.3.3.

3.4.2.1.1 Resin suspension: 96 microwell platform

Figure 3.4 shows still images of mixing of all six resins in the 96 microwell model at 800 rpm. As can be clearly seen, each resin remained settled at the bottom of the well without a single resin bead suspended in the liquid. This indicates that the strength of

liquid mixing near the base of the well was not sufficient to suspend the resins in this well dimension.

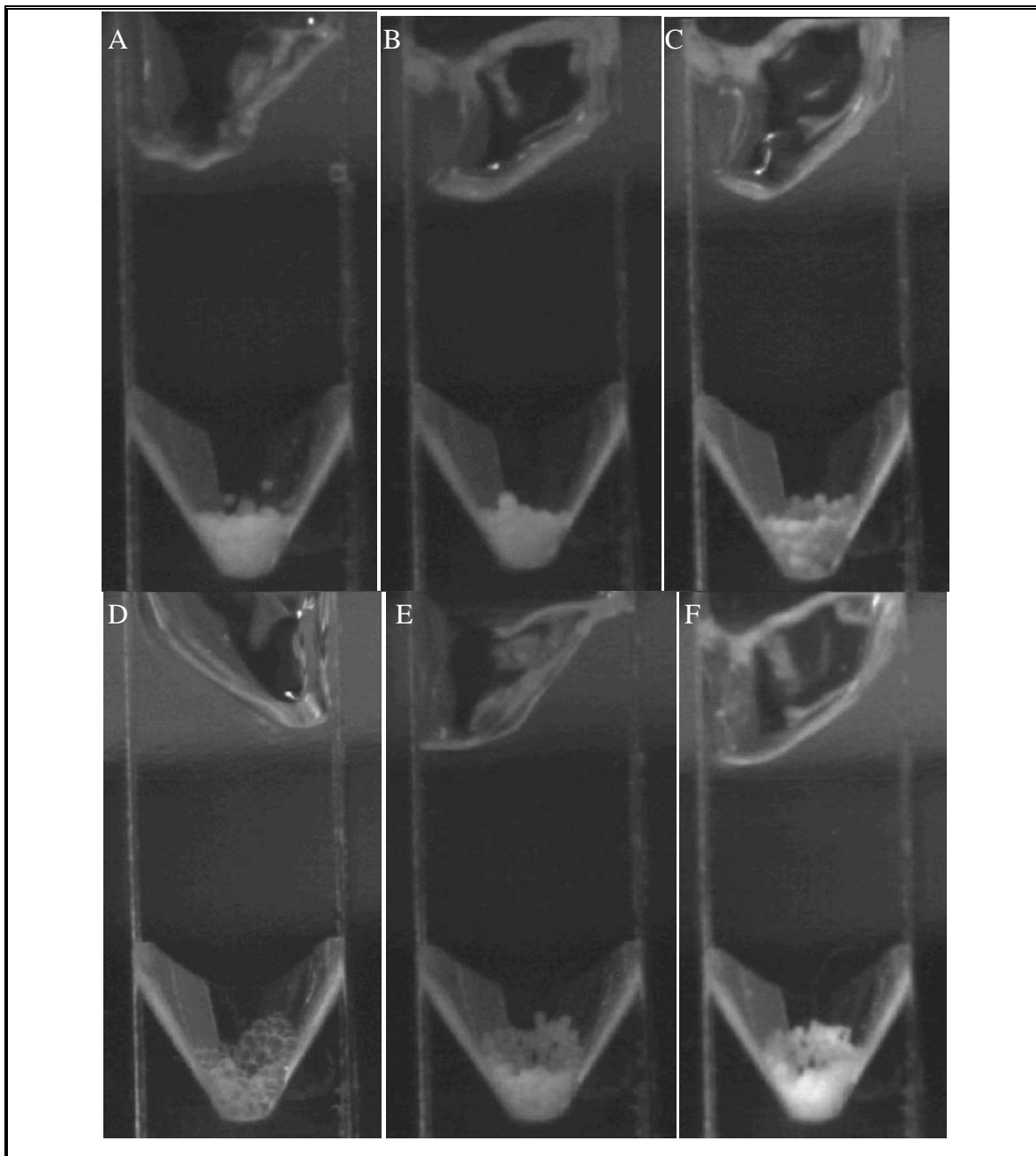


Figure 3.4 High speed camera images of (A) XAD7 (B) IRC50 (C) L493 (D) XAD4 (E) XAD16 (F) XAD1180 resins obtained under the following conditions: 800rpm, 3mm throw, 0.01g resin, 1ml volume [well geometry displayed in Table 2.2].

3.4.2.1.2 Resin suspension: 24 microwell platform

Figure 3.5 charts the maximum percentage of suspension of all six resins in the 24 wells microplate mimic up to a maximum mixing speed of 800 rpm, measured by observing the number of resin beads suspended out of the total number of resin beads added to the well. All six resins achieved suspension in the well at similar agitation speeds. XAD1180 resins were able to be suspended at a speed of 325rpm and resins IRC50 and L493, which needed greater agitation, were able to achieve suspension at speeds of 350rpm.

A similar trend is seen with regards to the optimum speeds required for maximum suspension with the exception of one resin, IRC50, where a significant increase of agitation is needed before maximum suspension is achieved. Resins XAD4, XAD16, XAD1180, XAD7 and L493 (ascending order) achieved maximum suspension in the range of 375-450rpm, however, maximum suspension of IRC50 was achieved at 800rpm despite it being 35% less dense at 0.66g/ml than the next dense resins (1.02g/ml). An explanation for this is the observation of 'clumps' of IRC50 beads in the high speed images of the well (Figure 3.6). This would result in needing high agitation speeds for the breakup of these resin 'clumps' and also for the suspension of these resin 'clumps'.

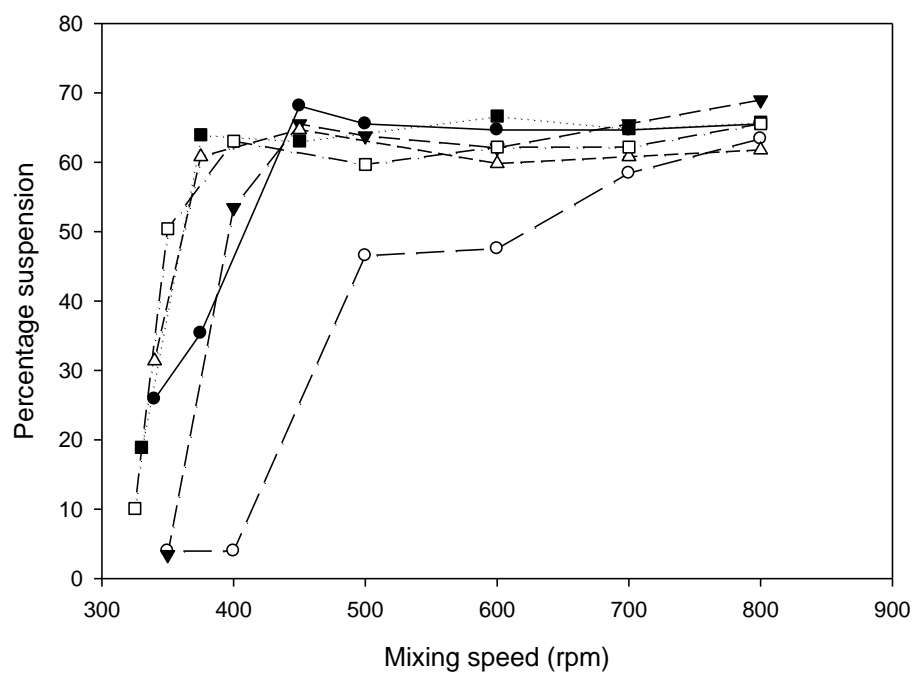


Figure 3.5 Suspension percentages of resins (●) XAD7 (○) IRC50 (▼) L493 (Δ) XAD4 (■) XAD16 and (□) XAD1180 in a well mimic from the 24 well microplate performed as described in section 2.3.3.

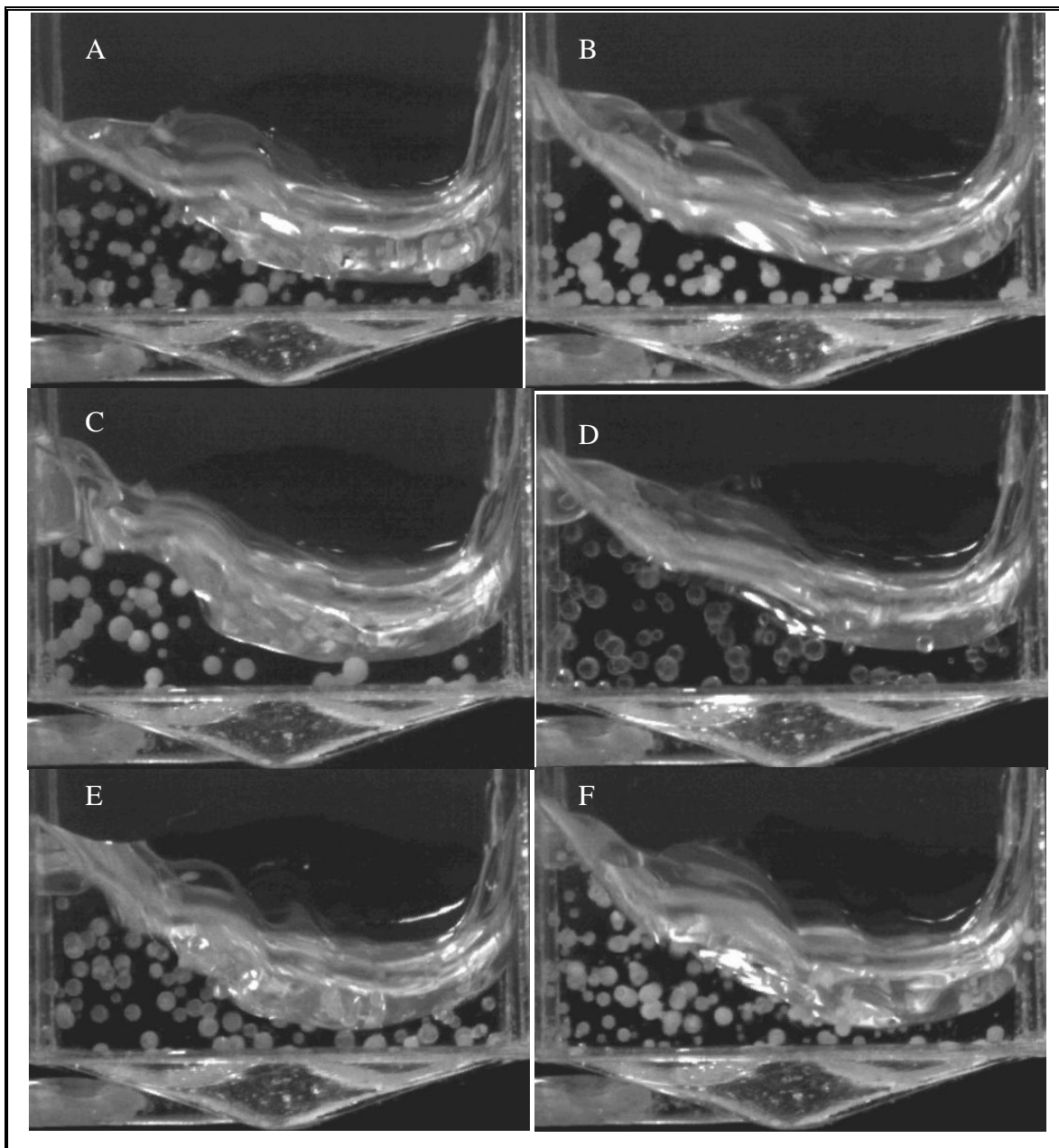


Figure 3.6 High speed camera images of (A) XAD7 (B) IRC50 (C) L493 (D) XAD4 (E) XAD16 (F) XAD1180 resins obtained in a well mimic from a 24 wells microplate platform under the following conditions: 800rpm, 3mm throw, 0.15g resin, 1.5ml volume [well geometry displayed in Table 2.2].

3.4.3 Determination of adsorption isotherms from microwell experiments

Figures 3.7 to 3.12 show the results from adsorption of ketone and lactone on all six resins in 96 and 24 microwell plates. For the purpose of comparison, adsorption data in figures 3.7 to 3.12 are fitted to only the Langmuir model and include the Langmuir model for bench scale adsorption.

The Langmuir adsorption model shows a good fit to the adsorption of both ketone and lactone on all six resins when using the 96 and 24 microwell plates. However the exception to this is the adsorption of ketone and lactone on IRC50 when using the 96 microwell platform. The convex shape of all adsorption isotherms, figures 3.7 to 3.12, when using either the 96 or 24 microwell plates indicates favourable adsorption, with all isotherms moving towards saturation.

A key observation from figures 3.7 to 3.12 is the large error bars (representing one standard deviation) associated with the adsorption data generated using the 96 wells microplate platform, particularly when nearing saturation. These large variances in adsorption can be attributed to the lack of resin suspension in the wells of the 96 wells microplate platform as seen in section 3.4.2.1.1. The adsorption process involves the adsorbate attaching itself to the surface of an adsorbent. The greater the exposure of adsorbent surface to the adsorbate the high chance of adsorption. Thus without resin suspension in the wells, resins will remain settled at the bottom, exposing less surface to which the adsorbates, in this case ketone and lactone, can adsorb onto.

This problem is exacerbated in the adsorption of ketone and lactone on IRC50 in the 96 wells microplate platform because the IRC50 beads tend to clump together (section 3.4.2.1.2), hence preventing further exposure of surface area to the solutes and resulting in a poor fit to data from the ml-scale adsorption studies.

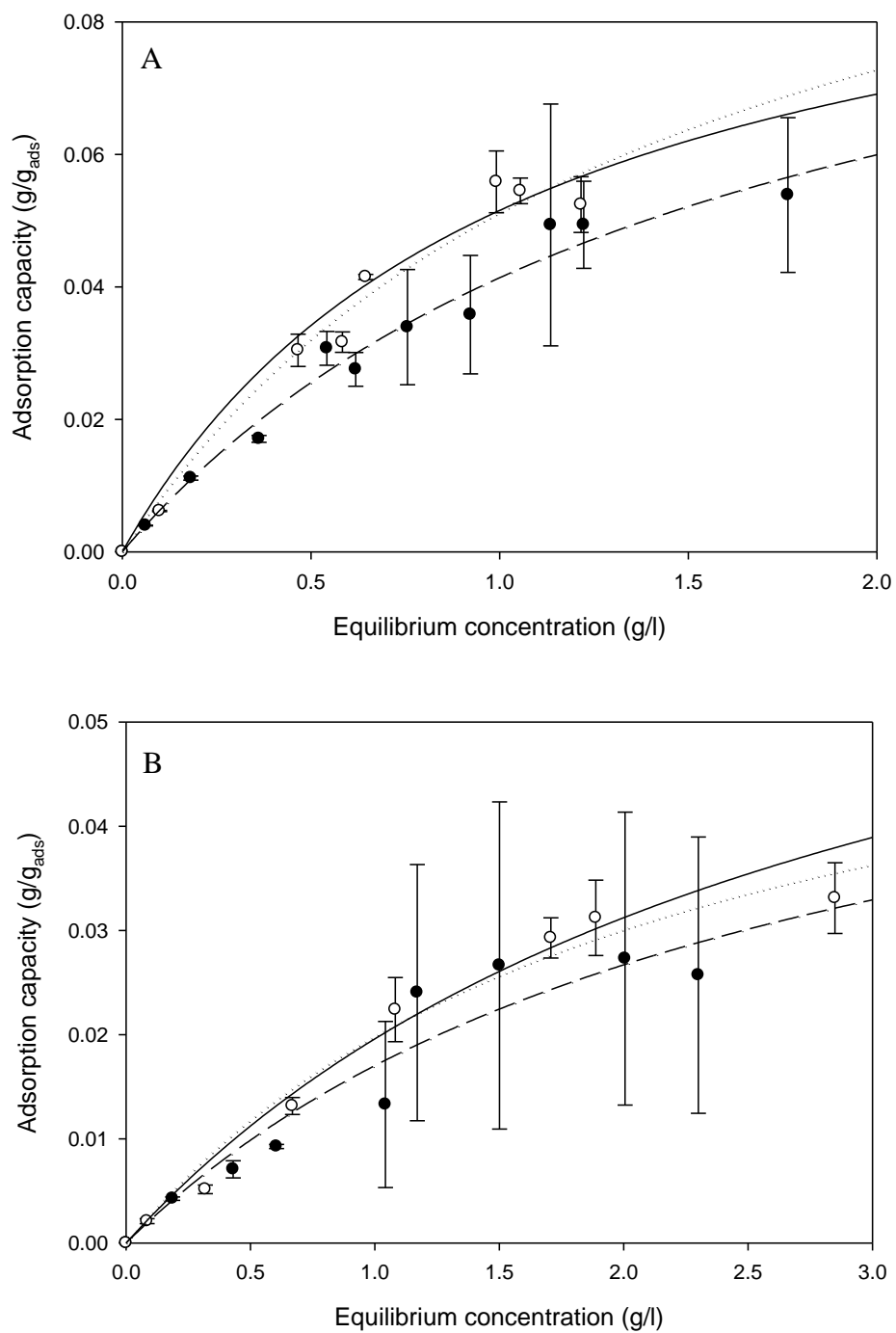


Figure 3.7 Adsorption isotherms generated using XAD7 for the adsorption of (A) ketone (B) lactone in the (●) 96 wells and (○) 24 wells microplate platforms in experiments described in section 2.3.2.1. Lines represent the Langmuir mathematical model fitted to the data as described in section 3.3.2 (solid line determined from ml scale; medium dashed line from 96 wells microplate; dotted line from 24 wells microplate). Error bars represent one standard deviation based on triplicate experiments.

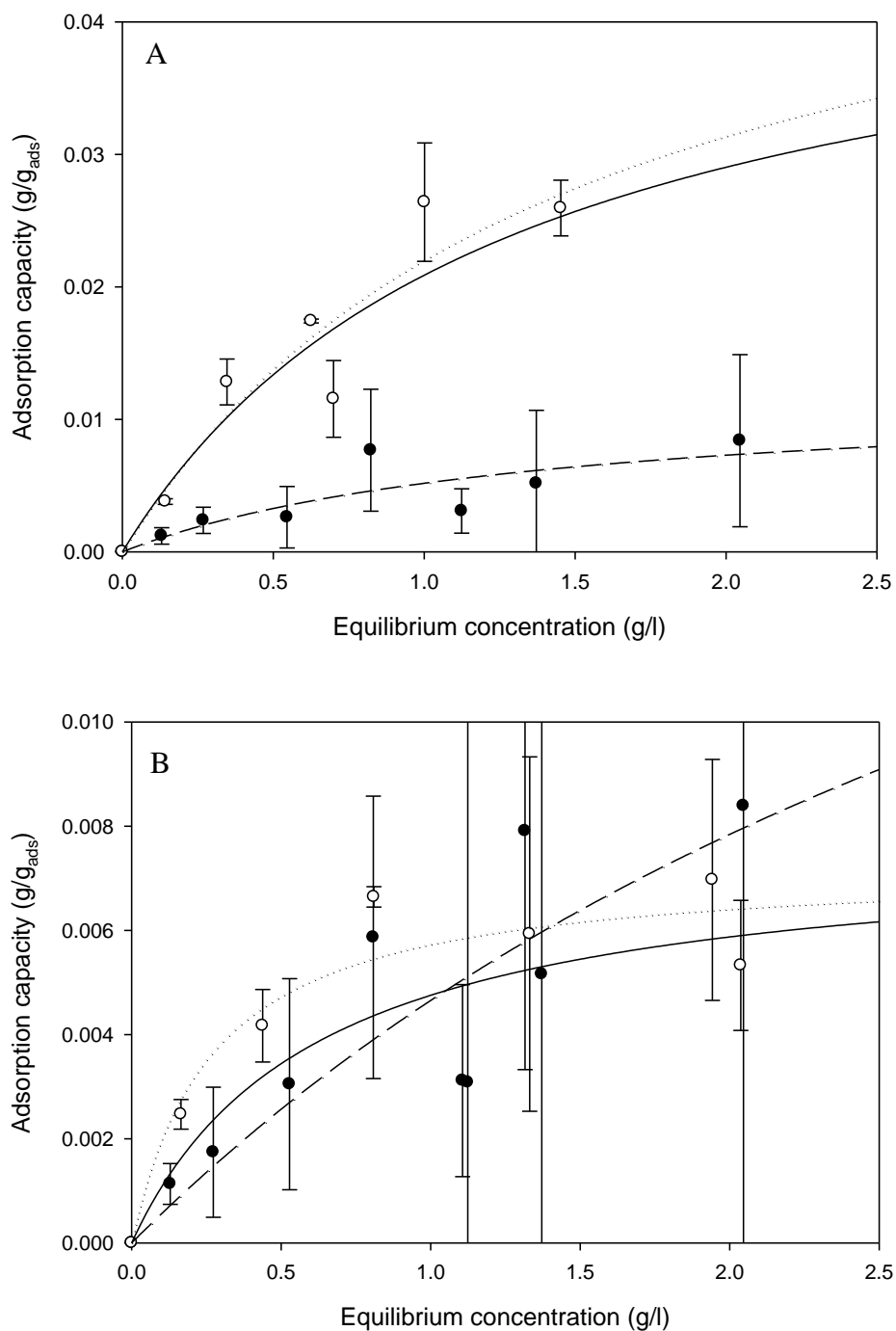


Figure 3.8 Adsorption isotherms generated using IRC50 for the adsorption of (A) ketone (B) lactone in the (●) 96 wells and (○) 24 wells microplate platforms in experiments described in section 2.3.2.1. Lines represent the Langmuir mathematical model fitted to the data as described in section 3.3.2 (solid line determined from ml scale; medium dashed line from 96 wells microplate; dotted line from 24 wells microplate). Error bars represent one standard deviation based on triplicate experiments.

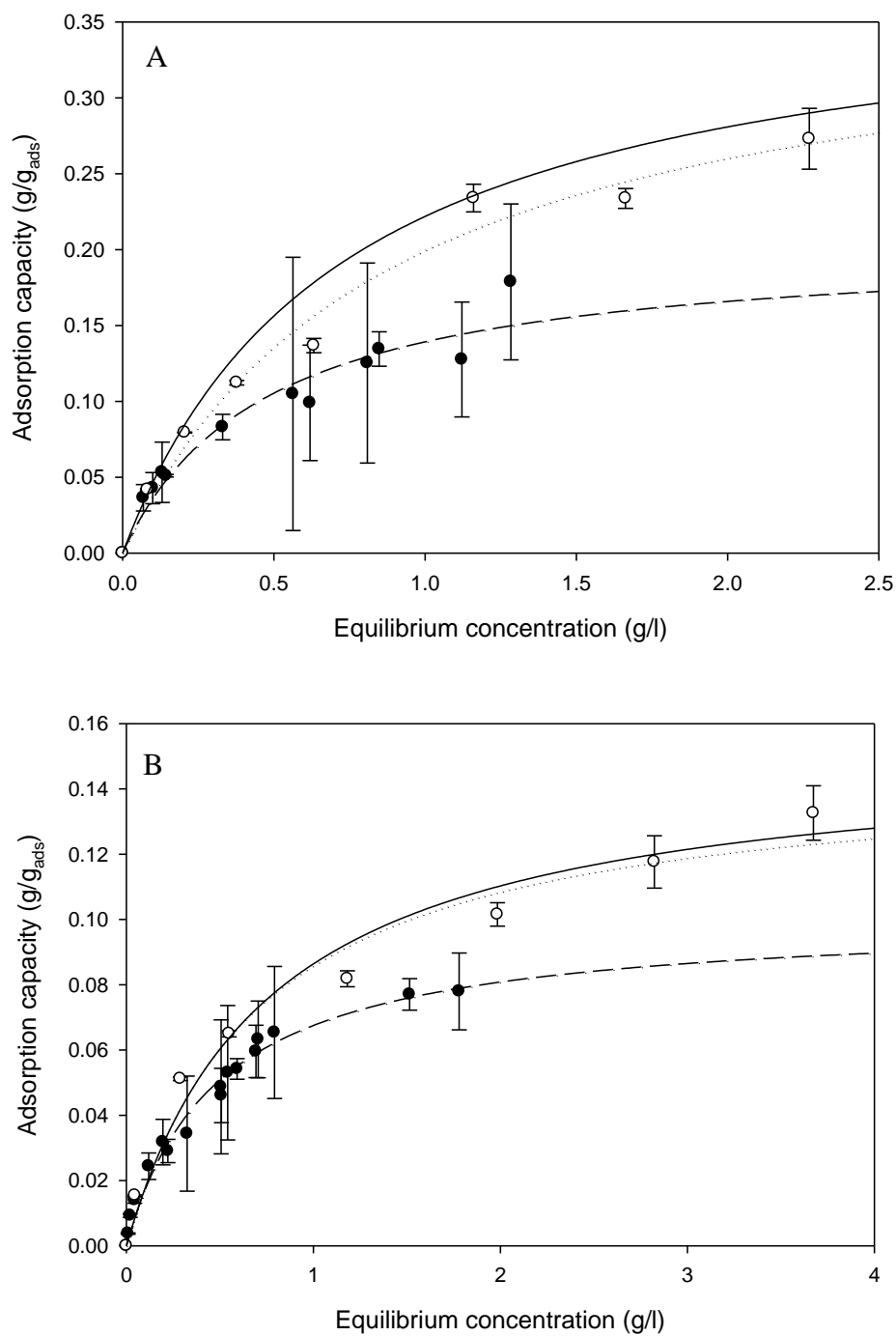


Figure 3.9 Adsorption isotherms generated using L493 for the adsorption of (A) ketone (B) lactone in the (●) 96 wells and (○) 24 wells microplate platforms in experiments described in section 2.3.2.1. Lines represent the Langmuir mathematical model fitted to the data as described in section 3.3.2 (solid line determined from ml scale; medium dashed line from 96 wells microplate; dotted line from 24 wells microplate). Error bars represent one standard deviation based on triplicate experiments.

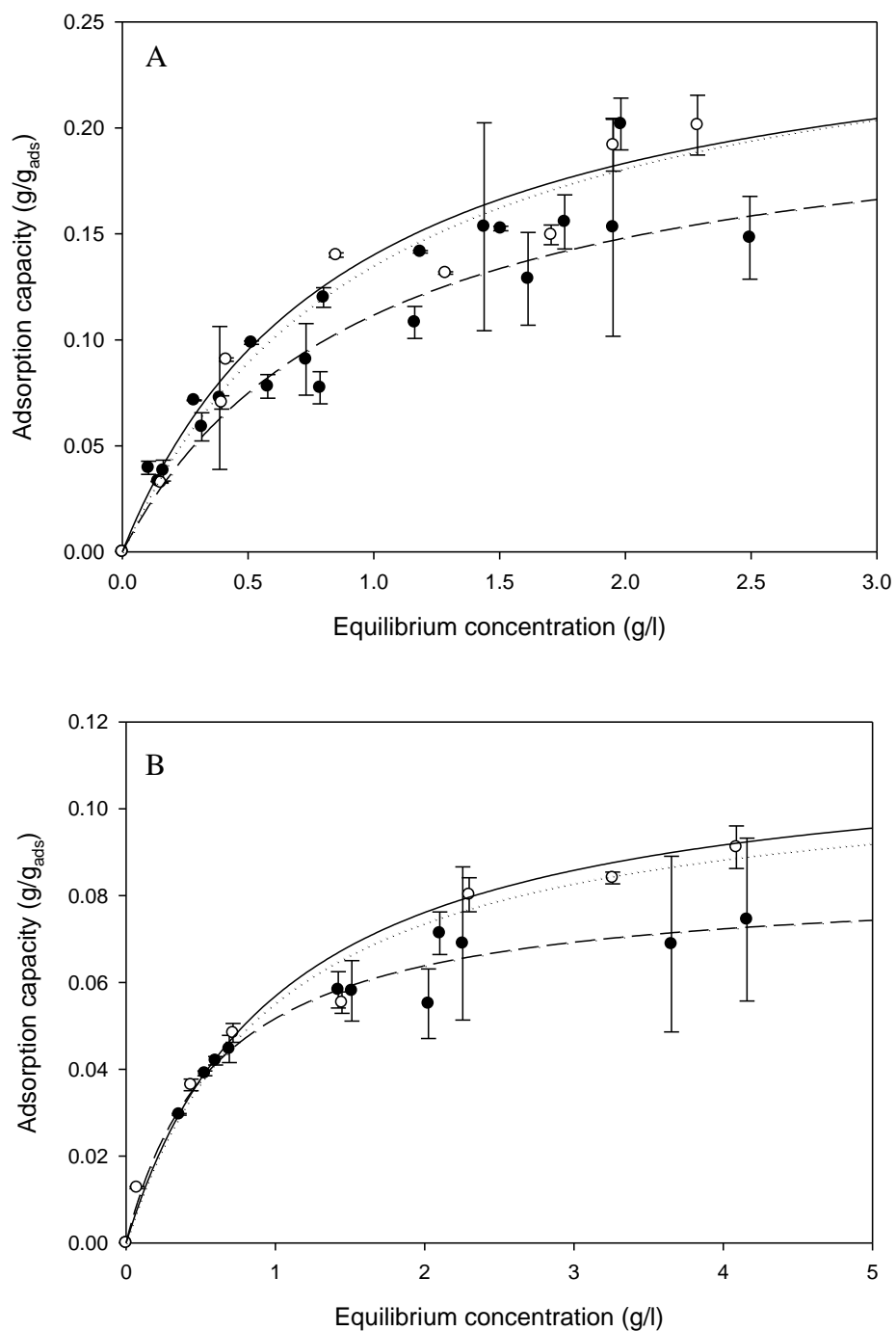


Figure 3.10 Adsorption isotherms generated using XAD4 for the adsorption of (A) ketone (B) lactone in the (●) 96 wells and (○) 24 wells microplate platforms in experiments described in section 2.3.2.1. Lines represent the Langmuir mathematical model fitted to the data as described in section 3.3.2 (solid line determined from ml scale; medium dashed line from 96 wells microplate; dotted line from 24 wells microplate). Error bars represent one standard deviation based on triplicate experiments.

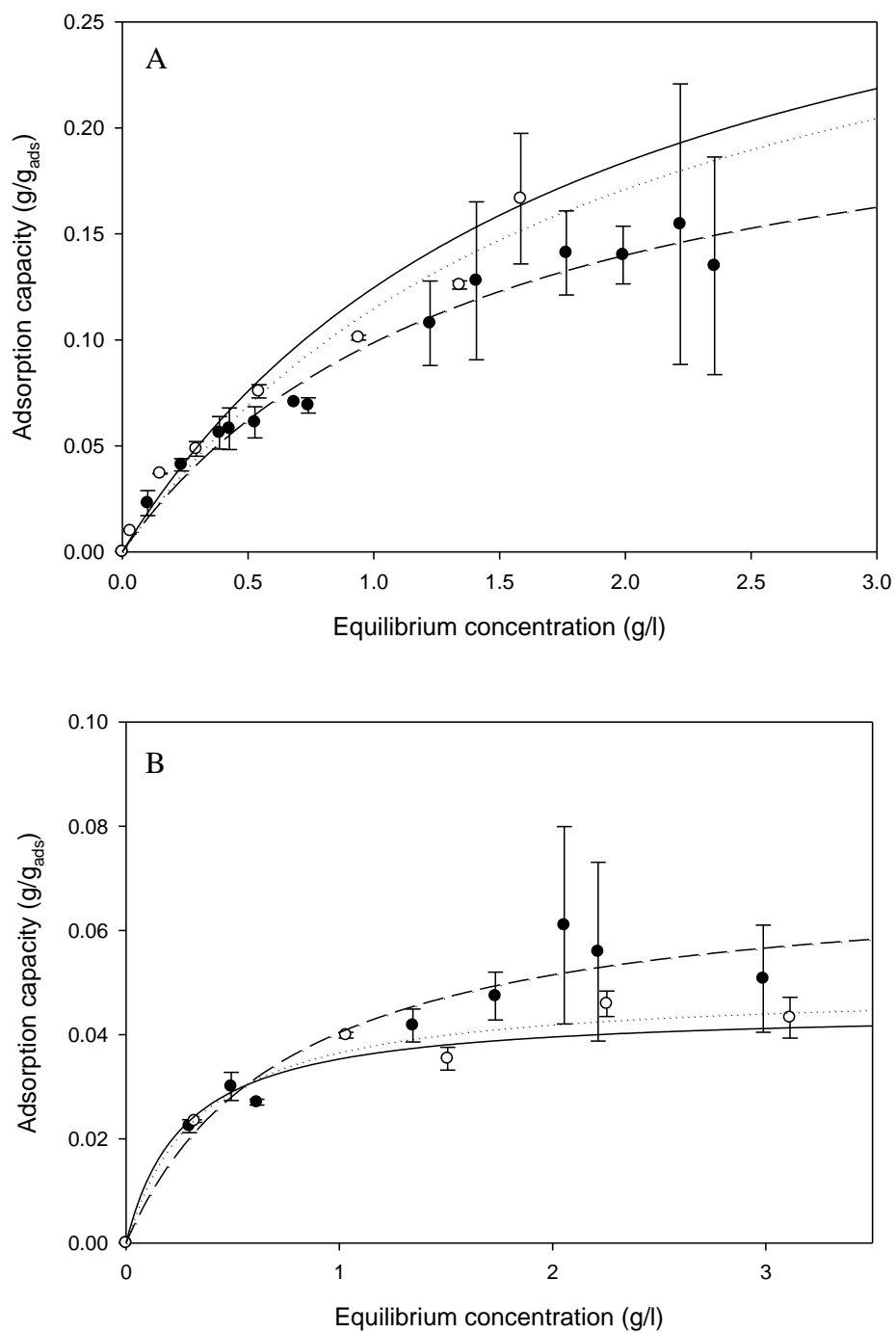


Figure 3.11 Adsorption isotherms generated using XAD16 for the adsorption of (A) ketone (B) lactone in the (●) 96 wells and (○) 24 wells microplate platforms in experiments described in section 2.3.2.1. Lines represent the Langmuir mathematical model fitted to the data as described in section 3.3.2 (solid line determined from ml scale; medium dashed line from 96 wells microplate; dotted line from 24 wells microplate). Error bars represent one standard deviation based on triplicate experiments.

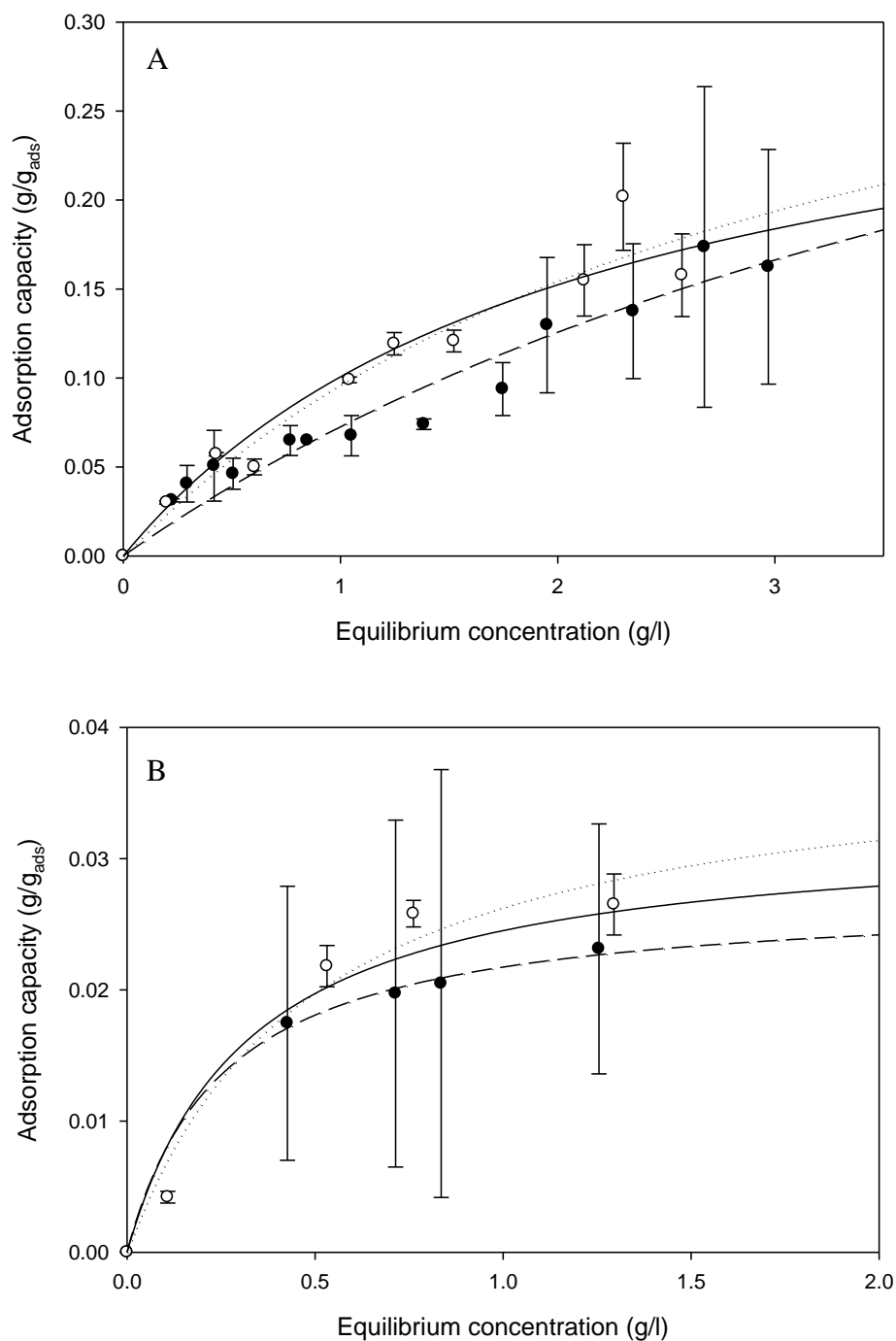


Figure 3.12 Adsorption isotherms generated using XAD1180 for the adsorption of (A) ketone (B) lactone in the (●) 96 wells and (○) 24 wells microplate platforms in experiments described in section 2.3.2.1. Lines represent the Langmuir mathematical model fitted to the data as described in section 3.3.2 (solid line determined from ml scale; medium dashed line from 96 wells microplate; dotted line from 24 wells microplate). Error bars represent one standard deviation based on triplicate experiments.

Figures A.3 to A.8 (thesis Appendix) show the Langmuir adsorption models as in figures 3.7 to 3.12 with the addition of 95% confidence interval bands for the Langmuir adsorption model determined for the adsorption results from the ml-scale. A confidence interval band shows a probability/estimate of the fitted regression lines falling within it and the higher the percentage of confidence interval is, the tighter the band will be. In the case of figures A.3 to A.8, the percentage of confidence interval is set at 95% and those adsorption models, generated from the 96 wells and 24 wells microplate, that fall within the band show a very good fit to the adsorption model generated at the ml-scale and hence the confidence to use the microplate platforms for HTRS.

The adsorption models generated in the 24 wells microplate, all fall within the 95% confidence interval band as seen in figures A.3 to A.8, however only the Langmuir model determine for adsorption of lactone on XAD1180 in the 96 wells microplate shows a good fit to the model from the ml-scale. The possible reason for the poor fit of adsorption models generated in the 96 wells microplate platform is the same as the one alluded to in the discussion at the beginning to this section. The lack of resin suspension reduces that surface available to the ketone and lactone to adsorb on to, resulting in poor adsorption.

Table 3.3 summarises the parameters from the Langmuir adsorption isotherm shown in figures 3.7 to 3.12 and compares the adsorption of ketone and lactone on all six resins at the 96 well, 24 well and bench scales.

Table 3.3 Comparison of Langmuir parameters for adsorption on ketone and lactone at the three different scales

Resin	Compound	Bench scale		96 microwell		24 microwell	
		Q_{\max} (g/g _{adsorbent})	K_A	Q_{\max} (g/g _{adsorbent})	K_A	Q_{\max} (g/g _{adsorbent})	K_A
XAD7	Ketone	0.105	0.967	0.109	0.614	0.126	0.684
	Lactone	0.077	0.342	0.062	0.380	0.062	0.470
IRC50	Ketone	0.048	0.781	0.012	0.721	0.055	0.679
	Lactone	0.008	1.621	0.025	0.230	0.007	3.738
L493	Ketone	0.383	1.381	0.205	2.113	0.374	1.143
	Lactone	0.152	1.307	0.101	2.035	0.147	1.407
XAD4	Ketone	0.265	1.118	0.220	1.034	0.273	0.980
	Lactone	0.115	0.975	0.084	1.627	0.110	1.007
XAD16	Ketone	0.351	0.552	0.240	0.698	0.335	0.526
	Lactone	0.045	3.677	0.071	1.323	0.049	2.943
XAD1180	Ketone	0.313	0.474	0.471	0.182	0.394	0.324
	Lactone	0.032	3.109	0.027	3.934	0.039	2.053

Adsorption in the 24 wells microplate also demonstrates similar adsorption capacity at a ketone equilibrium concentration of 0.5g/l to adsorption capacities found at the ml-scale, compared to the 96 wells microplate as can be seen in table 3.4. The difference of adsorption capacity between the 24 wells microplate platform and the ml-scale does not exceed 12%, however the difference, when using the 96 wells microplate platform, ranges from as low as 5% to as high as 91%.

Table 3.4 Comparison of adsorption capacities of six resins at three different scales, at a ketone equilibrium concentration of 0.5g/l

Resin	Q_{ads} (g/g _{adsorbent}) at C_{eq} 0.5g/l ketone (percentage difference to ml-scale)		
	ml-scale	96 microwell	24 microwell
XAD7	0.035	0.024 (37%)	0.031 (12%)
IRC50	0.012	0.0045 (91%)	0.012 (0%)
L493	0.21	0.2 (5%)	0.2 (5%)
XAD4	0.11	0.082 (29%)	0.1 (9.5%)
XAD16	0.082	0.061 (29%)	0.076 (7.6%)
XAD1180	0.059	0.056 (5.2%)	0.054 (8.8%)

3.5 Adsorption kinetics studies

The successful mimic of equilibrium adsorption in the 24 wells microplate platform and the larger variance in adsorption in the 96 wells microplate platform, determined the 24 wells microplate as the platform to use to perform kinetics studies on all six resins. These experiments were performed as described in section 2.3.2.2 to determine the degree of selectivity of the resins for one compound over the other by comparing the initial rates of adsorption of ketone and lactone on resins. The results will show which type of resin is suitable to be used as the substrate feeding tool and which type of resin will be effective to be used for product removal in the dual resin SFPR bioconversion strategy.

Over the course of the Baeyer-Villiger bioconversion, with the conversion of substrate and formation of product, there will not be a state of equilibrium with respect to adsorption of ketone and lactone on resins. Understanding dynamic interactions of substrate and product with resins alongside interactions at equilibrium, i.e. adsorption isotherms, would help better design of resin based SFPR bioconversion strategies

Figures 3.13 to 3.18 show the combined adsorption of ketone and lactone, each at an initial concentration of 1g/l, on each of the six resins over time. The data shown in these figures are of the initial ketone and lactone load on resin before equilibrium has been reached. It is important to add that the concentration of both ketone and lactone in solution at the start of the experiment is set as 1g/l because this will not lead to resin saturation and therefore the interactions will be based only on the affinity of resin for the two compounds and not competition over scarce adsorption sites.

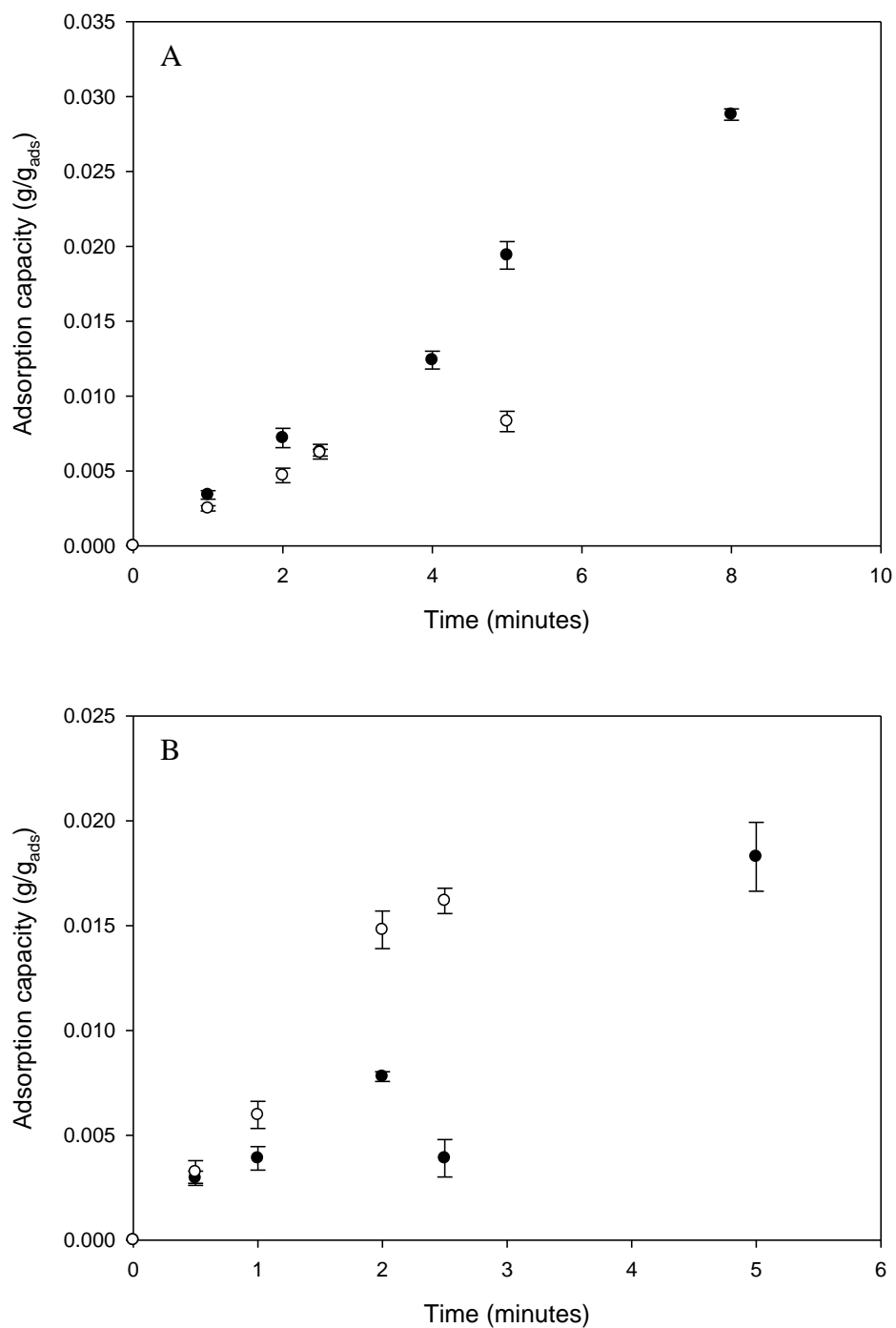


Figure 3.13 Time course of the dual compound adsorption of (●) ketone and (○) lactone on (A) XAD7 and (B) IRC50 in experiments described in section 2.3.2.2. Error bars represent one standard deviation based on triplicate experiments.

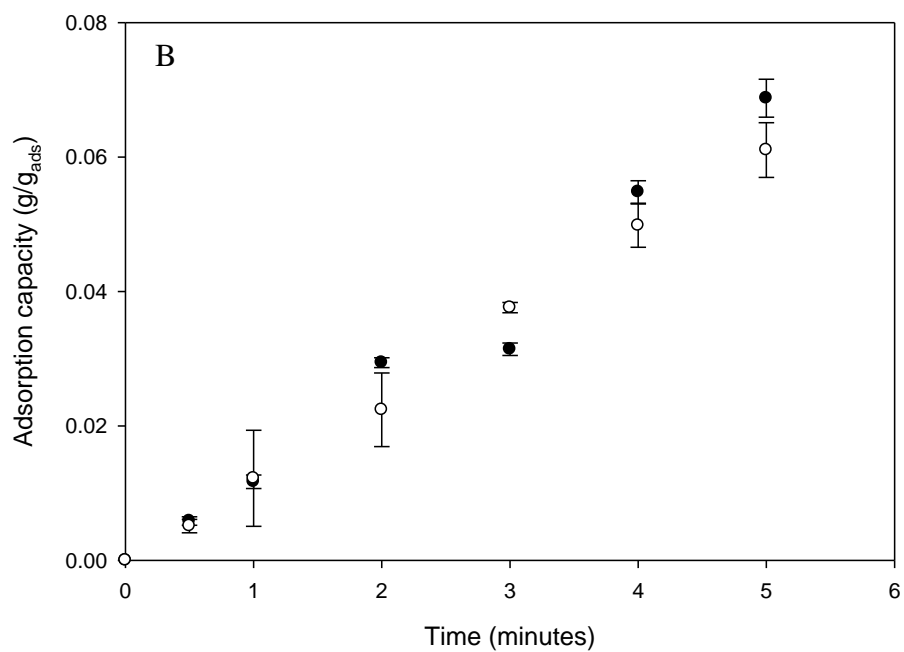
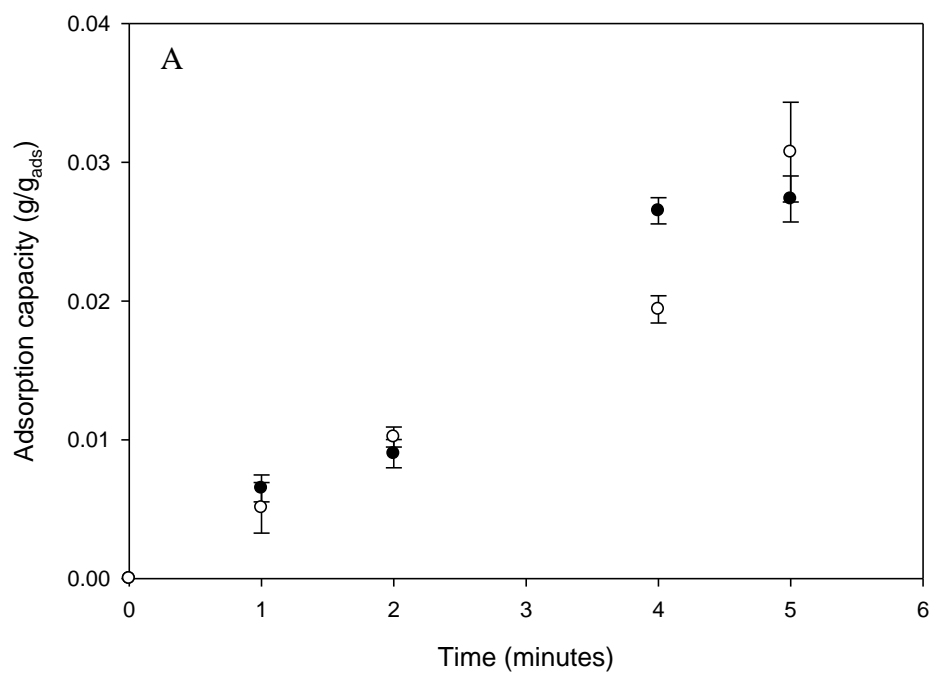


Figure 3.14 Time course of the dual compound adsorption of (●) ketone and (○) lactone on (A) L493 and (B) XAD4 in experiments described in section 2.3.2.2. Error bars represent one standard deviation based on triplicate experiments.

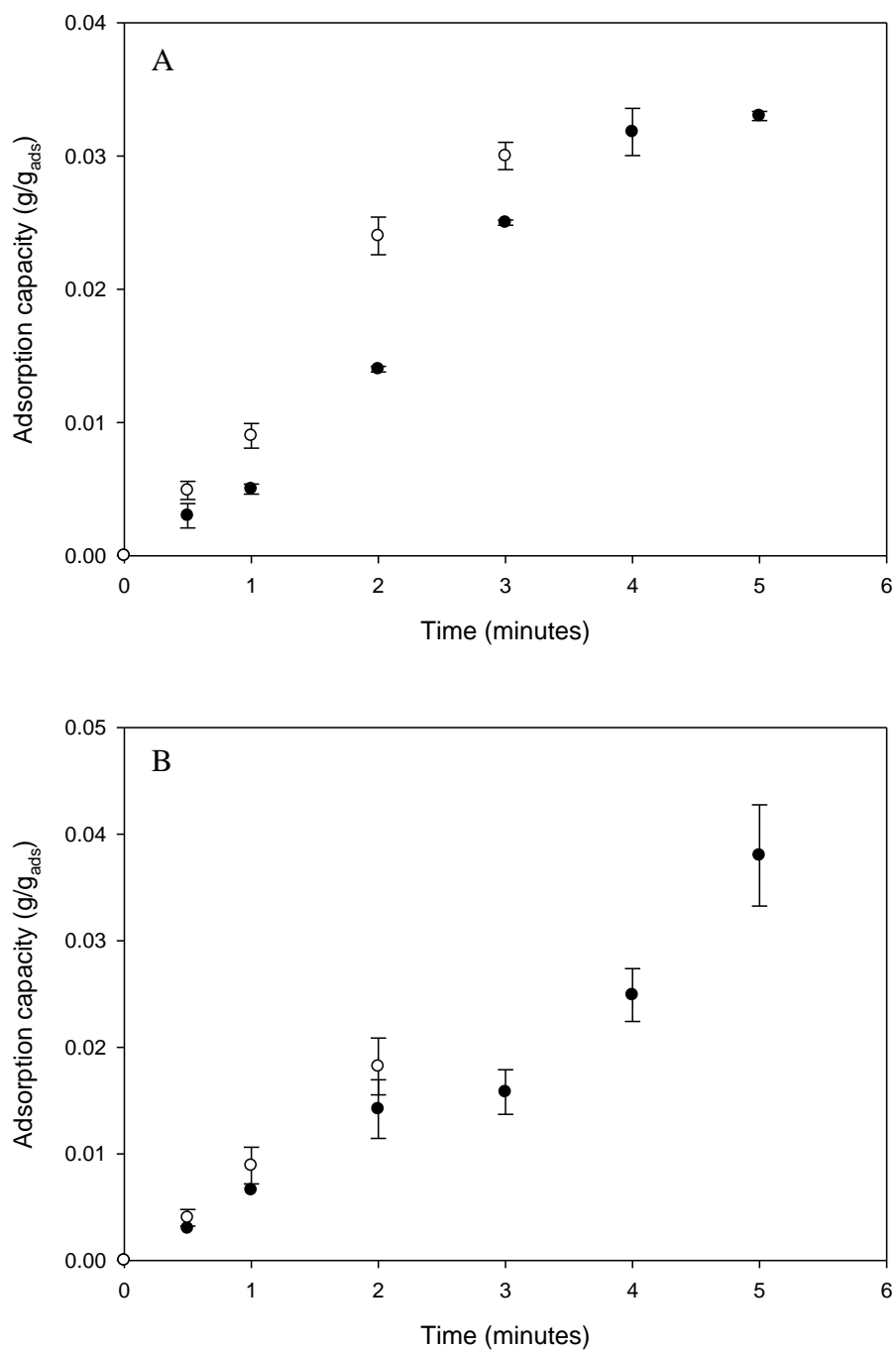


Figure 3.15 Time course of the dual compound adsorption of (●) ketone and (○) lactone on (A) XAD16 and (B) XAD1180 in experiments described in section 2.3.2.2. Error bars represent one standard deviation based on triplicate experiments.

Table 3.5 shows the selectivity of each resin for ketone and lactone. The greatest selectivity achieved for ketone is seen with resin XAD7 and resin IRC50 shows greater selectivity for lactone than any other resin tested. Overall, resins do demonstrate selectivity for one compound of the other. Resins XAD16 and XAD1180 show similar affinities for lactone over ketone, whereas resins L493 and XAD4 show similar, but slight, selectivity for ketone over lactone.

Table 3.5 Selectivity for ketone and lactone, as determined by equation 4, for each of the six resins

XAD7	IRC50	L493	XAD4	XAD16	XAD1180
1.84	0.49	1.04	1.08	0.70	0.76

3.6 HTRS efficiency

The highlights of the above described HTRS method, in a 24 wells microplate platform, are the speed and ease of performing adsorption isotherm (section 3.4.3) and adsorption kinetic (section 3.5) studies. The amounts of raw material used in the HTRS are significantly less than used for the ml-scale adsorption studies (section 3.4.1), for example 98.5% less resin is needed for performing HTRS based on 1% (w/v) of resin. This has the significant impact of reducing costs especially when screening the vast number of resins that are commercially available.

Reducing the amount of raw material also reduces the experiments' footprint and simplifies the practicality aspect by bringing numerous experiments together in one microplate (which then allows the use of a multichannel pipette). This was crucial when performing adsorption kinetic experiments where accurate sampling, with respect to timing, is a necessity.

Finally, implementing the HTRS method reduces the investigation time by performing numerous experiments in parallel and, in the case of adsorption isotherm studies, reducing the experiment duration. It needs a minimum of 10 hours to perform adsorption isotherm studies at the bench scale but only 3-4 hours using the HTRS method.

3.7 Conclusions

This chapter has presented a study of adsorption of ketone and lactone on six different resins at three different scales- bench, 96 microwell and 24 microwell platforms. Results were fitted to Langmuir and Freundlich adsorption isotherm models and compared. High speed image analysis was also performed to get an understanding of mixing of resins in the 96 microwell and 24 microwell platforms.

Out of the six resins, L493 showed the highest maximum adsorption capacity for both ketone, $0.38\text{g/g}_{\text{adsorbent}}$, and lactone, $0.15\text{g/g}_{\text{adsorbent}}$. More importantly, the highest adsorption capacity for ketone at an equilibrium concentration of 0.5g/l was also seen with the L493 resin, $0.21\text{ g/g}_{\text{adsorbent}}$.

Results from high throughput adsorption studies showed similar trends however greater variance was observed with the 96 microwell platform and a more accurate mimicry of the bench scale adsorption study from the 24 microwell platform.

Zhang et al (2008) reported that fluid mixing is more intensive in the 96 microwell platform than in the 24 microwell platform, however for the suspension of resins, based on resin suspension experiments, better suspension is achieved in the 24 microwell platform.

It was decided to perform kinetics study using the 24 microwell platform, based on the equilibrium adsorption experiments and also because the high throughput nature of experiments was demonstrated.

The kinetics study performed showed the adsorption dynamics of combined adsorption of ketone and lactone on all six resins. It was found that resin XAD7 has the greatest selectivity for ketone and IRC50 for lactone.

Thus, from the results generated from the equilibrium adsorption and kinetics studies in this chapter, it can be concluded that the best resins to be used for an effective SFPR strategy are XAD7 for the desorption of ketone, and IRC50 for the adsorption of lactone.

Chapter 4. Demonstrating a ‘proof of concept’ of the novel dual resin SFPR strategy in shake flasks

4.1 Aims

The objective of this chapter is to design a novel dual resin SFPR strategy for the Baeyer-Villiger bioconversion. The performance of the process will be experimentally investigated to determine whether employing the dual resin SFPR increases the productivity in comparison to bioconversions carried out without resins or using a single resin SFPR.

4.2 Introduction

The whole cell catalysed Baeyer-Villiger bioconversion’s inability to produce large amounts of the lactone at both high concentrations of substrate and product necessitates a strategy to overcome these inhibitions. Attempts to implement a resin based strategy have successfully resulted in an increase of product concentration. These strategies have used a single type of resin either as an ISPR tool or SFPR tool (section 1.4.2).

The investigation of this chapter is to implement a dual resin SFPR strategy to carry out a Baeyer-Villiger bioconversion. This strategy will use two different types of resins, one for substrate feeding and the other for product removal. The choice of resins is based on the results from the resin screening in the previous chapter.

4.3 Results

4.3.1 Demonstration of substrate inhibition in the BV bioconversion

Prior to investigation of the dual resin SFPR strategy, the reaction rate for the BV bioconversion was determined at initial substrate concentrations of 0.4g/l, where product formation is at its optimum (Doig *et al*, 2003), and 3g/l, 7.5 times larger than the optimum substrate concentration.

Bioconversions were performed in 50mM phosphate buffer with a working volume of 10% (v/v) after preliminary experiments demonstrated better substrate conversion under these conditions than performing the bioconversion in fermentation media, directly after cell growth, with a working volume of 20% (figure A.10 in Appendix). Using a buffer as the medium for bioconversion gives the benefit of better pH stabilisation and any negative effects on the enzymatic or metabolic activity possibly caused by undefined by-products and/or fermentation media components is eradicated. An additional point to mention is that the centrifugation and resuspension of cells caused no damage to the cells.

A lower working volume results in a higher gas-liquid interface to liquid volume ratio, at constant fixed rates, thus enabling a larger liquid surface for oxygen transfer for better aeration in the culture. A sufficient oxygen supply is particularly important in an oxidation reaction such as the Baeyer-Villiger reaction and the improved reaction rate seen with decreasing the working volume is in line with the report of effect of limited oxygen supply to conversion in this reaction by Baldwin and Woodley (2006).

Figure 4.1 shows the profile of lactone formation at the above mentioned ketone concentrations without resins. It can be observed that an increase in substrate concentration has an adverse effect on the rate of lactone production. At the initial substrate concentration of 0.4g/l, lactone production is achieved at a rate of 1.52g/l/h whereas the rate of lactone formation is dramatically decreased with a starting ketone concentration of 3g/l, to a rate of 0.34g/l/h. The whole cell biocatalyst activity at 0.4g/l

and 3.0g/l initial ketone concentrations are determined to be 25.5U/g_{DCW}, ±0.12%, and 5.7U/g_{DCW}, ±0.16%, respectively.

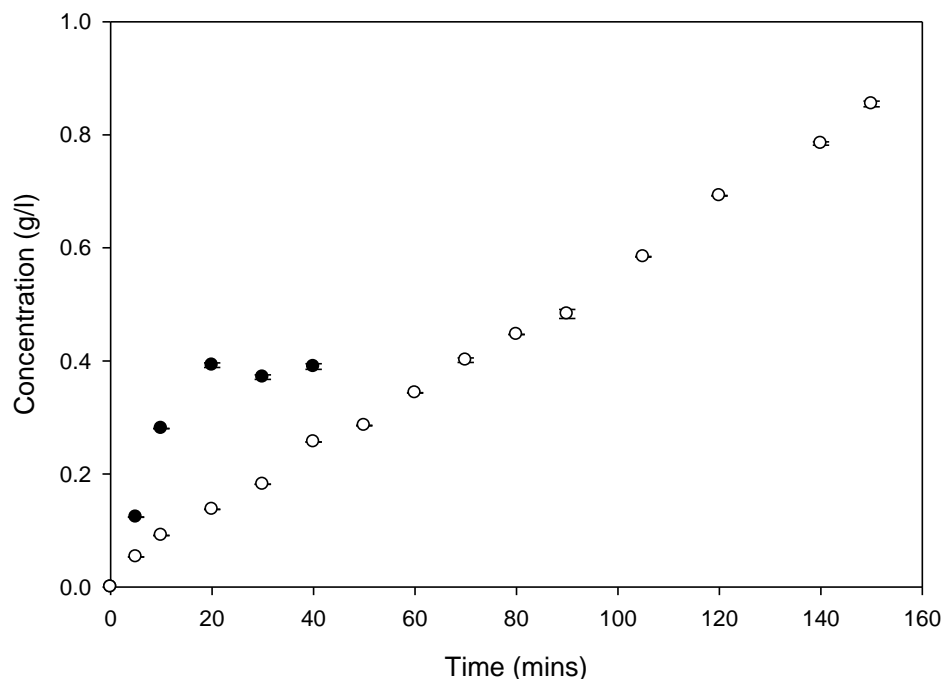


Figure 4.1 Production of lactone by *E. coli* TOP10 [pQR239] biocatalyst (8g_{DCW}/l) using initial ketone concentrations of (●) 0.4g/l and (○) 3g/l, without the use of a resin SFPR strategy as described in section 2.5.1. Error bars represent one standard deviation based on triplicate experiments.

This set of experiments demonstrates the substrate inhibition in this bioconversion and also sets a bench mark for the resin based SFPR bioconversions. The subsequent resin based bioconversions will therefore be carried out with an initial substrate concentration of 3g/l to compare their performances with that of the performances of the bioconversions without resins.

4.3.2 Single resin SFPR strategy

Hilker *et al.* (2004a) described a single resin SFPR (using L493 as the resin) to carry out a BV bioconversion and deemed it the best example of a ‘highly productive’ strategy for this reaction. Thus another bench mark was determined from the single resin strategy which is to be compared to the dual resin SFPR strategy.

Figure 4.2 shows the results from the single resin SFPR strategy to perform the BV bioconversion. Specifically, this figure shows the accumulation of both ketone and lactone in the aqueous phase and also the adsorbed concentration on L493 (observed as vertical bars). The experiment utilised resin L493 (ketone loaded to the capacity of $0.21\text{g/g}_{\text{resin}}$) which exhibited the highest maximum adsorption capacity and the highest adsorption capacity at an equilibrium ketone concentration of 0.5g/l out of the six resins investigated in Chapter 3.

The ketone concentration in the aqueous phase decreased in parallel with lactone formation for the first 100 minutes of the reaction and decreased to below 0.5g/l , as expected based on the adsorption studies in section 3.4.1. Also, lactone concentration in the aqueous phase did not exceed 1.08g/l over the course of the reaction, showing that it did not contribute to any reaction inhibition. This demonstrates that both desorption of the substrate and adsorption of the product were adequate enough as not to limit the reaction by lack of ketone in the aqueous phase and hinder the reaction by an unwanted accumulation of lactone.

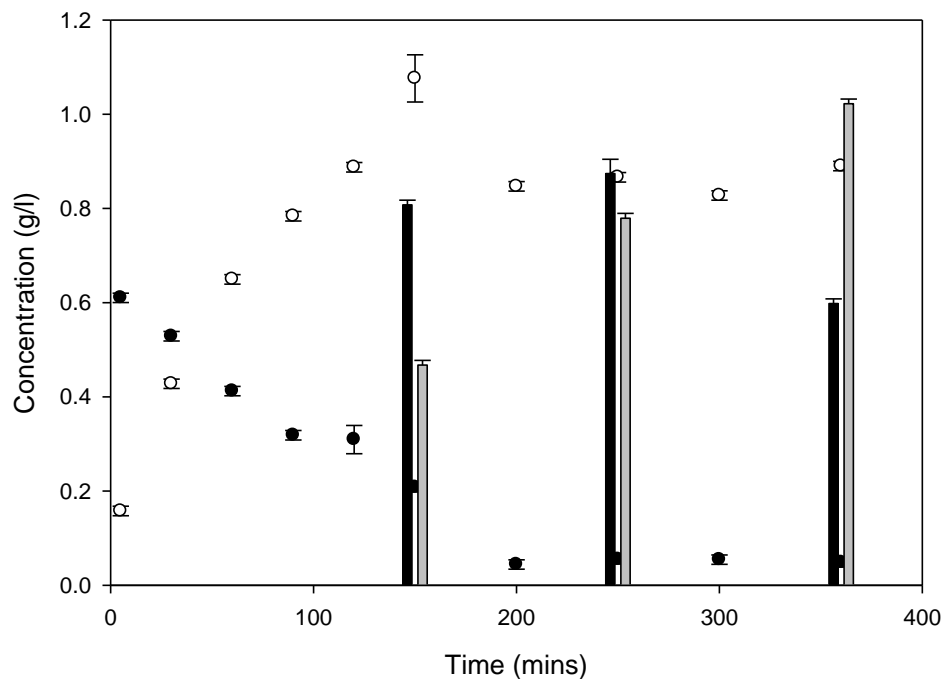


Figure 4.2 Single resin SFPR strategy, with use of L493 (8g/l) resin, for the production of lactone by *E. coli* TOP10 [pQR239] biocatalyst (8g_{DCW}/l) using an initial ketone concentration of 3g/l on the resin as described in section 2.5.2. (●) ketone in aqueous phase, (○) lactone in aqueous phase, (■) ketone adsorbed on L493 and (□) lactone adsorbed on L493. Error bars represent one standard deviation based on triplicate experiments.

There was a linear increase of lactone accumulation on the L493 resin over the 6 hours of the reaction however there was not a linear desorption of ketone from L493 as expected. The amount of ketone bound to the resin did decrease to 0.81g/l after 2.5 hours from 3g/l at the start of the reaction but after 4 hours it increased slightly to 0.87g/l. After 2.5 hours the ketone concentration in the aqueous phase is decreased to ca. 0.05g/l and became constant indicating an equilibrium state for the reaction has occurred which meant that ketone had to re-adsorb onto the resin. The increase in ketone accumulation could have suggested a significant experimental error if it was not for the fact that ketone and lactone recovery, from both the aqueous phase and resin, at 150, 250 and 360 minutes remained constant at 85%, the overall ketone concentration decreased

in parallel with overall lactone production and by 6 hours ketone accumulation on the resin had decreased.

Overall productivity of lactone using the single resin SFPR strategy was 0.73g/l/h and out of the total lactone produced 53% of lactone accumulated on the resin. The whole cell biocatalyst activity was determined to be 24.6U/g_{DCW}, $\pm 5.2\%$.

4.3.3 Dual resin SFPR strategy

Two combinations of resins were investigated based on the adsorption capacity and adsorption kinetic studies in Chapter 3. The first combination used L493 (ketone loaded to the capacity of 0.21g/g_{resin}) for the substrate feed as it exhibited the highest capacity for ketone and the second combination utilised XAD7 (ketone loaded to the capacity of 0.035g/g_{resin}) to feed the ketone as it exhibited the highest selectivity for ketone. Both combinations used IRC50 (amount added to system to the capacity of 0.008 g/g_{resin}) as the product removal tool due to its high selectivity of lactone over ketone.

Preliminary experiments (data not shown) of the dual resin SFPR strategy were carried out with the total amount of IRC50, required for product removal, added all at once. This resulted in poor conversion to lactone possibly due to ketone being adsorbed faster onto IRC50 than the cell uptake rate of the substrate (assumption being that rate of substrate conversion is proportional to uptake rate). Therefore a method of sequential addition of IRC50 into the system was employed based on the rate of adsorption of ketone onto IRC50, 0.198g/g_{resin}/h, determined in section 3.5. However it is important to note that adsorption of ketone by IRC50 cannot be completely eliminated.

Dual resin SFPR strategies were performed using two methods: (1) both resins were free in suspension in the aqueous phase and (2) IRC50 was held in a filter bag separated from the resin loaded with ketone. The latter method allowed the analysis of solute accumulation on each resin used in the dual resin SFPR strategy.

4.3.3.1 Dual resin SFPR using two resins free in suspension

Figures 4.3 and 4.4 show the conversion of ketone to lactone using L493 and XAD7 as tools for substrate feeding, respectively. The vertical bars show solute accumulation on both the resins used for ketone feeding and product removal.

Overall productivity of lactone using L493 and XAD7 as the substrate feeding tools in the dual resin SFPR strategy were 0.90g/l/h and 0.96g/l/h, respectively. The whole cell biocatalyst activity using the L493-IRC50 and XAD7-IRC50 combinations are determined to be 22.5U/g_{DCW}, ±9.1%, and 23.9U/g_{DCW}, ±8.4%, respectively. Lactone accumulation on resins in the L493-IRC50 combination was achieved to 85% and with the XAD7-IRC50 combination 87% of lactone accumulated onto both resins.

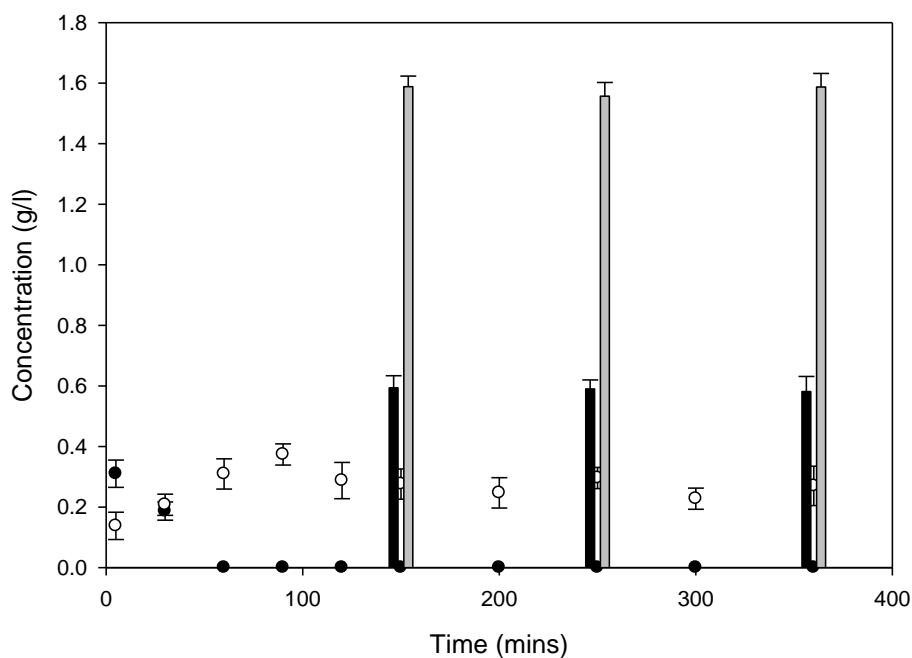


Figure 4.3 Dual resin SFPR, with use of L493 (8g/l) and IRC50 (300g/l) as substrate and product reservoirs respectively, for the production of lactone by *E. coli* TOP10 [pQR239] biocatalyst (8g_{DCW}/l) using an initial ketone concentration of 3g/l, as described in section 2.5.3.1. (●) ketone in aqueous phase, (○) lactone in aqueous phase, (■) ketone adsorbed on both resins and (▨) lactone adsorbed on both resins. 1g of fresh IRC50 added every 10 minutes, from $t=10$ mins, to a total of 20g. Error bars represent one standard deviation based on triplicate experiments.

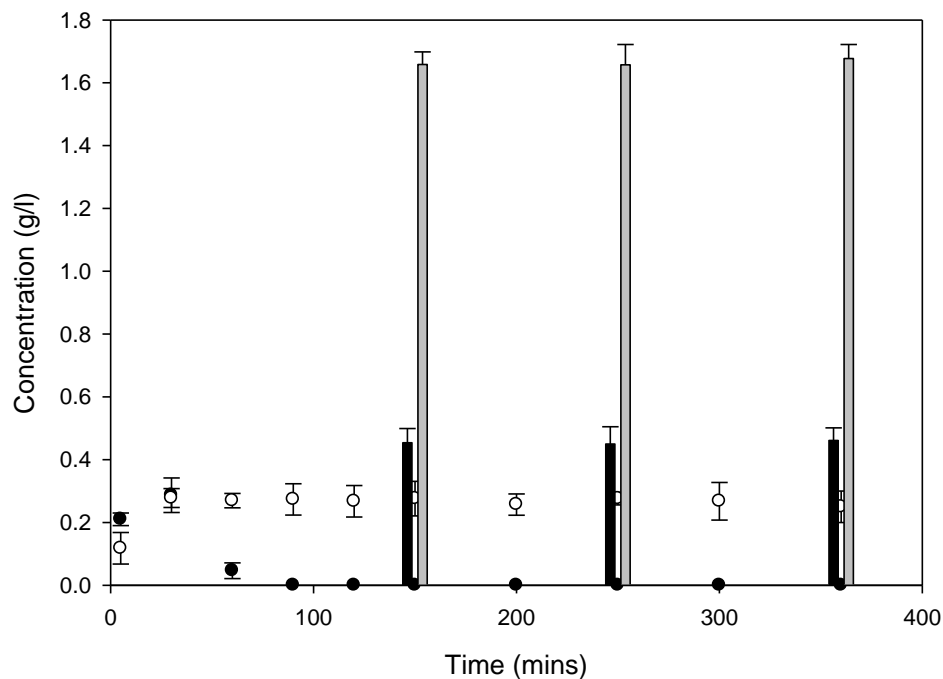


Figure 4.4 Dual resin SFPR, with use of XAD7 (60g/l) and IRC50 (300g/l) as substrate and product reservoirs respectively, for the production of lactone by *E. coli* TOP10 [pQR239] biocatalyst (8g_{DCW}/l) using an initial ketone concentration of 3g/l, as described in section 2.5.3.1. (●) ketone in aqueous phase, (○) lactone in aqueous phase, (■) ketone adsorbed on both resins and (■) lactone adsorbed on both resins. 1g of fresh IRC50 added every 10 minutes, from $t=10$ mins, to a total of 20g. Error bars represent one standard deviation based on triplicate experiments.

The aqueous phase concentration of both substrate and product for both experiments were low enough to prevent any solute inhibition. However with regards to ketone concentration, which was close to zero after ca. 60 minutes, it can be suggested that availability of ketone for conversion was a rate-limiting step. Also, the concentration of ketone and lactone accumulated on resins in both experiments remained constant from 2.5 hours onwards and with no increase of lactone concentration in the aqueous phase there a possibility that the reaction had stopped before 2.5 hours. Preliminary experiments (data not shown) showed that bioconversion is still carried out prior to 2.5 hours at negligible ketone concentrations.

Analysis of glycerol concentration post experiments were carried out to determine if there were insufficient amounts of glycerol available for bioconversion to take place. Concentrations of 8.1g/l, $\pm 15.7\%$, and 7.6g/l, $\pm 16.3\%$, of glycerol were still available in the bioconversion medium when using the L493-IRC50 and XAD7-IRC50 combinations, respectively. Doig *et al.* (2003) stated that below 5g/l of aqueous glycerol concentration reduces enzyme specific activity therefore lack of glycerol is not responsible for the apparent stoppage of bioconversion.

Also, after filtering off the aqueous phase from the resins bioconversions were carried out at a substrate concentration of 0.2g/l, which showed full conversion and no decrease of reaction rate. One explanation for the apparent stoppage of product formation is the competition between the resins and cells for the ketone, as mentioned earlier in the introduction of section 4.3.3. The ketone in solution will adsorb onto fresh IRC50 resin that is sequentially added and also re-adsorb onto the resin used as the substrate feeding tool.

4.3.3.2 Dual resin SFPR with the substrate feeding resin in filter bag

Figures 4.5 and 4.6 show the conversion of ketone to lactone using L493 and XAD7 as tools for substrate feed, whilst contained in a filter bag, respectively, and IRC50 for product removal. The vertical bars show solute accumulation on both the resins used for ketone feeding and product removal.

Separation of the two types of resins helps to analyse each resins' effectiveness of playing the role assigned to them, for example, whether the resin chosen for product removal, based on its high selectivity for lactone over ketone, is able to achieve complete adsorption of the product during the bioconversion, thus preventing the other type of resin from removing the lactone.

Overall productivity of lactone for both resin combinations was 0.91g/l/h, whilst the whole cell biocatalyst activity using the L493-IRC50 and XAD7-IRC50 combinations are determined to be 21.8U/g_{DCW}, ±11.1%, and 21.3U/g_{DCW}, ±12.3%, respectively. Lactone accumulation on resins with the L493-IRC50 combination was achieved to 87% and with the XAD7-IRC50 combination 85% of lactone accumulated onto both resins.

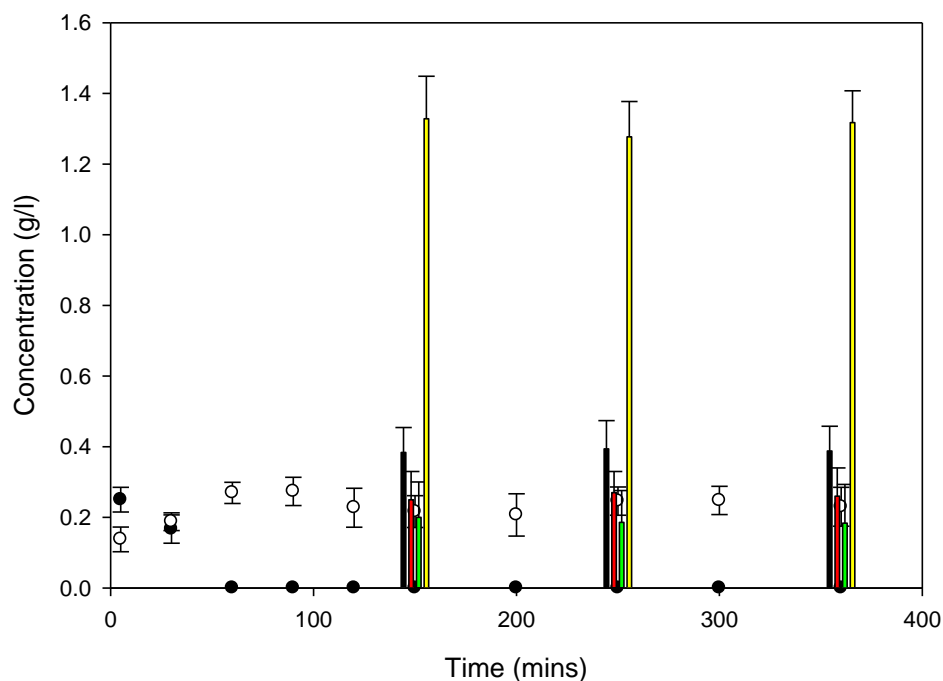


Figure 4.5 Dual resin SFPR, with use of L493 (8g/l) and IRC50 (300g/l) as substrate and product reservoirs respectively, for the production of lactone by *E. coli* TOP10 [pQR239] biocatalyst (8g_{DCW}/l) using an initial ketone concentration of 3g/l, as described in section 2.5.3.2. (●) ketone in aqueous phase, (○) lactone in aqueous phase, (■) ketone adsorbed on L493, (■) lactone adsorbed on L493, (■) ketone adsorbed on IRC50 and (■) lactone adsorbed on IRC50. 1g of fresh IRC50 added every 10 minutes, from $t=10$ mins, to a total of 20g. Error bars represent one standard deviation based on triplicate experiments.

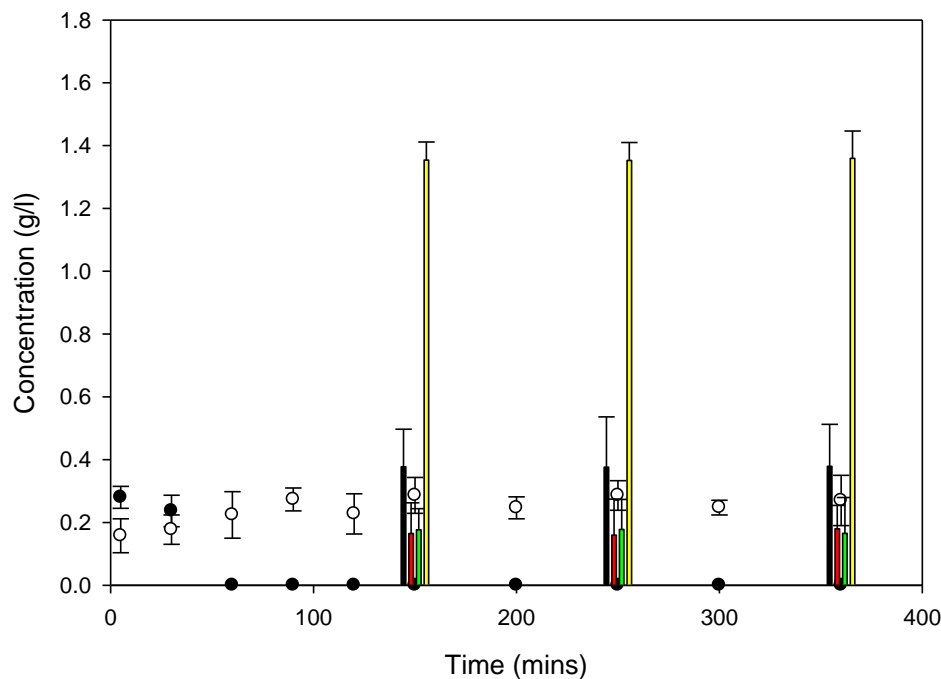


Figure 4.6 Dual resin SFPR, with use of XAD7 (60g/l) and IRC50 (300g/l) as substrate and product reservoirs respectively, for the production of lactone by *E. coli* TOP10 [pQR239] biocatalyst (8g_{DCW}/l) using an initial ketone concentration of 3g/l, as described in section 2.5.3.2. (●) ketone in aqueous phase, (○) lactone in aqueous phase, (■) ketone adsorbed on XAD7 (■) lactone adsorbed on XAD7, (■) ketone on IRC50 and (■) lactone on IRC50. 1g of fresh IRC50 added every 10 minutes, from $t=10$ mins, to a total of 20g. Error bars represent one standard deviation based on triplicate experiments.

The apparent observation from figures 4.5 and 4.6 is the high concentration of lactone accumulated on IRC50 (yellow bar). This is the resin chosen, based on the adsorption kinetics studies in the previous chapter, for product removal because of its high selectivity for the lactone over the ketone. 84% of the lactone accumulated on resins in the L493-IRC50 combination was found on IRC50 and as much as 88% of adsorbed lactone was present on IRC50 in the XAD7-IRC50 combination.

As seen with the previous method, where both resins are free in suspension in the aqueous phase, overall lactone production stops before 2.5 hours, with a possible explanation mentioned earlier in the introduction of section 4.3.3

4.3.4 Comparison of single resin and dual resin SFPR

Productivities of the experiments have been summarised in table 4.1 to compare the performance of the three strategies employed for Baeyer Villiger bioconversion. Productivities have been calculated by including the volume of resins in the overall productivity, as shown in equation 5 below.

$$Productivity = \frac{Product (g) / Total volume of aqueous and solid phase (L)}{Time (h)}$$

Equation [5]

Comparison is based on data from the resin based strategies up to 2.5 hours after start of experiment, because of the influence that the resins have of re-adsorbing the substrate.

Using productivity for comparison of the different strategies is based on the aim of overcoming decline of reaction rate due to the eventual biocatalyst inhibition at high substrate and product concentrations. Comparing productivities will demonstrate whether the dual resin strategy overcomes this problem.

In table 4.1, column 3, an increase in productivity is observed when a resin based strategy is employed at an initial substrate concentration of 3g/l. There is also an improvement of between 0.04-0.07g/l/h when the dual resin strategy is used instead of the single resin strategy, except when using the XAD7-IRC50 resins combination whilst employing a filter bag, where there is a decrease of 0.02g/l/h. The largest increase of productivity using the dual resin strategy compared to the single resin strategy is 10% observed with the L493-IRC50 resins combinations. This demonstrates that the dual resin strategy, with this resins combination, produces an improved performance at higher substrate and product concentrations than the single resin strategy.

Table 4.1 also shows, in column 4, the productivities that have been generated without taking into account the volume of the resins. This further comparison will show what

impact an increased amount of resins has when using the dual resin strategy over the single resin strategy. There is a similar trend to that mentioned above, that is an increase in productivity, when a resin based strategy is employed at an initial substrate concentration of 3g/l, is observed. There is also an improvement of between 0.17-0.23g/l/h when the dual resin strategy is used instead of the single resin strategy.

When comparing the productivities with and without taking into account the volume of resins, there is a drop of as much as 23% (XAD7-IRC50 resins combination in filter bag) in the productivities of the dual resin bioconversion when considering the volume of the resins. The single resin SFPR strategy requires considerably a smaller amount of resins ($0.05\text{g}_{\text{Lactone}}/\text{g}_{\text{resin}}$) compared to the dual resin SFPR strategy ($0.005\text{-}0.006\text{g}_{\text{Lactone}}/\text{g}_{\text{resin}}$) simply because of the need of a second type of resin for product removal, which has the lowest capacity amongst the resins tested (Chapter 3, table 3.1). At the initial ketone concentration of 3.0g/l, the single resin SFPR strategy required 0.6g of resin whereas the dual resin SFPR strategy needed 15.6g and 19g of resins for the L493:IRC50 and XAD7:IRC50 combinations, respectively.

Table 4.1 Comparison of performance of three different strategies to undertake Baeyer Villiger bioconversion. Results based on data after 2.5 hours of bioconversion.

		Productivity (g/l/h) [vol. of aqueous phase+resins]	Productivity (g/l/h) [vol. of aqueous phase only]	Lactone on resin (g/g_{resin})
Resin-free	0.4g/l*	N/A	1.52	N/A
	3g/l	N/A	0.34	N/A
Single resin	L493	0.72	0.73	0.05
Dual resin: free in suspension	L493-IRC50	0.79	0.90	0.006
	XAD7-IRC50	0.76	0.96	0.005
Dual resin: filter bag	L493-IRC50	0.79	0.91	0.006
	XAD7-IRC50	0.70	0.91	0.005

(*performed to completion)

The ratio of lactone accumulated on the resin used for product removal to lactone accumulated on the resin used as the substrate feed tool with the dual resin SFPR strategy have also been calculated. The XAD7-IRC50 combination demonstrated better performance, 7.56g/g, than the L493-IRC50 combination, 5.07g/g, as expected because resin XAD7 was chosen for its greater affinity for ketone than lactone based on adsorption kinetic studies in section 3.5.

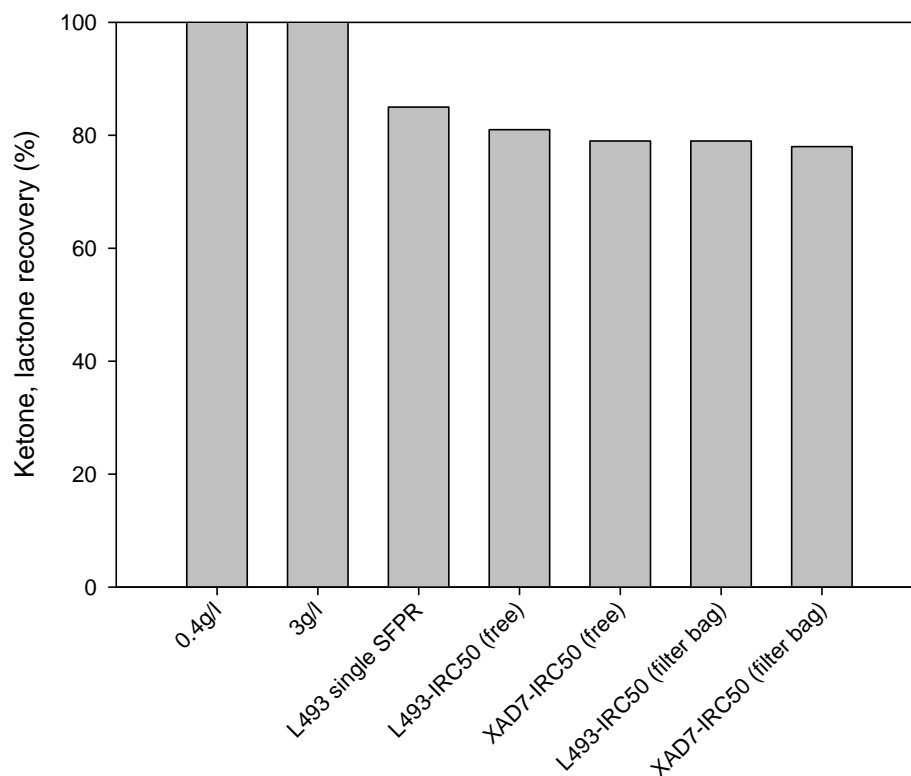


Figure 4.7 Calculated mass balances from all bioconversions performed without resins ('0.4g/l' and '3g/l'), with the single resin SFPR strategy ('L493 single SFPR') and with the dual resin SFPR strategy where both types of resins are free in suspension ('L493-IRC50 (free)' and 'XAD7-IRC50 (free)') and where they have been physically separated ('L493-IRC50 (filter bag)' and 'XAD7-IRC50 (filter bag)'). Results after 2.5 hours of bioconversion.

The mass balances of all the bioconversions performed in this chapter have been calculated and plotted in figure 4.7. Where the bioconversions have been performed without resins (with initial ketone concentrations of 0.4g/l and 3g/l), solute recovery was at 100%, whereas substrate and product recovery from bioconversions performed with the implementation of a resin based SFPR strategy, the calculated mass balances ranged from 79% to 85%.

The error with respect to mass balance seen in the bioconversions where resin based SFPR strategies have been employed, can only be an experimental error associated with

the use of the resins as the calculated mass balance of both bioconversions without the use of resins were 100%. It was observed during the resin based bioconversions that resin beads would be thrown up onto the inner walls of the shake flask, by the movement of the agitated liquid, and remain stuck on the inner walls away from the aqueous phase. This reduced the efficient desorption/adsorption of substrate and lactone and caused prevent complete recovery of resins after the bioconversion was stopped. Also the loss occurring at every stage of resin use, i.e. the several steps involved from the preparation of the resins all the way to the GC analysis of load on resin, would accumulate and contribute to the significant loss.

4.4 Conclusions

This chapter investigated the feasibility of performing a novel dual resin SFPR strategy to overcome substrate and product inhibition in the Baeyer-Villiger bioconversion. Using two different types of resin, one for substrate feeding and the other for product removal, the performance of the dual resin SFPR strategy was compared to a single resin SFPR strategy.

An increase of product concentration was observed with the dual resin SFPR strategy demonstrating the feasibility of this concept. It also gave an enhanced performance compared to the single resin SFPR strategy with regards to productivity. However, the shortcoming of this strategy was the greater amount of resin needed as a different type of resin is included for product removal and also the increased competition between resins and cells for the substrate. It was seen that as more fresh resin was sequentially added for product removal, it also removed substrate from the aqueous phase and hence the bioconversion becoming time dependent as seen by the reaction apparently stopping after 2.5 hours.

Chapter 5. Miniature stirred tank reactor evaluation of SFPR strategy

5.1 Aims

The objective of this chapter is to demonstrate the application of the novel dual resin SFPR strategy using a miniature stirred tank reactor (STR) and thus open a route to the scale-up of the process. The performance of the strategy is investigated experimentally to determine its suitability in a stirred tank reactor and hence whether application of the dual resin SFPR strategy increases the lactone concentration which can be achieved in this bioconversion with and without a single SFPR strategy.

5.2 Introduction

The implementation of the dual resin SFPR strategy in a miniature stirred tank reactor and demonstrating process efficiency at this scale would indicate potential for large scale application and hence making it an industrially relevant process.

The application of the dual resin SFPR strategy starts with the choice of process configuration, as discussed and shown in Chapter 1. Two simple reactor configurations have been investigated; the first configuration houses the two types of resins together inside the reactor, free in suspension and the second configuration houses one type of resin in a miniature column whilst the second type of resin remains in the reactor, free in suspension.

5.3 Results

5.3.1 Baeyer-Villiger bioconversion

As with the shake flask experiments (Chapter 4), BV bioconversion were carried out in the miniature reactor without the use of a resin SFPR strategy. The initial ketone concentrations of 0.4g/l and 3.0g/l set a benchmark to compare with the subsequent resin based SFPR experiments.

Lactone formation in the miniature reactor, at the initial ketone concentrations mentioned above, is shown in Figure 5.1. The profiles fit the expected trend seen from the shake flask experiments in section 4.3.1, where a decrease in lactone production is associated with the increase of starting ketone concentration. At 0.4g/l initial ketone, a lactone production rate of 1.80g/l/h is achieved, whereas at starting ketone concentration of 3.0g/l, lactone production is reduced to 0.38g/l/h. The whole cell biocatalyst activity at 0.4g/l and 3.0g/l initial ketone concentrations are determined to be 30.2U/g_{DCW}, \pm 0.6%, and 4.1U/g_{DCW}, \pm 6.7%, respectively.

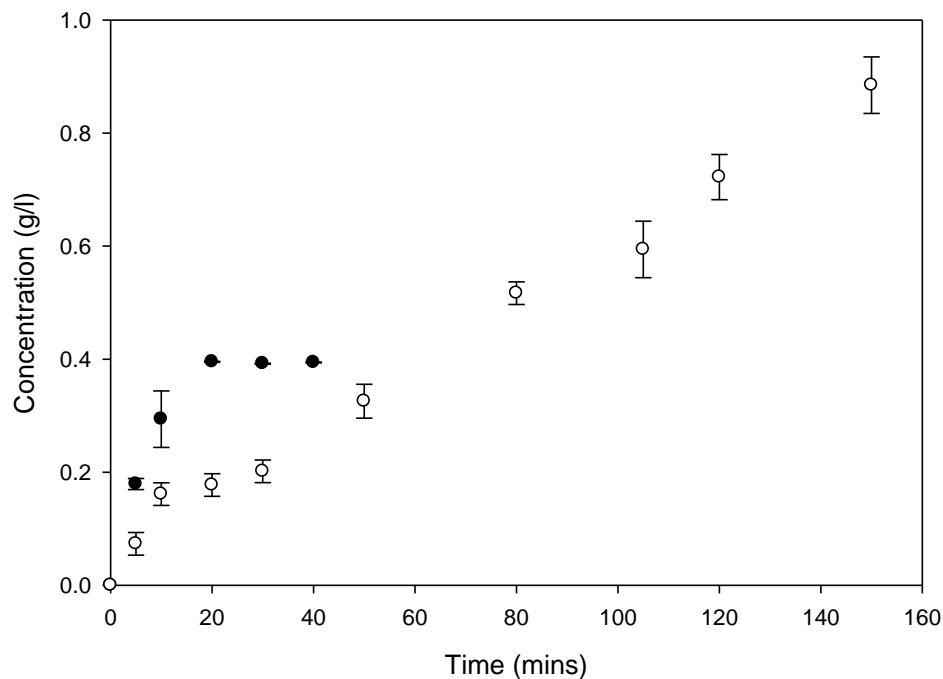


Figure 5.1 Production of lactone by *E. coli* TOP10 [pQR239] biocatalyst ($8g_{DCW/l}$) using initial ketone concentrations of (●) 0.4g/l and (○) 3g/l, without the use of a resin SFPR strategy in a miniature STR as described in section 2.6.2. Error bars represent one standard deviation based on triplicate experiments.

5.3.2 Single SFPR strategy

It was decided that all resin based SFPR bioconversions in this chapter were to be stopped after 2.5 hours based on the results of Chapter 4 where no change of lactone formation was seen beyond this time point.

The single SFPR strategy was demonstrated in the miniature reactor by using resin L493 free in suspension. Figure 5.2 shows the concentrations of both ketone and lactone in the aqueous phase and bound onto L493.

The aqueous concentrations of ketone and lactone remained below the concentrations that would inhibit the bioconversion. Aqueous ketone concentration was reduced to levels that have been considered negligible from 30 minutes onwards and hence the

availability of ketone for conversion is seen as a rate limiting step. Overall productivity of lactone, using the single resin SFPR strategy, was 0.82g/l/h and after 2.5 hours lactone production reached 68% based on the concentration of lactone in the aqueous phase and on the resin. The whole cell biocatalyst activity was determined to be 27.5U/g_{DCW}, ±4.7%.

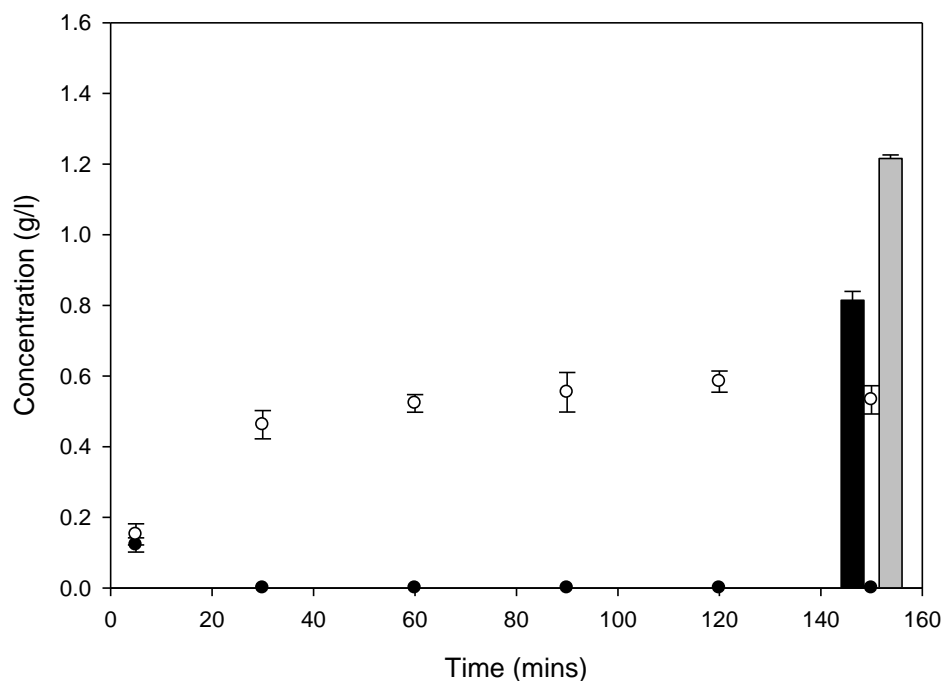


Figure 5.2 Single resin SFPR strategy, with use of L493 (8g/l) resin contained in a miniature STR, for the production of lactone by *E. coli* TOP10 [pQR239] biocatalyst (8g_{DCW}/l) using an initial ketone concentration of 3g/l on the resin. (●) ketone in aqueous phase, (○) lactone in aqueous phase, (■) ketone on L493 and (■) lactone on L493. Experiment performed as described in section 2.6.2. Error bars represent one standard deviation based on triplicate experiments.

A worry of using a resin based strategy in a reactor is the occurrence of settling of the resin at the base, however mixing in the reactor was observed to be effective for resin suspension as the resin fraction of L493 in this single resin strategy was only 1.2% (w/v).

5.3.3 Dual SFPR strategy

Two basic reactor configurations have been used for the dual resin SFPR strategy. The first is the direct introduction of resins into the reactor where the first type of resin that holds the substrate is added at the beginning of the reaction followed by the sequential addition of the second type of resin to adsorb the product from 10 minutes onwards.

Figures 5.3 and 5.4 show the conversion of ketone to lactone using L493 and XAD7 as tools for substrate feed, respectively and IRC50 as the product removal resin. The vertical bars show solute accumulation on both the resins used for ketone feeding and product removal.

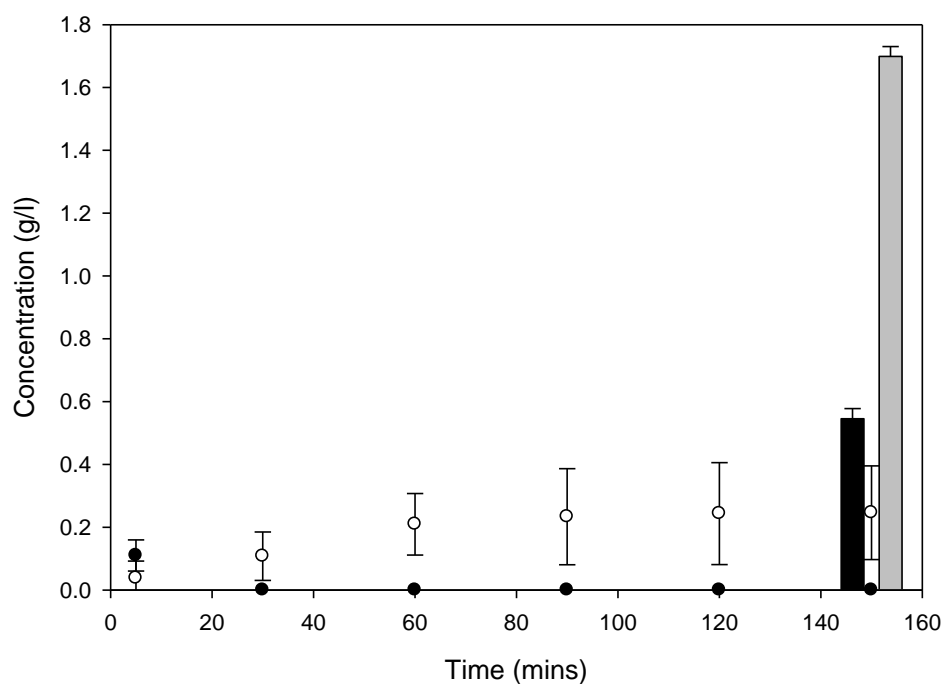


Figure 5.3 Dual resin SFPR, with use of L493 (8g/l) and IRC50 (300g/l) as substrate and product reservoirs respectively contained in a miniature STR, for the production of lactone by *E. coli* TOP10 [pQR239] biocatalyst (8g_{DCW}/l) using an initial ketone concentration of 3g/l. (●) ketone in aqueous phase, (○) lactone in aqueous phase, (■) ketone on resins and (■) lactone on resins. Experiment performed as described in section 2.6.3. 2g of fresh IRC50 added every 10 minutes, from $t=10$ mins. Error bars represent one standard deviation based on triplicate experiments.

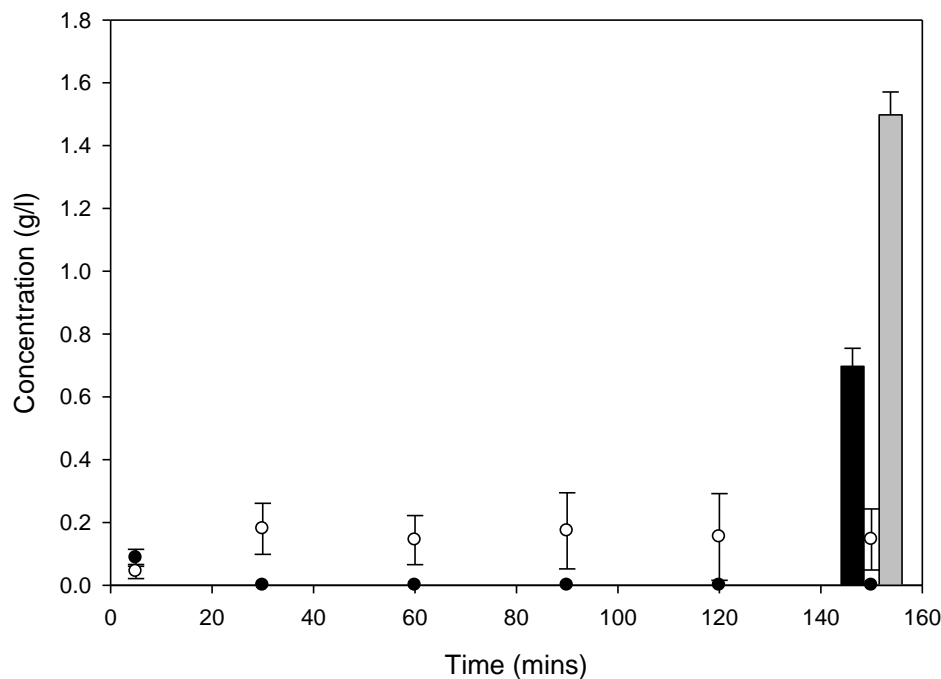


Figure 5.4 Dual resin SFPR, with use of XAD7 (60g/l) and IRC50 (300g/l) as substrate and product reservoirs respectively contained in a miniature STR, for the production of lactone by *E. coli* TOP10 [pQR239] biocatalyst (8g_{DCW}/l) using an initial ketone concentration of 3g/l. (●) ketone in aqueous phase, (○) lactone in aqueous phase, (■) ketone on resins and (■) lactone on resins. Experiment performed as described in section 2.6.3. 2g of fresh IRC50 added every 10 minutes, from $t=10$ mins. Error bars represent one standard deviation based on triplicate experiments.

The L493-IRC50 combination fared better than the XAD7-IRC50 dual resin combination by generating a productivity of 0.94g/l/h compared to 0.84g/l/h, respectively. The lower productivity seen with the XAD7-IRC50 dual resin combination can be attributed to the higher overall fraction of resins in the aqueous phase of 37% (w/v) in this combination compared to the 31.2% (w/v) in the L493-IRC50 combination.

This difference resulted in the decoupling of the magnetic stirrer above an agitation rate of 1500rpm using the XAD7-IRC50 combination whereas with the L493-IRC50 combination the agitation rate could be maintained at 2000rpm. In comparison, this resulted in less efficient mixing of resins in the XAD7-IRC50 combination and hence a

higher proportion of resins left settled at the base of the reactor. Ketone and lactone recovery was 5% lower using the XAD7-IRC50 combination compared to the process with the L493-IRC50 combination.

The whole cell biocatalyst activity using the L493-IRC50 and XAD7-IRC50 combinations are determined to be $23.8\text{U/g}_{\text{DCW}}, \pm 7.7\%$, and $25.2\text{U/g}_{\text{DCW}}, \pm 10.4\%$, respectively.

5.3.4 Recycle STR SFPR strategy

The second of the two reactor configurations used to implement the resin based SFPR strategy was the recycle reactor configuration. In this configuration the aqueous phase was pumped from the reactor to a column housing one type of resin and then recycled back into the reactor which held the second type of resin in the case of the dual resin SFPR strategy, as described in section 2.7.

As a filter was not used to prevent cells from circulating in the packed column, there is a risk of caking and hence blockage of cell culture circulation through the column. To see if caking occurs within the set bioconversion period, $8\text{g}_{\text{DCW}}/\text{l}$ of whole cells in 50mM phosphate buffer (without substrate or product) was continuously circulated through the packed column at a flow rate of 6.4ml/min. Flow rate was then monitored to observe for any change. Results are presented in figure A.12 (Appendix) and show no significant change in flow rate up to 180 minutes, demonstrating that any caking that takes place during the course of the set bioconversion time will not reduce time of circulation.

Figure 5.5 shows the results of implementing the single resin SFPR strategy and figure 5.6 shows the results of implementing the dual resin SFPR strategy. The L493-IRC50 combination is the only one of the two combinations for the dual resin SFPR strategy from Section 5.3.3 demonstrated here because of practical limitations.

The volume capacity of the column was only large enough to house the 1.2% (w/v) fraction of L493 needed for the implementation of the resin based SFPR strategy. The 7.1% (w/v) of XAD7 and 30% (w/v) of IRC50 fractions needed were too high to be housed in the miniature column.

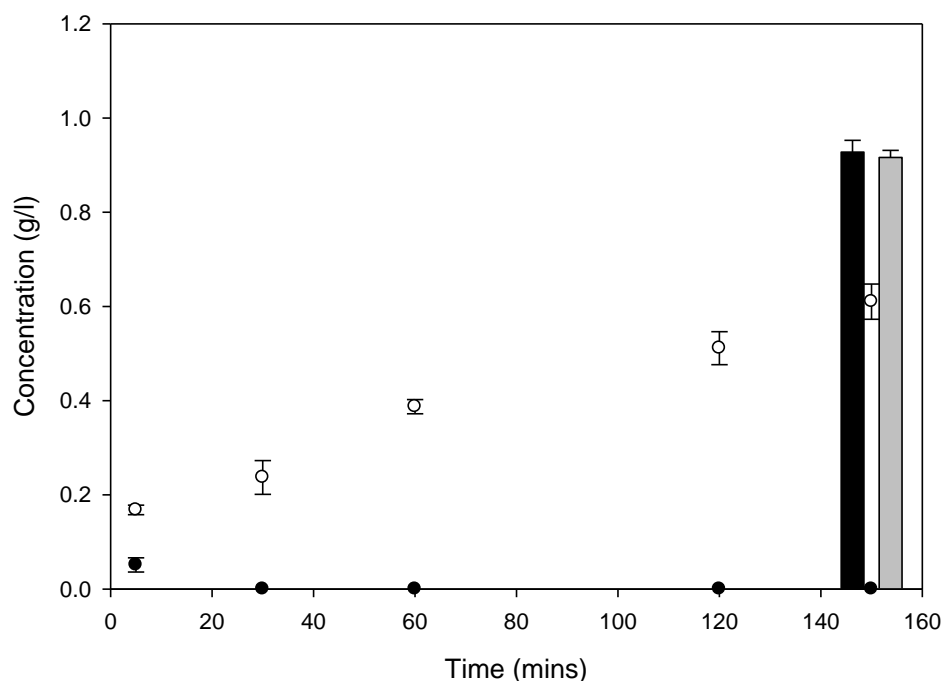


Figure 5.5 Single resin SFPR strategy, using a combination of a miniature STR and miniature column containing L493 (8g/l), for the production of lactone by *E. coli* TOP10 [pQR239] biocatalyst (8g_{DCW}/l) using an initial ketone concentration of 3g/l on the resin. (●) ketone in aqueous phase, (○) lactone in aqueous phase, (■) ketone on L493 and (■) lactone on L493. Experiment performed as described in section 2.7.4. 2g of fresh IRC50 added every 10 minutes, from $t=10$ mins. Error bars represent one standard deviation based on triplicate experiments.

Figure 5.5 shows ketone and lactone concentrations in the aqueous phase and bound to L493 inside the column. Ketone concentration in the aqueous phase is extremely low and hence is again considered negligible. A more gradual increase of lactone concentration is seen in the aqueous phase compared to that seen in Figure 5.2. Overall

productivity demonstrated by this configuration was 0.75g/l/h and a product formation of 62% was achieved after 2.5 hours.

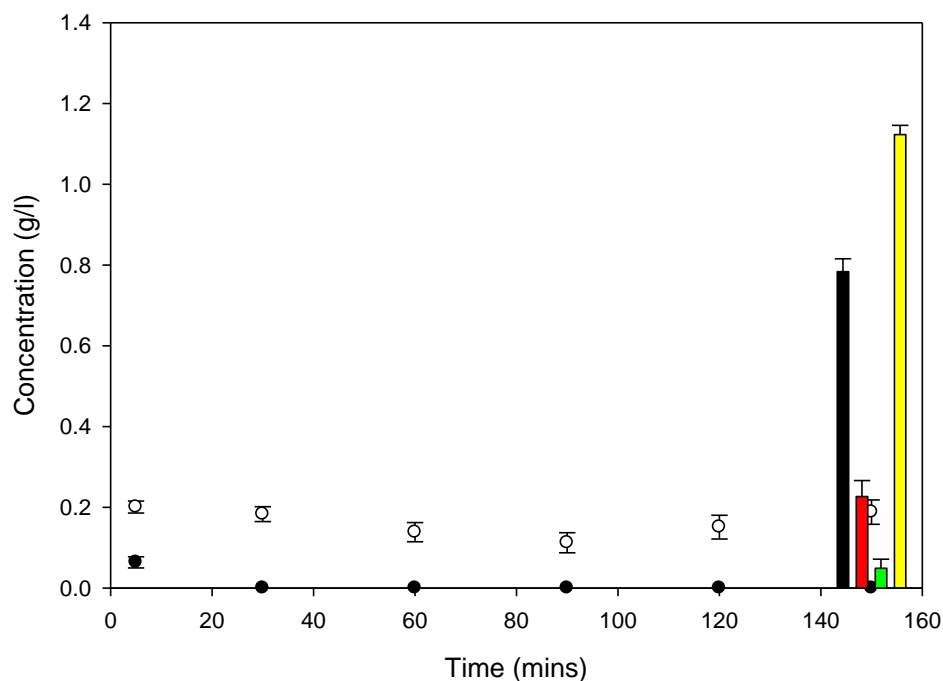


Figure 5.6 Dual resin SFPR, with use of L493 (8g/l) (housed in a miniature column) and IRC50 (300g/l) (free in suspension inside a miniature STR) as substrate and product reservoirs respectively, for the production of lactone by *E. coli* TOP10 [pQR239] biocatalyst (8g_{DCW}/l) using an initial ketone concentration of 3g/l. (●) ketone in aqueous phase, (○) lactone in aqueous phase, (■) ketone on L493, (■) lactone on L493, (■) ketone on IRC50 and (■) lactone on IRC50. Experiment performed as described in section 2.7.5. 2g of fresh IRC50 added every 10 minutes, from $t=10$ mins. Error bars represent one standard deviation based on triplicate experiments.

Figure 5.6 shows results from the implementation of the L493-IRC50 combination as the dual resin SFPR strategy with the recycle reactor configuration. This configuration allows the concentration of ketone and lactone on each type of resin to be displayed. Out of the total lactone produced, 73% was adsorbed onto IRC50, the resin seen as the most effective for product removal, compared to 15% adsorbed onto L493. Productivity improved from 0.75g/l/h in the single resin SFPR system to 0.78g/l/h and hence a slightly better yield of 65% was achieved. The whole cell biocatalyst activity using the

single resin SFPR and dual resin SFPR strategies in the recycle reactor configurations are determined to be $26.3\text{U/g}_{\text{DCW}}, \pm 7.1\%$, and $22.8\text{U/g}_{\text{DCW}}, \pm 11.6\%$, respectively.

5.3.5 Comparison of single and dual SFPR strategies

Table 5.1 below compares productivity and the load of solutes on resin for the different strategies. Productivities have been calculated by including the volume of resins (Equation 5).

All resin based SFPR systems in both reactor configurations (column 3) gave better performances than without using a resin based SFPR system at an initial ketone concentration of 3g/l (productivity= 0.38g/l/h) as seen in the shake flask experiments (Chapter 4).

There is a contrast when comparing the two reactor configurations with the performance of the recycle reactor configuration being lower than the configuration where resins are directly introduced into the reactor. This is true in regards to both single and dual resin SFPR strategies and hence makes the conventional reactor system a more attractive option of the two. The L493-IRC50 combination in the conventional reactor configuration achieves a 21% greater productivity than in the recycle reactor.

The dual resin SFPR strategy using the L493-IRC50 combination performed better than any other resin based SFPR strategy when carried out with both resins in the reactor. It reached a productivity of 0.85g/l/h after 2.5 hours of reaction, 5% higher than the productivity achieved with the single resin strategy in the conventional reactor configuration. This result supports the conclusion from Chapter 4 that there is a small improvement in the performance of the Baeyer-Villiger bioconversion using the dual resin strategy compared to the single resin strategy.

Table 5.1 Comparison of performance of three different strategies to undertake Baeyer Villiger bioconversion using two different reactor configurations- recycle reactor and conventional STR.

		Productivity (g/l/h) [vol. of aqueous phase+resins]	Productivity (g/l/h) [vol. of aqueous phase only]	Lactone on resin (g/g_{resin})
Resin-free	0.4g/l*	N/A	1.80	N/A
	3g/l	N/A	0.38	N/A
Single: free in suspension	L493	0.81	0.82	0.12
Single: column	L493	0.75	0.75	0.09
Dual: free in suspension	L493-IRC50	0.85	0.94	0.007
	XAD7-IRC50	0.76	0.84	0.005
Dual resin: column	L493-IRC50	0.70	0.78	0.005

*performed to completion

The data of the load of lactone on resins in Table 5.1 shows that lactone load on resin is significantly less when using the dual resin SFPR strategy compared to the use of the single resin SFPR strategy. This is because of the larger quantity of the second type of resin IRC50- used based on the adsorption kinetic studies- being needed to implement this system.

The ratio of lactone concentration accumulated on IRC50 to lactone concentration accumulated on L493 (IRC50:L493) in the dual resin SFPR strategy using the recycle reactor configuration was 4.95g/g, demonstrating the suitability of this resin combination.

Table 5.1 also shows the effect that the extra volume, as a result of the added resins, has on productivity by displaying, in column 4 the calculated productivities of the different bioconversions without taking the resin volume into account.

5.4 Conclusions

This chapter applied the novel dual resin SFPR strategy, which was proven to increase productivity of a Baeyer Villiger bioconversion, by using two different configurations of a miniature stirred tank reactor system- namely the conventional reactor configuration where both types of resins were inside the STR and a recycle reactor configuration with one type of resin housed in a miniature column.

The recycle reactor configuration performed worse out of the two reactor configurations for both single resin and dual resin SFPR strategies however the dual resin SFPR strategy showed similar performance to the single resin SFPR strategy. Ideally separation of the different types of resins will allow for regeneration and reuse of the resins, an attractive proposition for industrial processes.

As mentioned in the previous chapter, the shortcoming of the dual resin SFPR strategy was the higher amount of resin needed. This means that greater power is required for effective agitation of the resins for uniform distribution in the reactor.

Overall, this investigation has set up a base for optimising the dual resin SFPR strategy at the small scale and has also opened the way for scale up studies.

Chapter 6. Overall Conclusions

The research presented in this thesis is an evaluation of a novel dual resin substrate feed-product removal (SFPR) strategy by applying to the Baeyer-Villiger biooxidation reaction, catalysed by the recombinant *E. coli* TOP10 [pQR239]. Investigations began by performing adsorption studies to find the best combination of resins to implement in the dual resin SFPR strategy. Thereafter, ‘proof of concept’ was demonstrated for the dual resin SFPR strategy in shake flask experiments and then implementing it in two configurations using a miniature stirred tank reactor (STR). The key findings of this investigation are presented below:

- Adsorption studies carried out at the ml-scale to characterise six resins found that the resin with the highest surface area, Dowex Optipore L493, possessed the highest maximum adsorption capacity for bicyclo[3.2.0]hept-2-en-6-one and (1R,5S)-3-oxabicyclo[3.3.0]oct-6-en-2-one, the ketone substrate and lactone product of the Baeyer-Villiger bioconversion, respectively. These were determined as $Q_{\max} = 0.38\text{g/g}_{\text{resin}}$ for ketone and $Q_{\max} = 0.15\text{g/g}_{\text{resin}}$ for lactone after fitting adsorption data to the Langmuir and Freundlich adsorption models.
- A high throughput resin screening (HTRS) was investigated as an alternative to carrying out adsorption studies at the ml-scale. Two platforms were chosen to perform the adsorption studies, namely the 96 wells and 24 wells microplates, the latter of which determined as the platform that produces more accurate adsorption results and models that fit those generated at the ml-scale. Additionally, significantly better resin suspension is achieved in the 24 wells microplate.
- High throughput adsorption kinetics studies were performed in the 24 well microplate platform to determine selectivity of resins for ketone and the lactone compound, (1R,5S)-2-oxabicyclo[3.3.0]oct-6-en-3-one. Amberlite XAD7 was

found to have a higher selectivity for ketone over lactone and Amberlite IRC50 a higher selectivity for lactone over ketone than any other of the tested resins.

- Resin combinations of L493-IRC50 and XAD7-IRC50 were used to implement the dual resin SFPR strategy in shake flask experiments, where resins L493 and XAD7 were utilised as the substrate feeding tools and IRC50 resin as the product removal tool. The amounts of L493 and XAD7 used were based on their capacity for ketone at an equilibrium concentration of 0.5g/l and were 0.21g/g_{resin} and 0.035g/g_{resin}, respectively, to ensure aqueous substrate concentration during bioconversion was kept below the inhibitory concentration. The amount of IRC50 used was based on its maximum adsorption capacity for lactone, 0.008g/g_{resin}, to ensure complete removal of lactone product from the aqueous phase of the bioconversion.
- Carrying out the Baeyer-Villiger bioconversion with the implementation of the dual resin SFPR strategy in shake flasks saw an increase of productivity compared to the Baeyer-Villiger bioconversions carried out without resins by as much as 132% and with the single resin SFPR strategy by as much 10%, thus demonstrating a ‘proof of concept’ of the novel dual resin SFPR bioconversion strategy.
- Spatial separation of the two types of resins in the shake flask gave the opportunity to determine the proportion of the lactone product adsorbed onto resin Amberlite IRC50 which was used for product removal. 84% of total adsorbed lactone was adsorbed by IRC50 in the L493-IRC50 combination and 89% of total adsorbed lactone in the XAD7-IRC50 combination was adsorbed by IRC50. This shows selectivity of IRC50 for the lactone product over the ketone substrate as determined in the HTRS adsorption kinetic studies.
- The feasibility of implementing the dual resin SFPR strategy using a miniature reactor has also been demonstrated. A conventional stirred tank reactor (STR)

configuration, where both types of resins were added directly inside the STR, performed better than the recycle reactor configuration, where the resin used for substrate feeding was contained inside a miniature column.

Productivities achieved with the single and dual resin SFPR strategies in the conventional reactor configuration were 0.82g/l/h and 0.94g/l/h, respectively. A comparison with the single resin SFPR strategy as performed by Hilker *et al* (2004a) in a bubble column reactor shows similar productivity of 1g/l/h to that achieved with the dual resin SFPR strategy. However comparison is not directly possible because of the differences in process conditions- Hilker *et al* (2004a) performed the adsorption isotherm studies at 25°C and the Baeyer-Villiger reaction in fermentation media, with a cell concentration of 6.4g_{DCW}/l and at an initial substrate concentration of 25g/l, whereas in this research adsorption isotherm studies were carried out at 37°C, as this was the condition that the bioconversion was operated under, and bioconversions were performed in 50mM phosphate buffer, with a 8g_{DCW}/l cell concentration and at an initial ketone concentration of 3g/l (thus requiring a lower amount of resin). Nonetheless, the similar performances of the single and dual resin SFPR bioconversion strategies as performed in this research shows a promise for large scale processing just as Hilker *et al* (2005) did with the single resin SFPR strategy, which has gone on to be industrially applied by Sigma-Aldrich.

A shortcoming of implementing the dual resin SFPR strategy over the single resin SFPR strategy is the greater amount of resins required, due to the fact that two types of resin are required, one for substrate feeding and the other for product removal, rather than just the one type of resin that will perform both these roles in a single resin SFPR bioconversion.

A cost analysis shows that it is more expensive to run the dual resin SFPR strategy than the single resin SFPR strategy based on the combinations of resins used in this research. It costs £17.39 per gram of substrate when using the L493-IRC50 combination and £20.27 per gram of substrate when using the XAD7-IRC50 combination for implementing the dual resin SFPR strategy. This is a stark contrast to the cost needed to

run the single resin SFPR strategy where a mere £0.06 per gram of substrate is required when utilising resin L493. (Costs have been based on quotes from Sigma-Aldrich).

However, these costs are associated with the resins used in this research where the resin combinations were determined from screening six resins. Therefore by screening the vast number of resins available in the market, suitable resins that possess high adsorption capacities can off-set most of the cost as less will be needed to run the dual resin SFPR bioconversion strategy. The screening of hundreds of resins will be fast and efficient when done using the HTRS method developed from this research.

Another challenge is seen with the use of non-specific commercial resins in the dual resin strategy. Although differences in selectivity for the substrate and product can be applied, the non-specific nature of the resins prevents complete selectivity for one compound over the other especially when both are structurally and chemically similar; as is in the case with the substrate and product of the Baeyer-Villiger reaction investigated. However differences between the ketone and lactone, such as the 3-dimensional spatial arrangement of atoms and electron densities, can be exploited by designing resins specific to substrate and product, respectively.

Chapter 7. Future Work

The work presented in this thesis set a good base for the optimisation and scale-up of the dual resin SFPR bioconversion strategy. Investigations should be conducted to improve efficiency of the high throughput resin screening (HTRS) and validation of the dual resin SFPR strategy will need to be performed if it is to be commercially implemented. Further detail of the aforementioned work is presented below.

7.1 Automated HTRS and design of experiments (DoE)

The adsorption studies performed and presented in Chapter 3 characterised only six resins, so carrying out screening of a wider range of resins will ensure validation of the HTRS method. The natural extension to this is the automation of the HTRS methodology. The first step is investigating a more efficient resin handling and dispensing system than manually weighing the resins. Figure 7.1 shows results for early experiments of investigating the accuracy of pipetting slurry of resins by using wide bore tips (Biohit, Sartorius, Finland). The advantage of this method of dispensing resins into microwells, apart from speeding up manual addition, allows this procedure and therefore adsorption studies to be automated with a Tecan Genesis platform (Tecan, Reading, UK) available in the Department of Biochemical Engineering, UCL.

The HTRS can be further optimised by the use of design of experiments (DoE). This statistical approach will reduce the number of experiments and will maximise the quality of results gained from the HTRS. This is achieved by studying multiple experimental factors simultaneously as opposed to the ‘one factor at a time’ investigations, for example, factors such as temperature, solute concentration and time in the HTRS can be investigated simultaneously around a defined centre point.

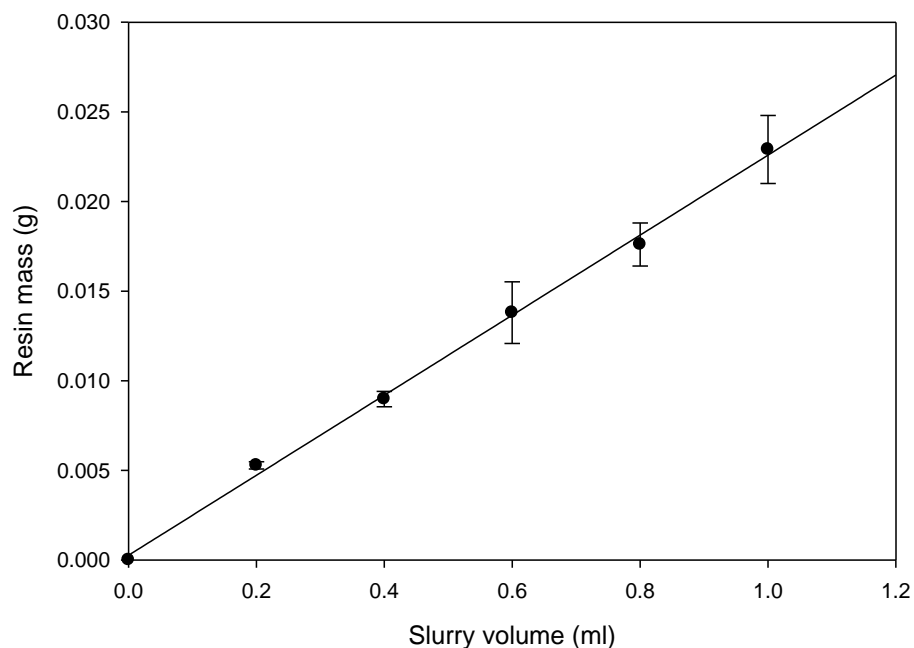


Figure 7.1 Mass of resin Amberlite IRC50 dispensed by a wide bore tip as slurry from a 10g/l resin suspension mixed by a 3 blade marine impeller at 350rpm. Error bars represent one standard deviation based on triplicate experiments.

7.2 Scale up of the dual resin SFPR bioconversion strategy

Implementation of the dual resin SFPR bioconversion strategy has opened the way for scale up studies in two reactor configurations- conventional and recycle reactors, thus criteria will need to be established that are required for larger scale designs of these two reactor configurations and then verification of the optimised process at pilot scale. There will be certain factors that are typically taken into consideration during reactor scale up but will be emphasised when scaling up a resin based SFPR bioconversion process, such as oxygen transfer and mixing. The extra volume that is added to the system as a result of using resins for performing the bioconversion will have an effect on other system requirements such as reactor size and considerations such cost per batch run.

A study of the influence of scale up parameters such as hydraulic retention time, superficial velocity and bed dimensions is paramount for process performance and

design of a recycle reactor configuration. Also in order for the resin based SFPR bioconversion process to be applied in a commercial setting when using the recycle reactor configuration it is important to consider validation issues such as containment of the whole cell biocatalyst and the sterility of the process, because this configuration operates by the recycling of bioconversion medium through an external resin column and back to the reactor.

An additional point to mention is the prospect for evaluation of the dual resin SFPR bioconversion strategy using a microscale platform and in fact an automated microscale platform based on recent research into rapid evaluation and optimisation of oxidative bioconversion processes using the Tecan Genesis platform has been developed recently (Baboo *et al.*, 2012).

Chapter 8. References

- Aldridge, S., 2013. Industry Backs Biocatalysis for Greener Manufacturing, *Nat. Biotechnol.*, 95-96.
- Alphand, V., Archelas, A. and Furtoss, R., 1989. Microbiological Transformations, 16. One-step Synthesis of a Pivotal Prostaglandin Chiral Synthon via a Highly Enantioselective Microbiological Baeyer-Villiger type reaction. *Tetrahedron Lett.*, 30, 3663-3664.
- Alphand, V., Carrea, G., Wohlgemuth, R., Furstoss, R. and Woodley, JM., 2003. Towards Large-scale Synthetic Applications of Baeyer-Villiger Monooxygenases. *Trends Biotechnol.*, 21, 318-323.
- Baboo, JZ., Galman, JL., Lye, GJ., Ward, JM., Hailes, HC. and Micheletti, M., 2012. An Automated Microscale Platform for Evaluation and Optimization of Oxidative Bioconversion Processes. *American Institute of Chemical Engineers.* 28, 392-405.
- Baeyer, A. and Villiger, V., 1899. Einwirkung des Caro'schen Reagens auf Ketone. *Berichte der deutschen chemischen Gesellschaft*, 32, 3625-3633.
- Baldwin, CVF., Wohlgemuth, R. and Woodley, JM., 2008. The first 200-L Scale Asymmetric Baeyer-Villiger Oxidation using a Whole-cell Biocatalyst. *Org. Process Res. Dev.*, 12, 660-665.
- Baldwin, CVF. and Woodley, JM., 2006. On Oxygen Limitation in a Whole Cell Biocatalytic Baeyer-Villiger Oxidation Process. *Biotechnol. Bioeng.*, 95, 362-369.
- Blaser, HU. and Schmidt, E., 2004. *Asymmetric Catalysis on Industrial Scale*. Weinheim: Wiley-VCH.

- Bornscheuer, UT., Huisman, GW., Kazlauskas, RJ., Lutz, S., Moore, JC. and Robins, K., 2012. Engineering the Third Wave of Biocatalysis, *Nature*, 185-194.
- Bull, AT., Bunch, AW. and Robinson, GK., 1999. Biocatalysts for Clean Industrial Products and Processes. *Current Opinion in Microbiology*, 2, 246-251.
- Chen, G., Kayser, MM., Mihovilovic, MD., Mrstik, ME., Martinez, CA. and Stewart, JD., 1999. Asymmetric Oxidations at Sulphur Catalysed by Engineered Strains that overexpress Cyclohexanone Monooxygenase. *New J. Chem.*, 23, 827-832.
- Chen, BH., Doig, SD., Lye, GJ. and Woodley, JM., 2002. Modelling of the Baeyer-Villiger Monooxygenase Catalysed Synthesis of Optically Pure Lactones. *Trans IChemE*, 80, 51-55.
- Conceicao, GJA., Moran, PJS. and Rodrigues, JAR., 2003. Highly Efficient Extractive Biocatalysis in the Asymmetric Reduction of an Acyclic Enone by the Yeast *Pichia stipitis*. *Tetrahedron: Asymmetry*, 14, 43-45.
- Creigee, R., 1948. Die Umlagerung der Dekalin-peroxyester als Folge von kationischem Sauerstoff. *Justus Liebigs Annalen der Chemie*, 560, 127-135.
- D'Arrigo, P., Lattanzio, M., Fantoni, GP. and Servi, S., 1998. Chemo-enzymatic Synthesis of the Active Enantiomer of the Anorressant 2-benzylmorpholine. *Tetrahedron: Asymmetry*, 9, 4012-4026.
- Duetz, WA., Ruedi, L., Hermann, R., O'Connor, K., Buchs, J. and Witholt, B., 2000. Methods for Intense Aeration, Growth, Storage and Replication of Bacterial Strains in Microtiter Plates. *Appl. Environ. Microbiol.*, 66, 2641-2646.
- Doig, SD., O'Sullivan, LM., Patel, S., Ward, JM. and Woodley, JM., 2001. Large Scale Production of Cyclohexanone Monooxygenase from *Escherichia coli* TOP10 pQR239. *Enzyme Microb. Technol.*, 28, 265-274.

- Doig, SD., Avenell, PJ., Bird, PA., Gallati, P., Lander, KS., Lye, GJ., Wohlgemuth, R. and Woodley., JM., 2002. Reactor Operation and Scale-up of Whole Cell Baeyer-Villiger Catalysed Lactone Synthesis. *Biotechnol. Prog.*, 18, 1039-1046.
- Doig, SD., Simpson, H., Alphand, V., Furstoss, R. and Woodley, JM., 2003. Characterisation of a Recombinant *Escherichia coli* TOP10 [pQR239] Whole-cell Biocatalyst for Stereoselective Baeyer-Villiger Oxidations. *Enzyme Microb. Technol.*, 32, 347-355.
- Donoghue, NA., Norris, DB. and Trudgill, PW., 1976. The Purification and Properties of Cyclohexanone Monooxygenase from *Nocardia globerula* CL1 and *Acinetobacter* NCIB 9871. *Eur. J. Biochem.*, 63, 175-192.
- Fahrenkamp-Uppenbrink, J., 2002. Chemistry Goes Green. *Science*, 297, 798.
- Gill, N. K., Appleton, M., Baganz, F. And Lye, G. J., 2008. Design and Characterisation of a Miniature Stirred Bioreactor System for Parallel Microbial Fermentations. *Biochem. Eng. J.*, 39, 164-176.
- Girard, P., Jordan, M., Tsao, M. and Wurm, FM., 2001. Small-scale Bioreactor System for Process Development and Optimisation. *Biochem. Eng. J.*, 7, 117-119.
- Hilker, I., Guteirrez, MC., Furstoss, R., Ward, J., Wohlgemuth, R. and Veronique, A., 2008. Preparative Scale Baeyer-Villiger Biooxidation at High Concentration using Recombinant *Escherichia coli* and *in situ* Substrate Feeding and Product Removal Process. *Nature Protocols*, 3, 546-554.
- Hilker, I., Wohlgemuth, R., Alphand, V. and Furstoss, R., 2005. Microbial Transformations 59. First Kilogram Scale Asymmetric Microbial Baeyer-Villiger Oxidation with Optimised Productivity using a Resin-based *in situ* SFPR Strategy. *Biotechnol. Bioeng.*, 92, 702-710.

- Hilker, I., Alphan, V., Wohlgemuth, R. and Furstoss, R., 2004a. Microbial Transformations, 56. Preparative Scale Asymmetric Baeyer-Villiger Oxidation using a Highly Productive “Two-in-One” Resin-Based *in situ* SFPR Concept. *Adv. Synth. Catal.*, 346, 203-214.
- Hilker, I., Gutierrez, MC., Alphan, V., Wohlgemuth, R. and Furstoss, R., 2004b. Microbiological Transformations, 57. Facile and Efficient Resin-Based *in situ* SFPR Preparative-Scale Synthesis of an Enantiopure “Unexpected” Lactone Regioisomer via a Baeyer-Villiger Oxidation Process. *Org. Lett.*, 6, 1955-1958.
- Jackson, NB., Liddell, JM. and Lye, GJ., 2006. An Automated Microscale Technique for the Quantitative and Parallel Analysis of Microfiltration Operations. *J. Membr. Sci.*, 276, 31-41.
- Kamerbeek, NM., Janssen, DB., van Berkel, WJH. and Fraaije, MW., 2003. Baeyer-Villiger Monooxygenases, an Emerging Family of Flavin-Dependent Biocatalysts. *Adv. Synth. Catal.*, 345, 667-678.
- Kim, P-Y., Pollard, DJ. and Woodley, JM., 2007. Substrate Supply for Effective Biocatalysis. *Biotechnol. Prog.*, 23, 74-82.
- Lye, GJ. and Woodley, JM., 1999. Application of *in situ* Product-Removal Techniques to Biocatalytic Processes. *Trends Biotechnol.*, 17, 395-402.
- Lye, GJ., Ayazi-Shamlou, P., Baganz, F., Dalby, PA. and Woodley, JM., 2003. Accelerated Design of Bioconversion Processes using Automated Microscale Processing Techniques. *Trends Biotechnol.*, 21, 29-37.
- Mihovilovic, MD., 2006. Enzyme Mediated Baeyer-Villiger Oxidations. *Current Organic Chemistry*, 10, 1265-1287.

- Mihovilovic, MD., Muller, B., Kayser, MM., Stewart, JD., Frohlich, J., Stanetty, P. and Spreitzer, H., 2001. Baeyer-Villiger Oxidations of Representative Heterocyclic Ketones by Whole Cells of Engineered *Escherichia coli* Expressing Cyclohexanone Monooxygenase. *J. Mol. Catal. B: Enzym.*, 11, 349-353.
- Murahashi, SI., Ono, S. and Imada, Y., 2002. Asymmetric Baeyer-Villiger reaction with Hydrogen Peroxide Catalysed by a Novel Planar-chiral Bisflavin. *Angewandte Chemie. International edition in English*, 41, 2366-2368.
- Persidis A., 1998. High throughput screening. *Nat. Biotechnol.*, 16, 488-489.
- Pollard, DJ. and Woodley, JM., 2007. Biocatalysis for Pharmaceutical Intermediates: the Future is Now. *Trends Biotechnol.*, 25, 66-73.
- Renz, M. and Meunier, B., 1999. 100 Years of Baeyer-Villiger Oxidation. *Eur. J. Org. Chem.*, 737-750.
- Rich, JO., Michels, PC. and Khmel'nitsky, YL., 2002. Combinatorial Biocatalysis. *Curr. Opin. Chem. Biol.*, 6, 161-167.
- Rozzell, JD., 1999. Commercial Scale Biocatalysis: Myths and Realities. *Bioorg. Med. Chem.*, 7, 2253-2261.
- Rudroff, F., Alphand, V., Furstoss, R. and Mihovilovic, MD., 2006. Optimising Fermentation Conditions of Recombinant *Escherichia coli* Expressing Cyclopentanone Monooxygenase. *Org. Process Res. Dev.*, 10, 599-604.
- Ryerson, CC., Ballou, DP. and Walsh, C., 1982. Mechanistic Studies on Cyclohexanone Oxygenase. *Biochemistry*, 21, 2644-2655.
- Schmid, A., Dordick, JS., Hauer, B., Kiener, A., Wubbolts, M. and Witholt, B., 2001. Industrial Biocatalysis Today and Tomorrow. *Nature*, 409, 258-268.

- Secundo, F., Zambianchi, F., Crippa, G., Carrea, G. and Tedeschi, G., 2005. Comparative Study of the Properties of Wild Type and Recombinant Cyclohexanone Monooxygenase, an Enzyme of Synthetic Interest. *J. Mol. Catal. B: Enzym.*, 34, 1-6.
- Sheng, D., Ballou, DP. and Massey, V., 2001. Mechanistic Studies of Cyclohexanone Monooxygenase: Chemical Properties of Intermediates Involved in Catalysis. *Biochemistry*, 40, 11156-11167.
- Shoemaker, HE., Mink, D. and Wubbolts, MG., 2003. Dispelling the Myths- Biocatalysis in Industrial Synthesis. *Science*, 299, 1649-1697.
- Simpson, HD., Alphand, V. and Furstoss, R., 2001. Microbiological Transformations 49. Asymmetric Biocatalysed Baeyer-Villiger Oxidation: Improvement using a Recombinant *Escherichia coli* Whole Cell Biocatalyst in the Presence of an Adsorbent Resin. *J. Mol. Catal. B: Enzym.*, 16, 101-108.
- Stahl, S., Greasham, R. and Chartrain, M., 2000. Implementation of a Rapid Microbial Screening Procedure for Biotransformation Activities. *Journal of Bioscience and Bioengineering*, 89, 367-371.
- Stark, D. and von Stockar, U., 2003. *In situ* Product Removal (ISPR) in Whole Cell Biotechnology During the Last Twenty Years. *Advances in Biochemical Engineering/Biotechnology*, 80, 149-175.
- Stewart, JD., Reed, KW. and Kayser, MM., 1996. 'Designer Yeast': A New Reagent for Enantioselective Baeyer-Villiger Oxidations. *Journal of the Chemical Society*, 1, 755-757.
- Stewart, JD., Reed, KW., Martinez, CA., Zhu, J., Chen, G. and Kayser, MM., 1998. Recombinant Bakers Yeast as a Whole-cell Catalyst for Asymmetric Baeyer-Villiger Oxidations. *Journal of American Chemical Society*, 120, 3541-3548.

- Straathof, A.J.J., Panke, S. and Schmid, A., 2002. The Production of Fine Chemicals by Biotransformations. *Curr. Opin. Biotechnol.*, 13, 548-556.
- Strukul, G., 1998. Transition Metal Catalysis in the Baeyer-Villiger Oxidation of Ketones. *Angewandte Chemie. International edition in English*, 37, 1198-1209.
- ten Brink, G.J., Arends, I.W.C.E. and Sheldon, R.A., 2004. The Baeyer-Villiger Reaction: New Developments toward Greener Procedures. *Chem. Rev.*, 104, 4105-4123.
- Uyttebroek, M., Ortega-Calvo, J.-J., Breugelmans, P. and Springael, D., 2006. Comparison of mineralization of solid-sorbed phenanthrene by polycyclic aromatic hydrocarbon (PAH)-degrading *Mycobacterium* spp. and *Sphingomonas* spp. *Appl. Microbiol. Biotechnol.*, 72, 829–836.
- Vicenzi, J.T., Zmijewski, M.J., Reinhard, M.R., Landen, B.E., Muth, W.L. and Marler, P.G., 1997. Large-scale Stereoselective Enzymatic Ketone Reduction with *in situ* Product Removal via Polymeric Adsorbent Resins. *Enzyme Microb. Technol.*, 20, 494-499.
- Watanabe, A., Uchida, T., Ito, K. and Katsuki, T., 2002. Highly Enantioselective Baeyer-Villiger Oxidation using Zr(salen) Complex as Catalyst. *Tetrahedron Lett.*, 43, 4481-4485.
- Watson, W.J.W., 2012. How do the Fine Chemical, Pharmaceutical, and Other Related Industries Approach Green Chemistry and Sustainability? *Green Chem.*, 14, 251-259.
- Willets, A., 1997. Structural Studies and Synthetic Applications of Baeyer-Villiger Monooxygenases. *Trends Biotechnol.*, 15, 55-62.

- Woodley, JM., Bisschops, M., Straathof, AJJ. and Ottens, M., 2008. Perspective Future Directions for *in-situ* Product Removal (ISPR). *J. Chem. Technol. Biotechnol.*, 83, 121-123.
- Woodley, JM., Breuer, M. and Mink, D., 2013 (article in press). A Future Perspective on the Role of Industrial Biotechnology for Chemicals Production, *Chem. Eng. Res. Des.*
- Wohlgemuth, R., 2007. Interfacing Biocatalysis and Organic Synthesis. *J. Chem. Technol. Biotechnol.*, 82, 1055-1062.
- Zambianchi, F., Pasta, P., Carrea, G., Colona, S., Gaggero, N. and Woodley, JM., 2002. Use of Isolated Cyclohexanone from Recombinant *Escherichia coli* as a Biocatalyst for Baeyer-Villiger and Sulfide Oxidations. *Biotechnol. Bioeng.*, 78, 489-496.
- Zambianchi, F., Raimondi, S., Pasta, P., Carrea, G., Gaggero, N. and Woodley, JM., 2004. Comparison of Cyclohexanone Monooxygenase as an Isolated Enzyme and Whole Cell Biocatalyst for the Enantioselective Oxidation of 1,3-dithiane. *J. Mol. Catal. B: Enzym.*, 31, 165-171.
- Zhang, H., Lamping, SR., Pickering, SCR., Lye, GJ. and Shamlou, PA., 2008. Engineering Characterisation of a Single Well from 24-well and 96-well Microtitre Plates. *Biochem. Eng. J.*, 40, 138-149

List of Abbreviations and Symbols

Å	Angstrom
ATP	Adenosine-5`-triphosphate
BVMO	Baeyer-Villger Monooxygenase
C_{eq}	Equilibrium concentration
C_i	Initial concentration
CHMO	Cyclohexanone Monooxygenase
d_i	Impeller diameter
d_T	Reactor diameter
DCM	Dicholoromethane
DCW	Dry cell weight
DoE	Design of Experiments
DOT	Dissolved oxygen tension %
DSW	Deep square well
FID	Flame ionisation detector
fps	Frames per second

GC	Gas chromatography
HTRS	High throughput resin screening
ISPR	<i>in-situ</i> product removal
K_A	Langmuir isotherm equilibrium constant
K_F	Freundlich isotherm equilibrium constant
K_K	Initial rate of adsorption of ketone
K_L	Initial rate of adsorption of lactone
n	Freundlich isotherm constant
NAD	Nicotinamide adenine dinucleotide (oxidised)
NADH	Nicotinamide adenine dinucleotide (reduced)
M	Mass of resin
OD_{600nm}	Optical density measured at absorbance wavelength of 600nm
OD	Optical density
psi	Pound-force per square inch
Q_{ads}	Adsorption capacity
Q_{max}	Maximum adsorption capacity

R^2	Regression coefficient
rpm	Revolutions per minute
$S_{K,L}$	Selectivity
SFPR	Substrate feed-product removal
STR	Stirred tank reactor
t	Time
U	Enzyme unit defined as μmol of product formed per minute
UV	Ultraviolet
V	Total volume
vvm	Vessel volume per minute
v/v	Volume per volume
w/v	Weight per volume (g/ml)

Appendix

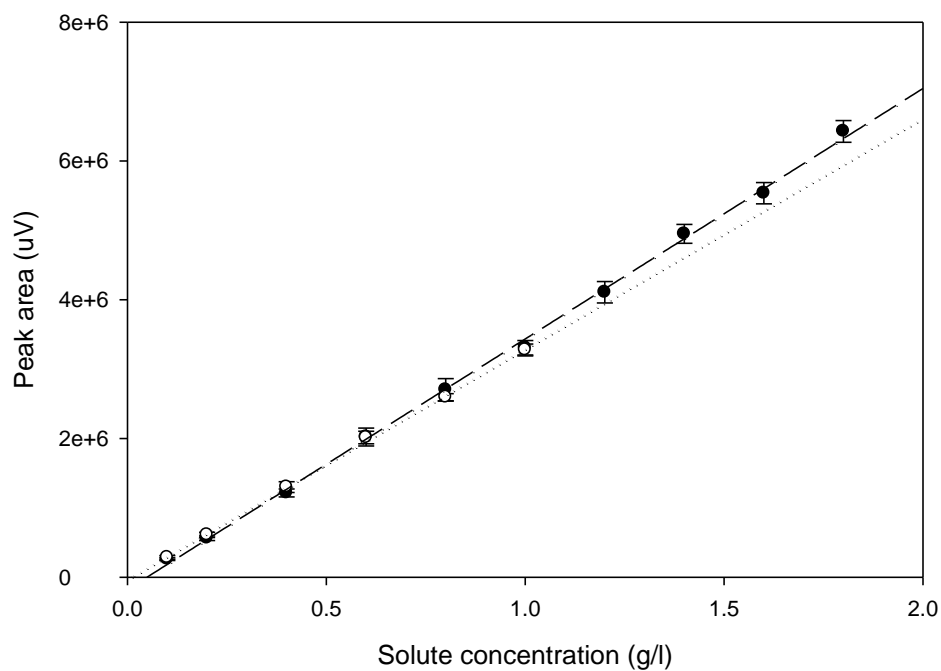


Figure A.1 Calibration curves for ketone (●) and lactone (○) in ethyl acetate. Samples were prepared as described in section 2.2.1.1 and analysed as described in section 2.2.1.2. Both fitted lines have R^2 values >0.99 and error bars show one standard deviation based on triplicate experiments.

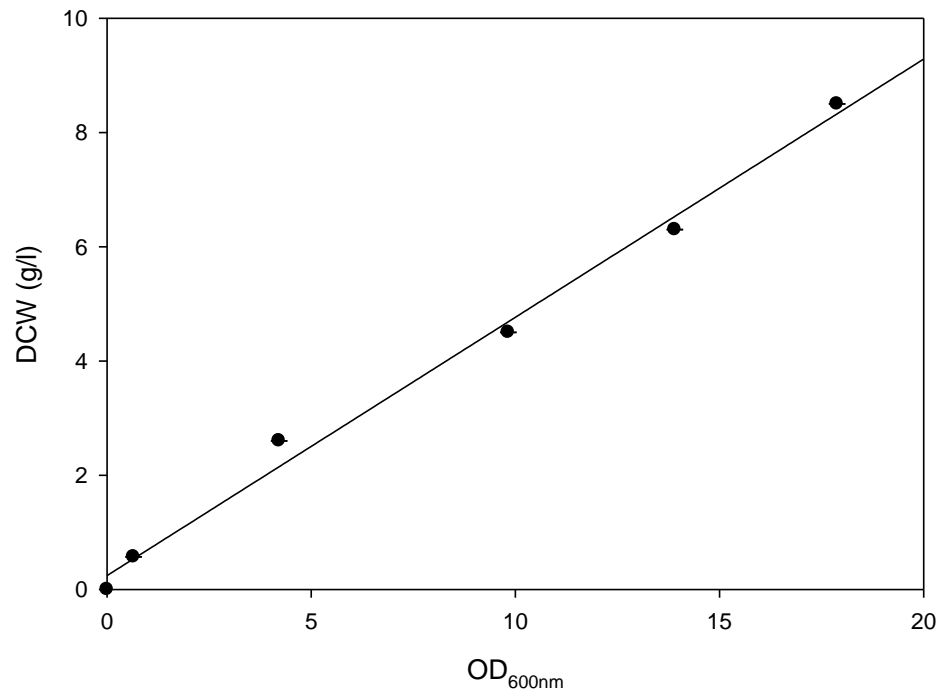


Figure A.2 Calibration of OD_{600nm} measurements from an *E. coli* TOP10 [pQR239] fermentation with DCW measurements determined as described in section 2.2.2. Fitted line has an R^2 value of > 0.99 and error bars represent one standard deviation based on triplicate experiments.

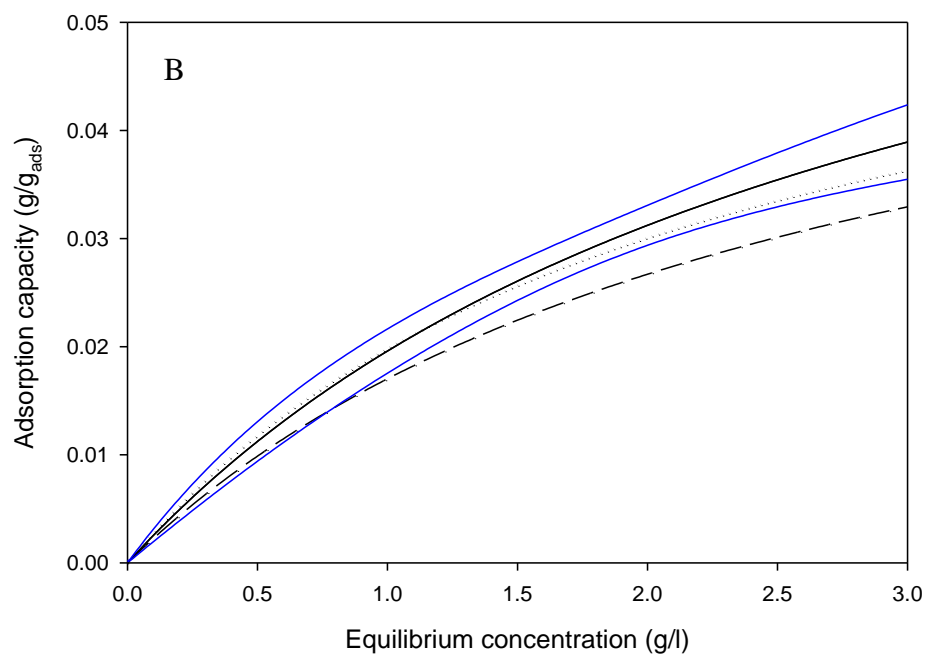
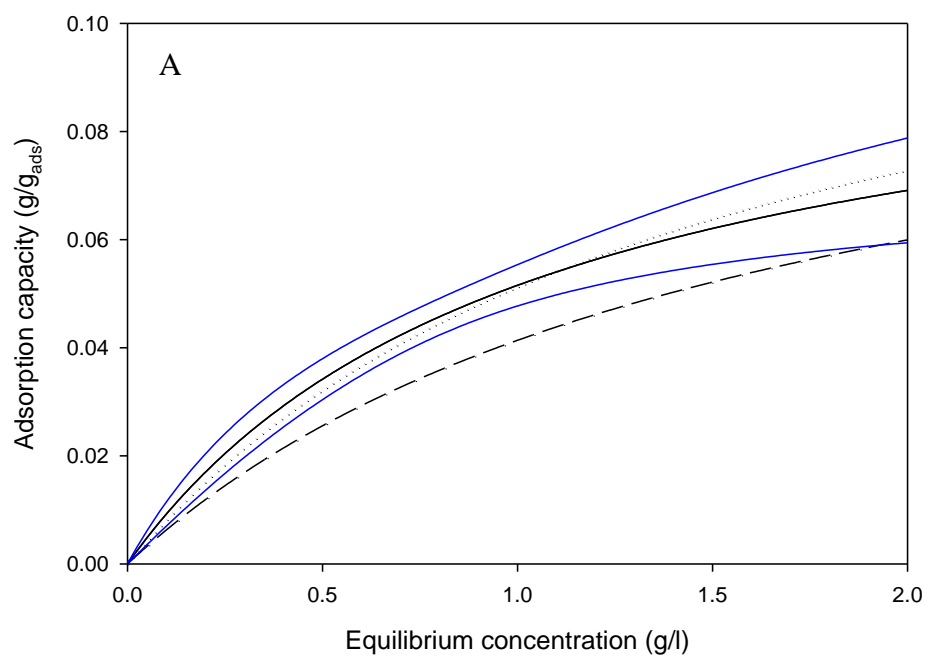


Figure A.3 Adsorption isotherms generated using XAD7 for the adsorption of (A) ketone (B) lactone in the 96 wells and 24 wells microplate platforms in experiments described in section 2.3.2.1. Black lines represent the Langmuir mathematical model fitted to the data as described in section 3.3.2 and the blue solid lines represent the 95% confidence interval band for the Langmuir model determined for adsorption at ml-scale (solid line: ml-scale; medium dashed line: 96 wells; dotted line: 24 wells).

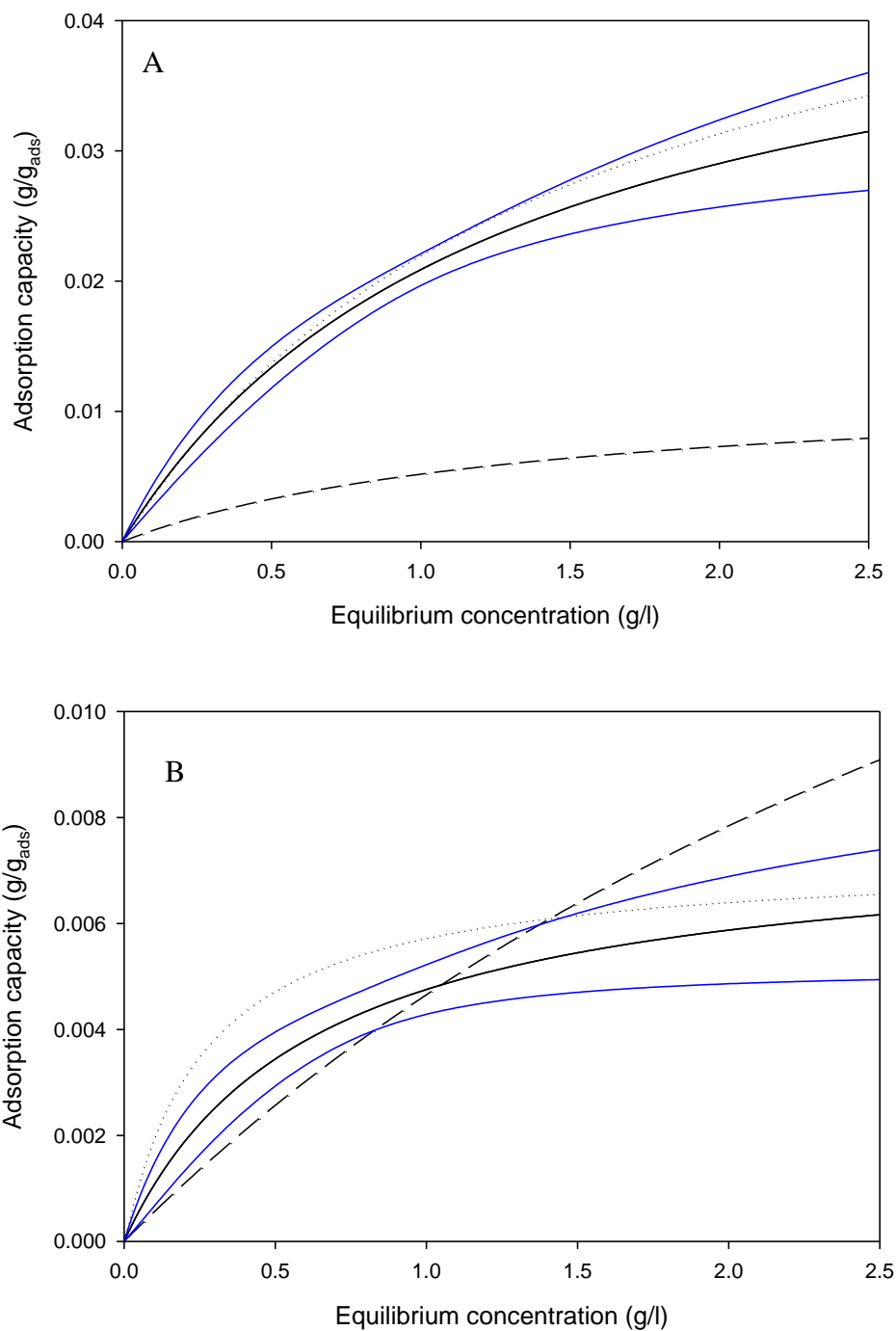


Figure A.4 Adsorption isotherms generated using IRC50 for the adsorption of (A) ketone (B) lactone in the 96 wells and 24 wells microplate platforms in experiments described in section 2.3.2.1. Black lines represent the Langmuir mathematical model fitted to the data as described in section 3.3.2 and the blue solid lines represent the 95% confidence interval band for the Langmuir model determined for adsorption at ml-scale (solid line: ml-scale; medium dashed line:96 wells; dotted line: 24 wells).

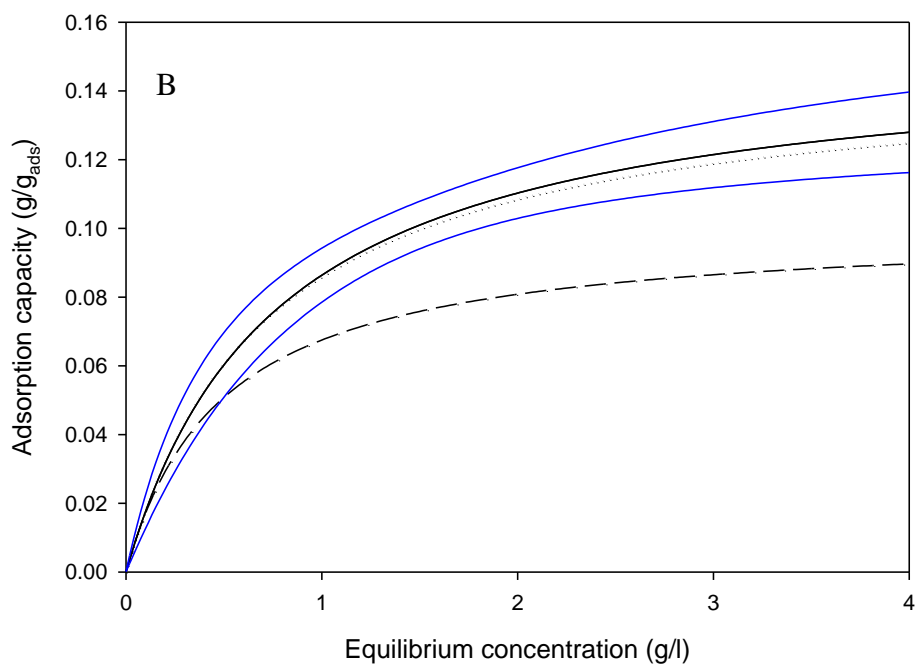
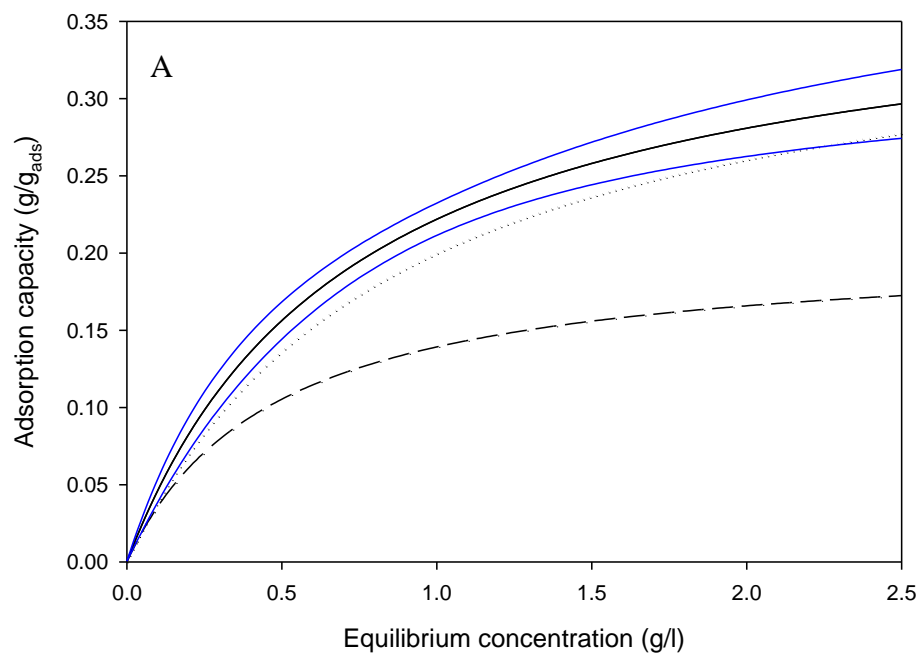


Figure A.5 Adsorption isotherms generated using L493 for the adsorption of (A) ketone (B) lactone in the 96 wells and 24 wells microplate platforms in experiments described in section 2.3.2.1. Black lines represent the Langmuir mathematical model fitted to the data as described in section 3.3.2 and the blue solid lines represent the 95% confidence interval band for the Langmuir model determined for adsorption at ml-scale (solid line: ml-scale; medium dashed line: 96 wells; dotted line: 24 wells).

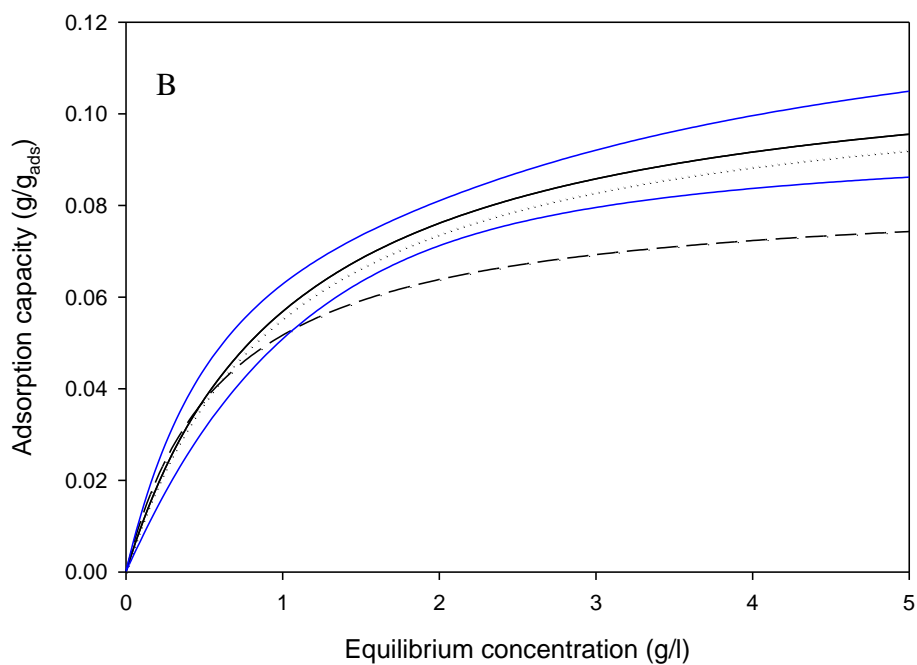
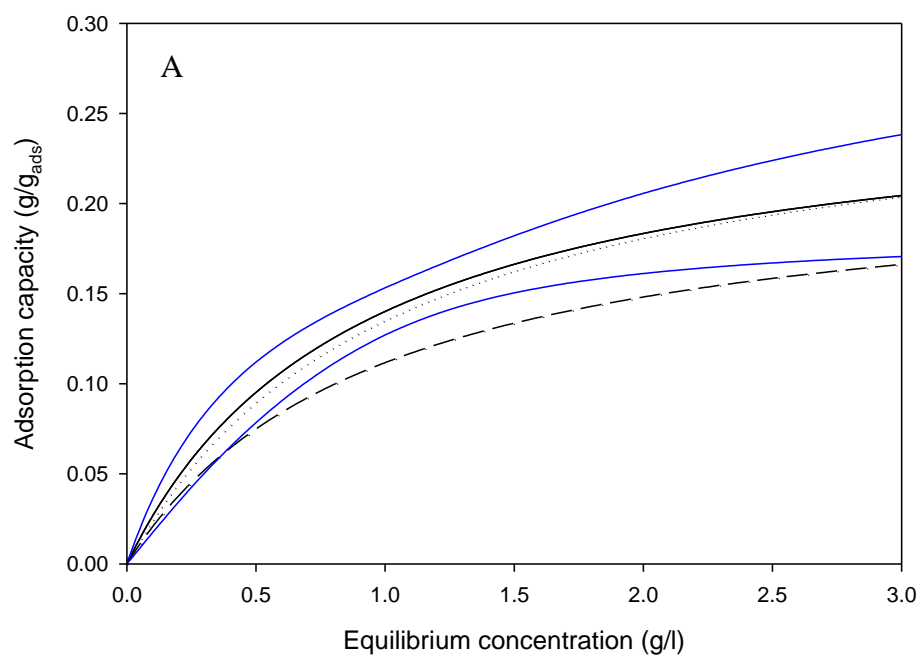


Figure A.6 Adsorption isotherms generated using XAD4 for the adsorption of (A) ketone (B) lactone in the 96 wells and 24 wells microplate platforms in experiments described in section 2.3.2.1. Black lines represent the Langmuir mathematical model fitted to the data as described in section 3.3.2 and the blue solid lines represent the 95% confidence interval band for the Langmuir model determined for adsorption at ml-scale (solid line: ml-scale; medium dashed line: 96 wells; dotted line: 24 wells).

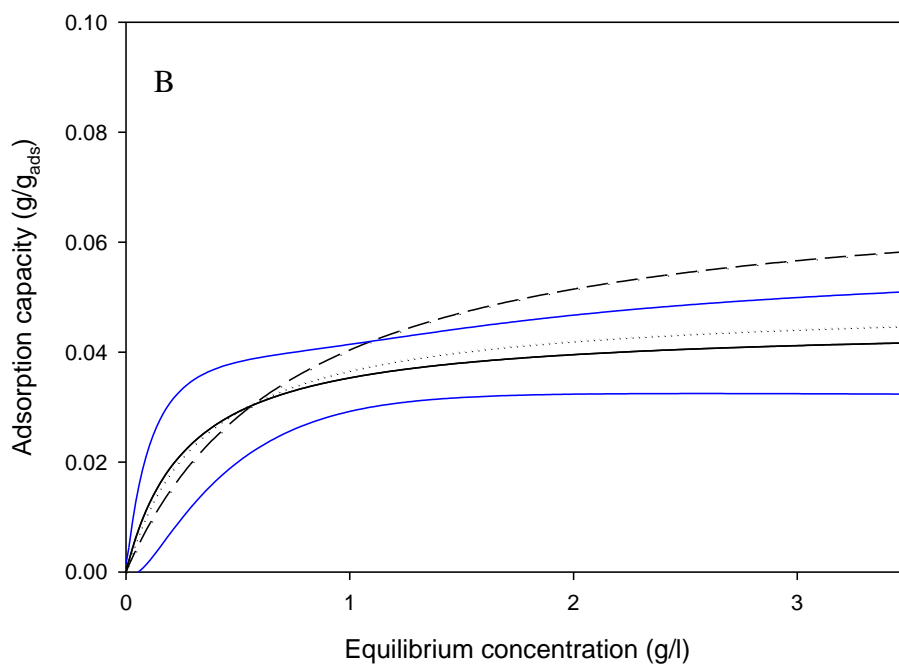
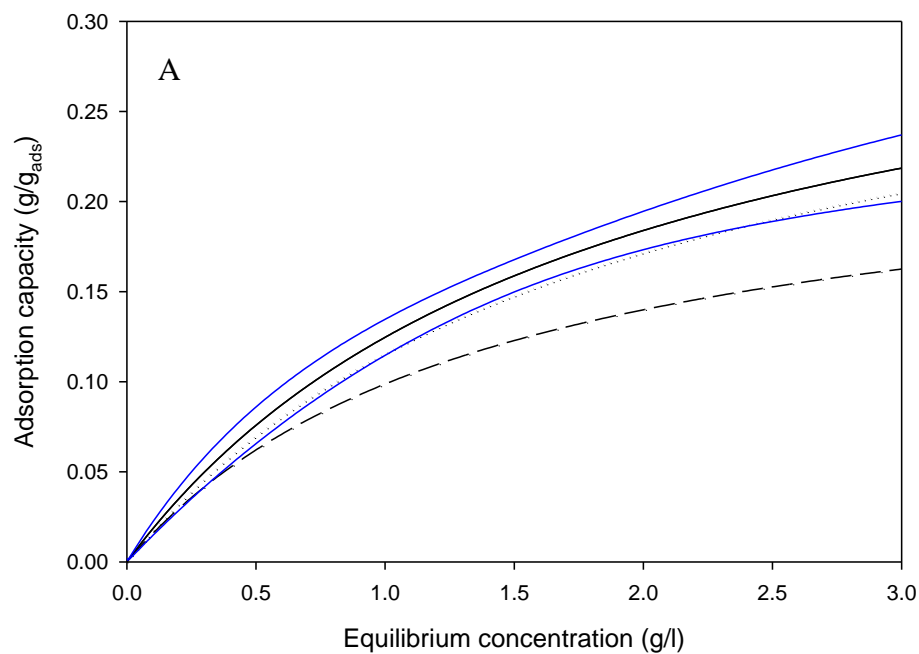


Figure A.7 Adsorption isotherms generated using XAD16 for the adsorption of (A) ketone (B) lactone in the 96 wells and 24 wells microplate platforms in experiments described in section 2.3.2.1. Black lines represent the Langmuir mathematical model fitted to the data as described in section 3.3.2 and the blue solid lines represent the 95% confidence interval band for the Langmuir model determined for adsorption at ml-scale (solid line: ml-scale; medium dashed line: 96 wells; dotted line: 24 wells).

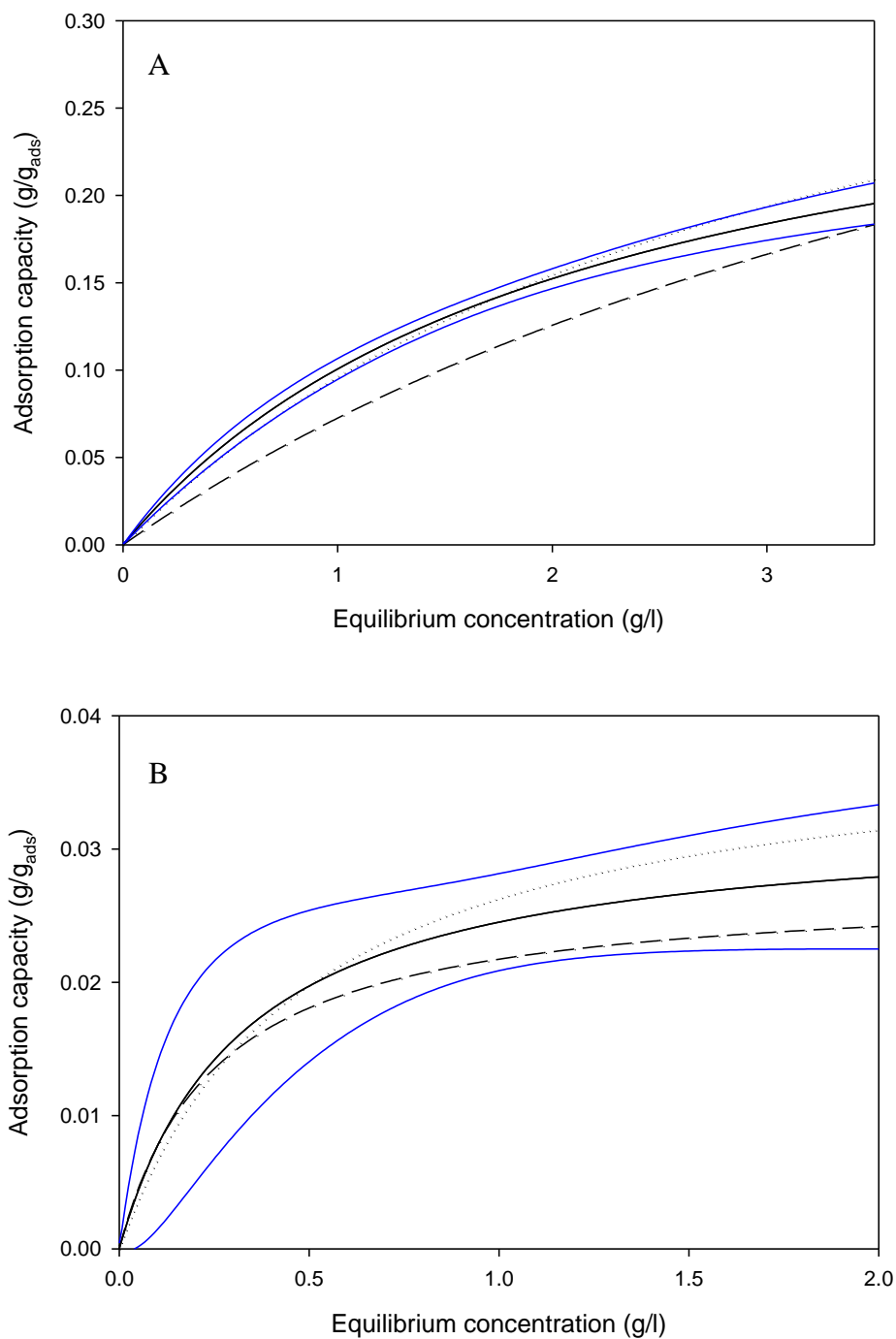


Figure A.8 Adsorption isotherms generated using XAD1180 for the adsorption of (A) ketone (B) lactone in the 96 wells and 24 wells microplate platforms in experiments described in section 2.3.2.1. Black lines represent the Langmuir mathematical model fitted to the data as described in section 3.3.2 and the blue solid lines represent the 95% confidence interval band for the Langmuir model determined for adsorption at ml-scale (solid line: ml-scale; medium dashed line: 96 wells; dotted line: 24 wells).

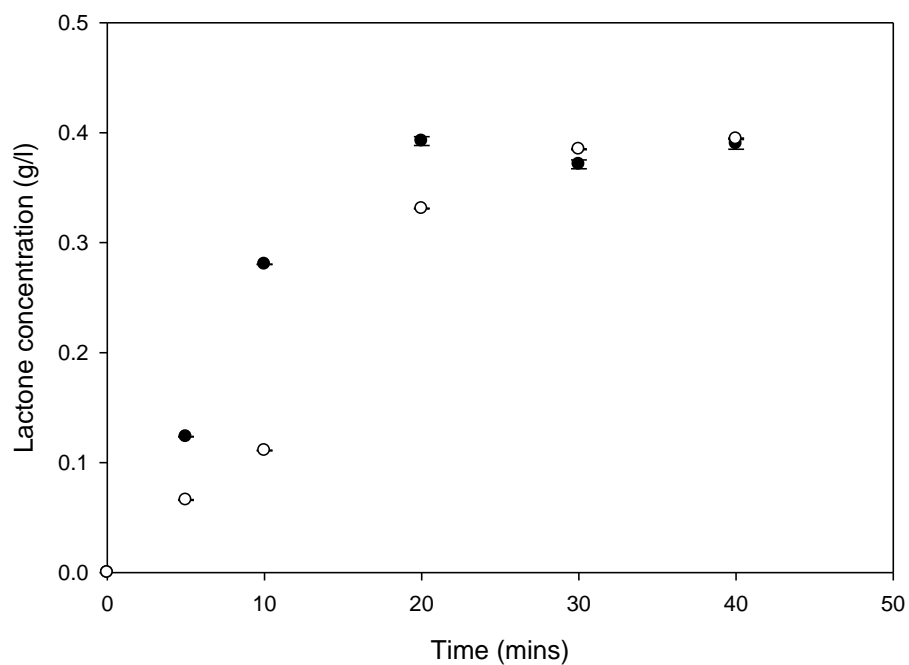


Figure A.9 Production of lactone by *E. coli* TOP10 [pQR239] biocatalyst ($8g_{DCW/l}$) using initial ketone concentration of $0.4g/l$ in (●) 50mM phosphate buffer (working volume 10%) and (○) fermentation media (working volume 20%), without the use of a resin SFPR strategy as described in section 2.5.1. Error bars represent one standard deviation based on triplicate repeats of experiments.

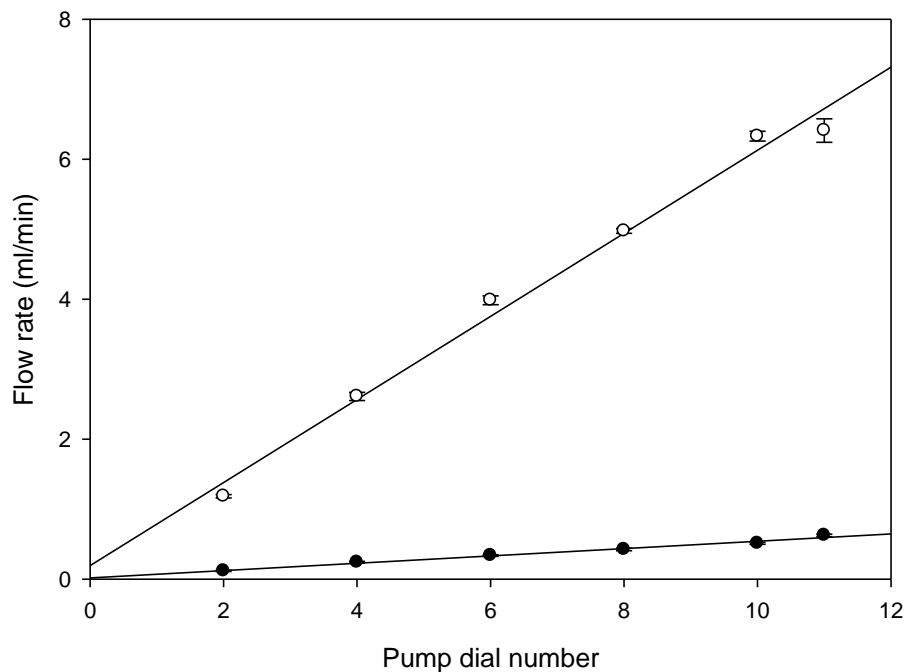


Figure A.10 Characterisation of the peristaltic Pump P-1 (Pharmacia Biotech, Sweden) by passing 50mM phosphate buffer through the Tricorn 5/50 column (GE Healthcare, Buckinghamshire, UK) packed with 1.2g of resin Optipore L493.(●) setting x1 and (○) setting x10. Error bars represent one standard deviation based on triplicate repeats of experiments.

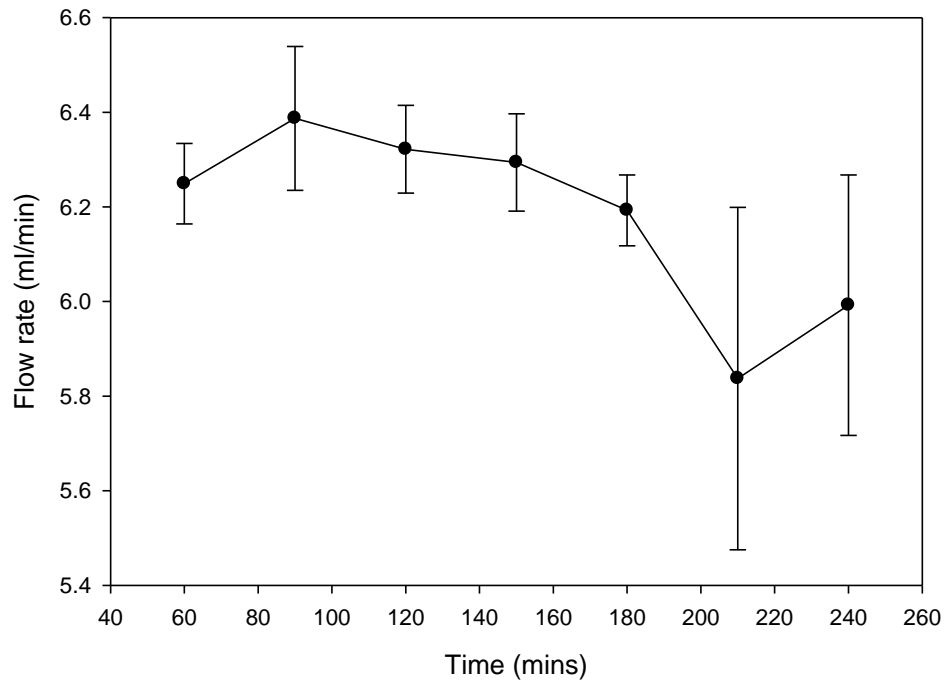
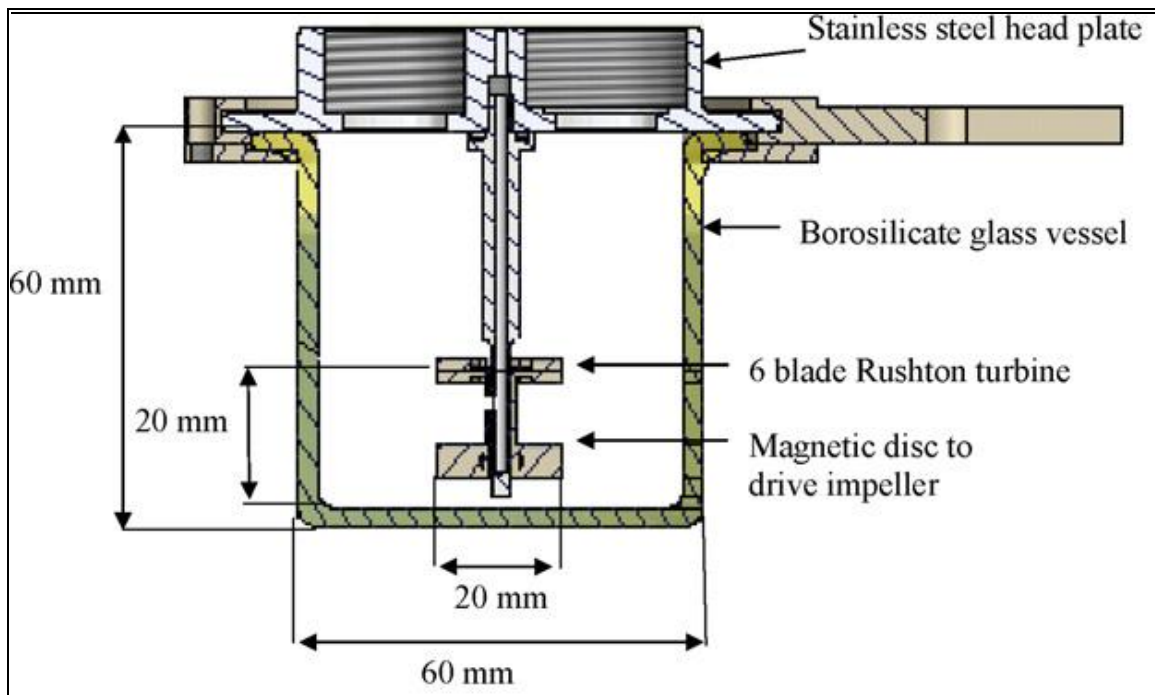


Figure A.11 Flow rate of 8g_{DCW}/l of cells resuspended in 50mM phosphate buffer passed through the Tricorn 5/50 column (GE Healthcare, Buckinghamshire, UK) packed with 1.2g of resin Optipore L493 using the the peristaltic Pump P-1 (Pharmacia Biotech, Sweden) at a flow rate of 6.4ml/min. Error bars represent one standard deviation based on triplicate repeats of experiments.



FigureA.12 Mechanical drawing of a cross section of the miniature stirred tank reactor (taken from Gill *et al* 2008).

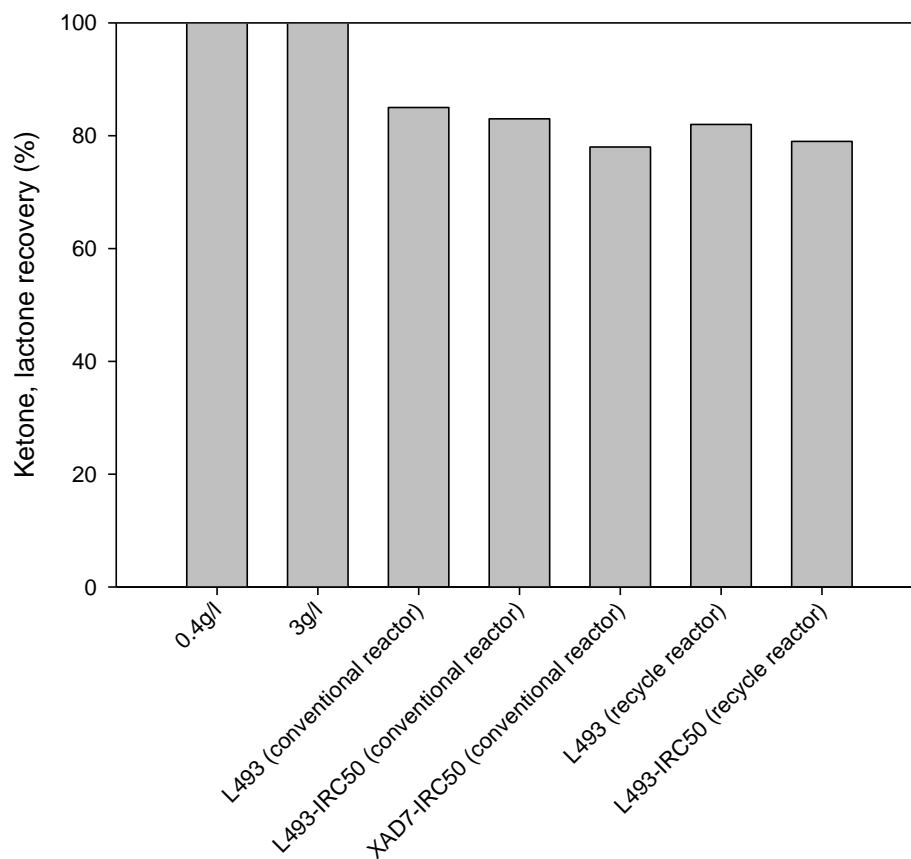


Figure A.13 Calculated mass balances from all bioconversions performed in the miniature STR without resins ('0.4g/l' and '3g/l'), with the single resin SFPR strategy in the conventional reactor ('L493 (conventional reactor)' and 'L493 (recycle reactor)') configurations and with the dual resin SFPR strategy in the conventional reactor ('L493-IRC50 (conventional reactor)' and 'XAD7-IRC50 (conventional reactor)') and recycle reactor ('L493-IRC50 (recycle reactor)') configurations. Results after 2.5 hours of bioconversion.